university of groningen

faculty of science and engineering

Research into residual stresses in metals for optical instrumentation

MASTER PROJECT THESIS

ASTRONOMY I&I

16 OCTOBER 2019

Author:
Kaushal Marthi
S3318206

Supervisors:
Dr. Lars Venema
Ir. Johan Pragt
Prof. Dr. Reynier Peletier

Summary

Optical instrumentation places stringent requirements on the precision of its components, particularly as progress dictates that the precision must continually improve. Depending on the wavelength of radiation which the instrument is measuring, the required precision can be tremendously fine. For example, in ultraviolet measurements the required precision can be at the nanometre scale [1]. Hence the need is present to account for factors which can affect the precision. With a better understanding of the mechanical properties, there is less need for safety measures to counteract possible undesired effects, improving the final quality of the product and reducing production risks.

In the case of optical instrumentation such as telescopes, the aluminium alloy 6061 tends to be frequently used, on the basis of heritage [2]. There is now however, a great desire to understand the material well such that, as the industry goes into higher levels of precision for its instrumentation, the material used can be well-understood and better-quality assessments can be made between competing materials.

An emerging issue in this field are residual stresses, which exist in components in the absence of an applied force and are ‘locked-in’ the material. These stresses can be released by a process which disrupts the equilibrium, such as machining, or simply by slowly releasing over time, a concept known as creep. A release of stress is accompanied by a deformation, which affects the dimensional stability of the part, and can diminish the image/data quality as a result. There is therefore the desire to form a deeper understanding of residual stresses.

The current thesis aimed to be able to form a refined definition of residual stresses, such that they can be measured without the need for specialised equipment. This definition would aim to relate residual stresses to existing material parameters which are measured through simple and/or standard tests.

Currently, there are already methods (of varying accuracy, complexity, cost and usefulness) for measuring residual stresses in materials [3]. These methods will return a value, or values, for the residual stress, again with varying degrees of usefulness. It is thought however, that it would be of more use to have the residual stresses related to existing material parameters. If the relation can be formed with parameters extracted from one or more of these simple tests, then it would logically mean that these tests could be used to estimate the residual stresses present in a piece of material.

Thus, the primary objective of this project was to form a definition of residual stresses as a material parameter in relation to the existing parameters. This definition was intended to be quantitative, such that it could be used to measure residual stresses. Naturally, it was not expected that a perfect, fully-formed relation and measurement procedure could be obtained during the course of this project, but progress in this direction was desired.

Simultaneously, literature would be studied to provide an overview of the existing residual stress measurement methods, with the intention of being able to identify useful measurement methods, and the possible analyses of these, in the event of the primary objective being unattainable. Additionally, it would be pertinent nonetheless to have the knowledge of these methods.

Finally, as non-essential objectives, it was decided to perform cursory research into the prediction of residual stresses as a result of certain processes, and the prediction of future deformation as a result of residual stresses.

The project was approached from a literature perspective, with the idea that the past knowledge and empirical relations could be used to provide links to residual stress. Additionally, the work would be theoretical, therefore experimental data would not be collected in this project in the interest of limiting the scope to reasonable boundaries.

Initially, the background theory relevant to this project was researched and presented. This consisted of building up from basic stress-strain theory to more complex ideas such as yield criteria, plasticity and strain-hardening. This background theory is necessary for the understanding of the measurement methods and the relation obtained later.

Subsequently, an overview of the current methods used for the measurement of residual stresses is presented. Three types of method exist: non-destructive, semi-destructive and destructive. A representative method of each type is selected for an overview: X-ray diffraction, hole-drilling, and the contour method, respectively. At the end, a table analysing the relative qualities of each method is given, although the choice is likely to be subjective, based on user preference and task.

The research into residual stresses and material parameters indicated that residual stresses existing in the surface of a material have an effect on hardness measurements. This relationship had already been suspected and observed [4]. The desire was therefore present to obtain a quantitative relation between these parameters.

To this end, a paper by Frankel et al. presented a model for the effect of residual stress on hardness using cylindrical stresses (radial and circumferential stresses) [5]. This model made use of the stresses applied by a hardness test, residual stresses, and yield stress in the von Mises yield criterion to obtain an expression.

The cylindrical stresses were modified to rectangular stresses through the initial use of an equi-biaxial stress state, used in Lee & Kwon's paper [6]. The modification led to an initial relation, which was used to justify the methodology by observing the similarity of the relation to the observed relation between hardness and yield stress [7] [8] [9].

The stress state was then made more complex through the use of a stress ratio parameter, κ, which described the ratio between the two orthogonal residual stress components present in the plane of the material, taken from a subsequent paper by Lee & Kwon [10] [11]. This stress

state was used to develop a more complex final form of the relation, shown below, where σ_{res} is the major residual stress component, σ_y is the yield stress, and P_m is the mean pressure or Meyer hardness.

$$\sigma_y^2 = (\kappa^2 - \kappa + 1)\sigma_{res}^2 + \frac{1}{3}(\kappa + 1)\sigma_{res}P_m + \frac{1}{9}P_m^2$$

This relation was hypothetically tested using arbitrarily varying values of the various parameters and observing the effects. A plot is also given using real values of σ_y and hardness from data tables as an example, however as the parameters of the test could not be controlled, confident conclusions cannot be formed from this plot.

The relation has potential for use in the estimation of residual stresses. The parameters in the relation, σ_y and P_m are ones which are measurable through standard tests that are widely used in the industry: the tensile test and hardness tests. Therefore, with the sufficient verification and support of data, the relation (or an improved form) could be used in the measurement of residual stresses using hardness measurements.

That being said, the relation certainly does have its drawbacks, primarily relating to the limitations of the usability of the relation, and the additional research and information required to use it. These drawbacks are of varying impact, nevertheless they are important to note.

The limitations of the relation lie with information that the relation is not able to incorporate. It cannot handle inelastic residual stresses without a local yield stress, it does not account for strain-hardening occurring during the indentation of a hardness test, and it can only measure the stresses near the surface.

The additional information required relates to the stress ratio parameter κ and a fit parameter used by Frankel et al., α [5]. These parameters are not known in advance and would need extensive testing to standardise them for certain processes.

Therefore, the primary need and recommendation is that further research is conducted, particularly since the relation must be supported by experimental data. Rough potential procedures are proposed for the procurement of for κ and α. The limitations of the relation can additionally be mitigated by further research to improve the equation such that it can incorporate some of the missing information. A list of a few proposed future actions is given below:

- Test relation thoroughly through performing hardness and residual stress measurements for various situations
- Standardise κ through measuring axiality of residual stresses as a result of various materials and manufacturing processes, e.g. cold-rolling.
- Standardise α through fitting hardness-residual stress data for various materials and processes.
- Incorporate strain-hardening due to indentation into the relation, for example by making σ_y in relation dependent on plastic deformation caused by indentation. Can use mathematical approximations to stress-strain curve to estimate 'new' yield stress.
- Obtain standard residual stress profiles for various processes and materials, such that surface measurements can be used to infer stresses deeper in the part.
- Incorporate local yield stresses into relation, such that it is not limited to elastic residual stresses.

As for the tertiary objectives, a small amount is presented on the prediction of the deformation caused by residual stresses. A thesis and paper by Spence contain a creep model for the progression of residual stresses over time, this is presented briefly at the end [12] [13].

In conclusion, the use of hardness to measure residual stresses as opposed to other methods is perhaps curious, given the lack of sensitivity of hardness measurements to residual stresses. The residual stress calculation from the relation also shows high sensitivity to measurement errors, affecting accuracy.

However, hardness tests are included as standard in the industry. Hence, making use of existing equipment, as well as relating residual stresses to material parameters makes the use of this theory an attractive option, despite its limitations. The theory may well be able to give some indication of the residual stresses present based on hardness measurements, or perhaps be a building block in more robust theories.

Acknowledgments

I would firstly very much like to thank my project supervisors at ASTRON, Lars Venema and Johan Pragt, for their vital guidance and invaluable patience during this project, and for taking the time and effort to help and counsel me.

I would also like to thank Eddy Elswijk for his technical input and discussions, and Reynier Peletier at the Kapteyn Institute for his guidance and advice.

Finally, I would like to thank my family for their constant support and encouragement during this process.

Contents

1 Introduction

1.1 Background

Optical instrumentation has stringent requirements on precision, particularly due to the demand for constant progress. Instruments need to continually become more precise, and certain types of measurement will require greater precision. For example, if one wishes to conduct measurements in the ultraviolet part of the spectrum, the wavelength can be of the order of 10^1 nanometres [1]. This would require nanometre-level precision. In order to meet these capabilities, it is necessary to know as much about the materials used as possible.

The study of materials tends to be a complicated and somewhat abstract field. This is especially true in alloys, due to the unpredictable way in which their structures often form. The importance of the field often lies in selecting the correct material or alloy for a given task, from the wide range available, and being able to identify any remaining problem sources in the selected material.

The nature and complexity of the study of materials means that materials tend to be divided up into classes. For example, metals, ceramics and polymers have their own classes [14]. The motivation for this division is that standard rules for one class of material may not apply for another class, hence within each class certain rules can be applied.

In this thesis, the focus will be on the class of metals, specifically aluminium alloys, which are widely used in telescope mirrors [2]. For metals, certain common parameters are used for selection. Common examples include the modulus of elasticity, E, the yield stress, hardness, and ultimate tensile stress. These are usually listed in a table of properties for a material. An example table for aluminium alloys is shown below in Table 1.1 [15].

Alloy and temper	Strength, MPa		Elongation, %		Hardness, Brinell No., 500 kgf load, 10 mm ball
	Ultimate	Yield	In 50 mm 1.60 mm thick specimen	In 5D 12.5 mm diam specimen	
5005-H32	140	115	11	...	36
5005-H34	160	140	8	...	41
5005-H36	180	165	6	...	46
5005-H38	200	185	5	...	51
5050-O	145	55	24	...	36
5050-H32	170	145	9	...	46
5050-H34	190	165	8	...	53
5050-H36	205	180	7	...	58
5050-H38	220	200	6	...	63
5052-O	195	90	25	27	47

Table 1.1: Example table of aluminium alloys material properties [15]

In particular, the aluminium alloy 6061 (Table 1.2 [16]) is frequently used in telescope optical paths, due to favourable characteristics such as dimensional stability and the heritage of the material [2]. The heritage of the material provides justification for the continued use; it has been proven to work well in the past, hence there is a good reason to continue using it. As the required precision increases however, the need to gain knowledge of factors which could affect stability becomes crucial.

Element	Maximum Unless Range is Specified
Silicon	.40 - .8
Iron	.7
Copper	.15 - .40
Manganese	.8 - 1.2
Magnesium	.8 - 1.2
Chromium	.04 - .35
Zinc	.25
Titanium	.15
Others Each	.05
Others Total	.15
Aluminum	Balance

Table 1.2: Aluminium alloy 6061 composition [16]

1.2 The Problem

A key factor of interest which is known to affect material performance is the stresses which exist in the absence of an external force, known as residual stresses. Residual stresses

are a by-product of all manufacturing and machining processes, to a greater or lesser extent [17]. Cold-rolling, a common manufacturing process, is one such example where residual stresses are generated due to plastic deformation [3] [18].

In optical components, the problems associated with residual stresses occur when the residual stresses are relieved and cause the part to deform. One of the key characteristics required for optical performance is dimensional stability. The part needs to hold its dimensions such that the optical path is not affected. Localised relaxation of residual stresses will lead to a non-uniform deformation, affecting the optical path and hence the image or data quality.

The first area of concern with regards to stress relaxation is machining. Typically, with optical components, machining is performed very carefully. An initial machining is done with a certain tolerance, after which the material is heat-treated to relieve stresses. The final delicate machining is then done after the heat treatment to minimise the effect of the machining.

However, residual stresses exist in an equilibrium within a material, due to the absence of an external force. Thus, a disturbance to the equilibrium such as machining would necessitate a re-establishment of the equilibrium, which is done through deformation of the material. It has been observed that after a piece has been machined, it can significantly deform.

The other area of concern is relaxation of residual stresses over an extended period of time, known as creep. Relatively low values of residual stress can exist comfortably in a material. However, over time a material with a low amount of stress can still deform, or creep. This was also identified by Newsander et al.: “the residual stress must be low throughout the part. Residual stress over time will relax and become manifest as dimensional changes” [2].

Therefore, any insight into the residual stresses existing within a piece of material has the potential to be crucial in the manufacture of optical components. A simple method for the measurement of these is additionally of importance, as existing residual stress measurement

methods generally require specialised equipment, which may not be readily accessible to a user wishing to measure the residual stress in a part.

1.3 Objectives and Plan

The primary objective of this project was therefore to attempt to gain an insight into residual stresses through the use of past literature, with the aim of being able to suggest a method for their measurement using readily available equipment. It was therefore deemed useful to quantitatively link the residual stresses to existing material parameters, particularly hardness, as there was already a link. Although there are other sources, residual stresses due to mechanical effects were primarily addressed.

A research into existing residual stress measurement methods was additionally deemed necessary, to help understand the issue, to illustrate the alternatives, and to potentially make use of in the eventuality that the primary objective was deemed unattainable.

Additional objectives included the prediction of residual stress creep over time, and prediction of residual stresses due to certain processes. These were deemed useful to have, but of lower importance than the above objectives, and not crucial for the completion of the project. The list of objectives, in order of importance, is given below.

Objective 1. **Defining residual stresses theoretically as a material parameter**, and/or relating it to existing defined material parameters such as strength, Young's modulus, hardness, etc. This should be a quantifiable parameter, whether it be a material constant that indicates propensity for residual stress formation, or another material parameter that is indicative of the residual stresses present in the material.

Objective 2. **Defining a method for on-site residual stress measurement and quantification:** This can be seen as both a continuation of, or separate from the first one, seeing as it is not known whether the first one is theoretically possible in the scope of this project, but perhaps progress can be made in that direction. If point 1 is achievable, then it should naturally lead to at least an idea for an on-site measurement, and point 2 is seen as a secondary objective. In the event that point 1 is not fully achievable within the scope of this project, then point 2 will be the primary objective, and the definition of a method for on-site measurement can be progressed through research into existing measurement methods for residual stresses. This research into existing measurement methods is necessary in any case. Thus, point 2 can be used to have a quantification of the residual stresses present. This quantification with measurement needs to include certain parameters which

help to (as fully as possible) define the residual stress in the sample, rather than just one single averaged number for the value. An own method of using the information from the existing measurement methods for analysis should be introduced.

Objective 3. **Predicting progression of residual stresses in relation to dimensional stability:** This could progress from point 1 or 2. If one can obtain a good idea of the residual stress distribution within either a test sample or final product, then one can try to predict how the potential relaxation of these stresses would affect the dimensional stability, and the timescales involved. This can be seen as a tertiary objective, of lesser importance than the first two, and is possible that it cannot be completed in the scope of this project.

Objective 4. **Predicting residual stresses:** Ideally would like to be able to use theory to be able to also predict what residual stresses are expected through the material as a result of certain processes, such that one can estimate what stresses can be expected in final product. Similarly to point 3, this is also a tertiary objective.

The overview of the objectives and their importance in the multiple eventualities is summarised in the flowchart shown below in Figure 1.1, in order to gain an indication of the expected progression of the project, which is dependent on the success of the primary objective. The tertiary objectives will also gain in importance in the eventuality of objective 1 being incomplete, and objective 2 becoming a primary objective.

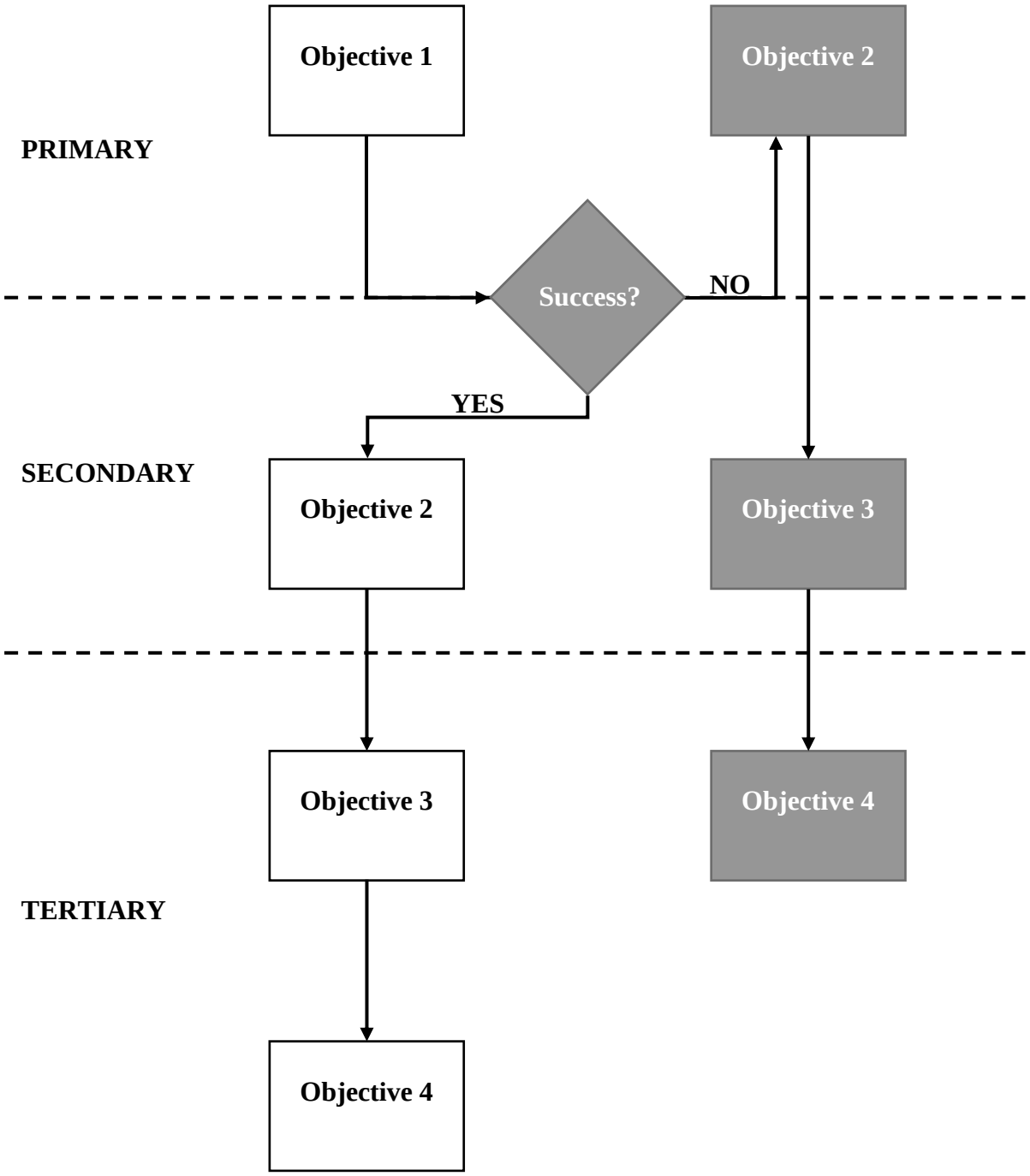

Figure 1.1: Flowchart of project objective hierarchies and eventualities

2 Background theory

This section describes the background theory required for this thesis. This section will provide an overview of the basics of stress-strain theory, up through some more complex theory, to give enough of an idea of the background concepts such that the discussions of the relations introduced later can be clear. This section will introduce stresses and strains, material curves, and will subsequently go into some theory in plasticity, to introduce and explain the concepts of yielding and strain-hardening. Finally, there will be some basic ideas of the formation of residual stresses in metals due to mechanical causes.

2.1 Stress-Strain theory

2.1.1 Stress-strain definitions

The force per unit area exerted in a material is known as the stress. In mechanics, stresses are essentially regions of pressure in a material. The transmission of an external force to the interior of the material is performed by particles exerting forces on their neighbours. In Figure 2.1 from Gere [19], a bar is under a force P which, when exerted on the bar with a cross-sectional area A, produces a uniformly distributed stress in the bar, σ, which is defined as in equation (2.1). This type of stress is known as a 'normal' stress since the force and the stress are acting perpendicularly to the cross-section.

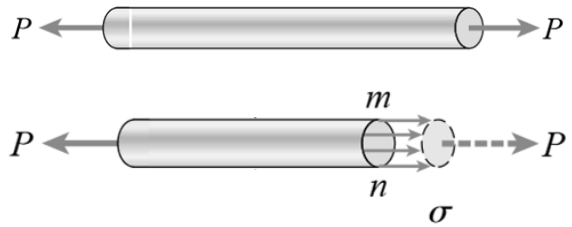

Figure 2.1: Figure from Gere, showing definition of stress in a bar, under a load P [19].

$$\sigma = \frac{P}{A} \tag{2.1}$$

Conversely to stress, the strain ε is a dimensionless entity representing the proportional deformation of an element due to stress. Considering the same bar as previously, the force P causes the bar to elongate by an amount δ, as seen in Figure 2.2. The strain experienced by the

bar is then defined as being the proportion of the elongation respective to the original length L of the bar, as shown in equation (2.2). This is also a 'normal' strain, as the deformation is perpendicular to the cross-section.

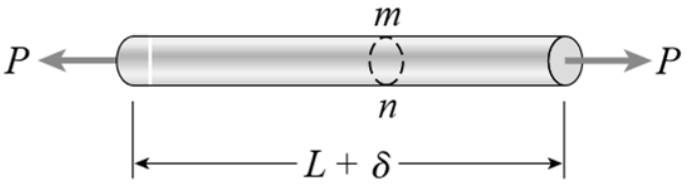

Figure 2.2: Figure from Gere, showing bar of original length L being extended by δ, under a load P [19]

$$\varepsilon = \frac{\delta}{L} \tag{2.2}$$

In most cases of interest, the stresses and strains will be more complex than in the simple situation shown above. The example shows members loaded axially, i.e. along their axis, and are therefore only one-dimensional in nature. Moreover, the loading state shown will result in a uniformly distributed stress in the cross-section. In reality this is rarely the case, and one tends to be more concerned with localised areas of stress and strain. Furthermore, there will be more complex types of stress, such as shear stresses.

Shear stresses, as opposed to the normal stresses described thus far, are stresses which act tangentially to a cross-section. A shearing effect would be one that would cause the faces of a cross-section to 'slide' over one another.

In Figure 2.3 from Megson [20], since the beam is fixed at one end, the application of the load P perpendicularly to the axis of the beam at the free end coupled with the reaction force acting oppositely at the fixed end, would cause a shearing effect in the material.

The cross-section in Figure 2.3 shows that the load causes the internal shear force S, which is equivalent to P and distributed over the cross-section. This distribution is not uniform, but the average shear stress τ_{av} is given by equation (2.3), with A being the area of the cross-section.

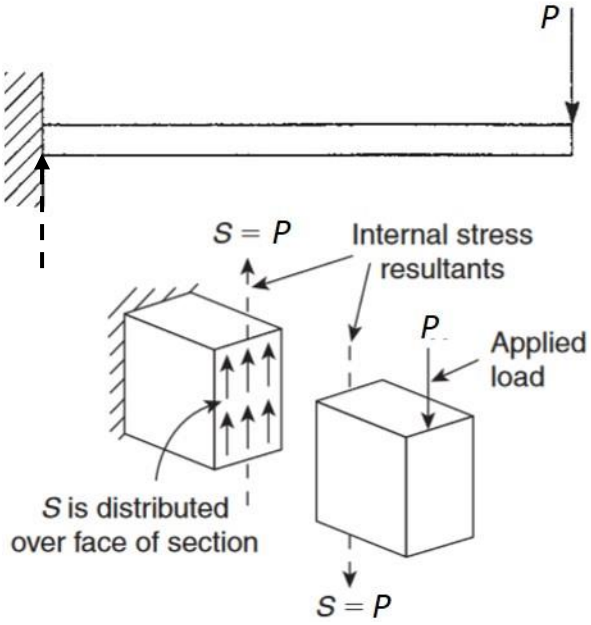

$$\tau_{av} = \frac{S}{A} = \frac{P}{A} \tag{2.3}$$

Figure 2.3: Figure(s) from Megson, showing shear load and resulting shear stress [20]

2.1.2 Stress element & stress tensor

A point can have multiple stresses of both types acting upon it in three dimensions. The description of all the stresses acting on a point is known as the 'state of stress', and is often portrayed by means of an infinitesimal volume element, as in Figure 2.4 a). The volume element depicts the stresses in the three dimensions acting at the point.

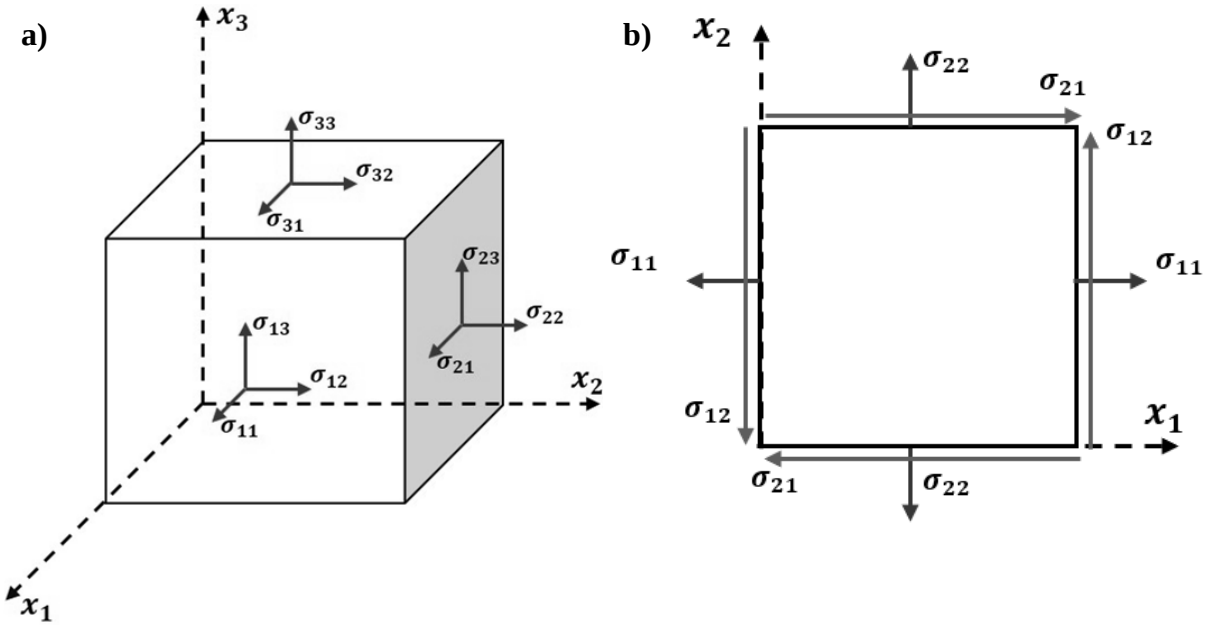

Figure 2.4: a) Figure showing an infinitesimal volume element at a point and stresses acting upon it, b) View of x_1 -x_2 plane of volume element showing stresses

The number convention for the subscripts of the stresses σ_{ij} is as follows: i represents the plane on which the stresses are acting, with the plane's number being designated by the axis to which it is perpendicular. j represents the direction of the stress itself, i.e. if the stress is parallel to the x_2 axis, then j will be 2. Therefore, normal stresses have identical subscripts, and shear stresses do not.

The stresses are described as single arrows in Figure 2.4 a), but a stress is in fact a set of two opposing arrows, as can be seen in Figure 2.4 b) showing the element in the x_1-x_2 plane. Each arrow representing a stress acting on a face of the element is coupled to an arrow pointing in the opposite direction, and on the opposing face of the element. This is necessary to maintain equilibrium in a particular direction. A set of two opposing arrows represents one stress. In normal stresses this will be either tensile or compressive, and in shear it will be 'clockwise' or 'anti-clockwise' shearing.

In order to maintain rotational equilibrium, certain shear stress values will be necessarily equivalent. Considering Figure 2.4 b) again, the shear stress couple σ_{12} would act to cause an anticlockwise moment and hence rotation. Hence, the couple σ_{21} must balance it out in the clockwise direction to maintain rotational equilibrium, therefore $\sigma_{12} = \sigma_{21}$. This is also true for the other shear stresses: $\sigma_{13} = \sigma_{31}$ and $\sigma_{23} = \sigma_{32}$.

Stresses are not defined as scalar or vector, but instead the stress state at a point is condensed into a singular quantity known as the stress tensor, shown in equation (2.4). Stresses are not scalar, as they have a necessity for magnitude and direction. A vector definition is not apt either, as the nature of stresses means that they cannot be summed in the manner that vectors are.

In three dimensions, the stress tensor takes the form of a 3-by-3 matrix, which is filled by the nine stresses that act on the point (three normal stresses and six shear stresses). The diagonal elements are the normal stresses, and the off-diagonal elements are the shear stresses.

Although the tensor has 9 components, the equivalence of the shear stresses leads to only 6 independent components.

$$\boldsymbol{\sigma_{ij}} = \begin{pmatrix} \sigma_{11} & \sigma_{12} & \sigma_{13} \\ \sigma_{21} & \sigma_{22} & \sigma_{23} \\ \sigma_{31} & \sigma_{32} & \sigma_{33} \end{pmatrix} \tag{2.4}$$

2.1.3 Plane stress & Biaxial stress

In certain situations, a simplifying assumption known as plane stress is used, which neglects the stresses connected to the third dimension or direction. An example of this is shown in Figure 2.5, where the stress state features only the stresses acting on the x_1 and x_2 faces, and also only the stresses acting in the x_1 and x_2 directions. The stresses associated with the third direction x_3, are excluded. This includes the shear stresses acting on the x_1 and x_2 faces, but in the x_3 direction. In essence, any stress which includes '3' in its subscript will disappear. The state will reduce into a two-dimensional problem, appearing as in Figure 2.4 b), resulting in the stress tensor shown in equation (2.5).

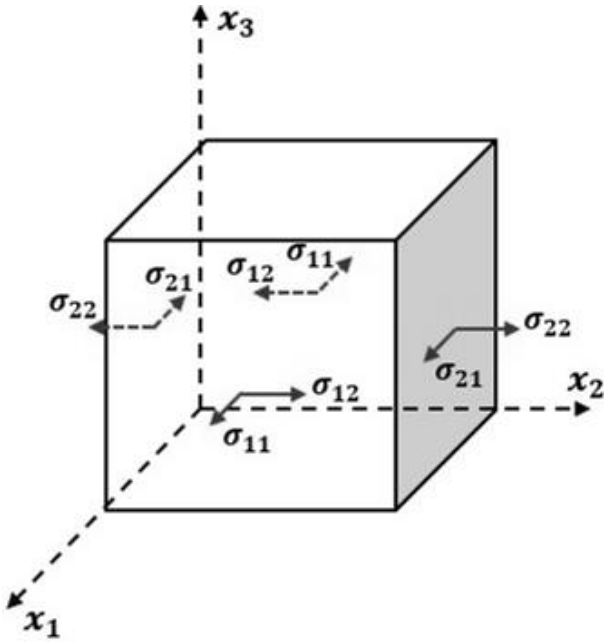

$$\boldsymbol{\sigma_{ij}} = \begin{pmatrix} \sigma_{11} & \sigma_{12} & 0 \\ \sigma_{21} & \sigma_{22} & 0 \\ 0 & 0 & 0 \end{pmatrix} = \begin{pmatrix} \sigma_{11} & \sigma_{12} \\ \sigma_{21} & \sigma_{22} \end{pmatrix} \tag{2.5}$$

Figure 2.5: Infinitesimal element with a plane stress assumption. Components of x_3 neglected

Another commonly used simplification, known as a biaxial stress state, further assumes that there are no shear stresses, thus the only stresses acting are the normal stresses in the x_1 and x_2 directions. When there are only normal stresses in one and three dimensions, this is known as a uniaxial and triaxial stress state, respectively. In these assumptions, the normal stresses are also the principal stresses, which will be seen later. The motivation for these assumptions is to simplify the stress state, for the easing of conceptual and mathematical handling.

2.1.4 Transformations and Principal Stresses

Although the state of stress at a point is an intrinsic property that does not change, the values of the stresses in the stress tensor change when a different orientation of the axes is chosen. A change in the axes' orientation involves a rotation by an angle θ. The original (plane stress) axes, x_1 and x_2, will be rotated to x_1' and x_2' (Figure 2.6). This causes a change in the stress values according to equation(s) (2.6), and therefore causes the transformation of the stress tensor.

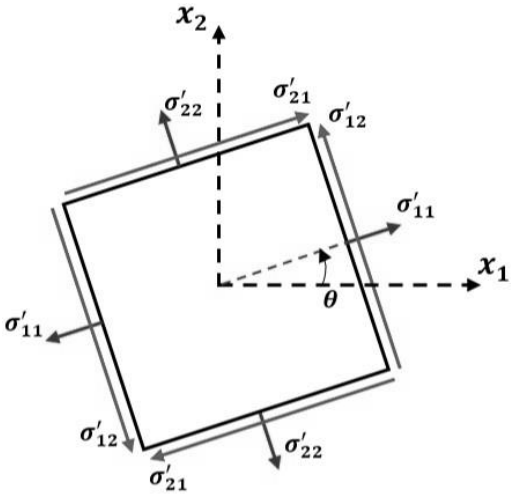

Figure 2.6: Rotated plane stress element

$$\sigma'_{11}, \sigma'_{22} = \frac{\sigma_{11} + \sigma_{22}}{2} \pm \frac{\sigma_{11} - \sigma_{22}}{2} \cos 2\theta \pm \sigma_{12} \sin 2\theta$$

$$\sigma'_{12} = \sigma'_{21} = -\frac{\sigma_{11} - \sigma_{22}}{2} \sin 2\theta + \sigma_{12} \cos 2\theta \quad \textbf{(2.6)}$$

It is subsequently logical that, for certain orientations of the axes, a normal stress will reach its maximum and minimum values, which are called principal stresses. For a particular normal stress, these can be found through the differentiation of the above equation. The result

of this procedure is equation (2.7) below, which calculates the principal angle θ_p for the principal stresses, σ_1(maximum) and σ_2(minimum). The maximum and minimum values are also known as the major and minor principal stresses, respectively.

The equation results in two values for θ_p which are 90^0 apart, hence orthogonal. This implies that, in plane stress, as one normal stress component reaches a maximum value, the other will be at the minimum value, as depicted in Figure 2.7. θ_p is used to find these values, and the resulting equation for the major and minor principal stresses is given in (2.8).

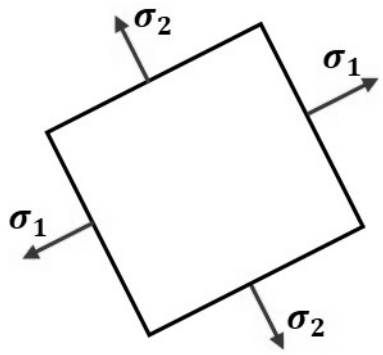

Figure 2.7: Principal stresses

$$\tan 2\theta_p = \frac{2\sigma_{12}}{\sigma_{11} - \sigma_{22}} \tag{2.7}$$

$$\sigma_{1,2} = \frac{\sigma_{11} + \sigma_{22}}{2} \pm \sqrt{\left(\frac{\sigma_{11} - \sigma_{22}}{2}\right)^2 + \sigma_{12}^2} \tag{2.8}$$

The principal orientation occurs when shear stresses are zero, thus for biaxial stress states, the normal stresses in the original orientation are already the principal stresses. This also holds true for uniaxial and triaxial stress states; the normal stresses are the principal stresses since there are no shear stresses present in these stress states.

The principal stresses above are for the in-plane stresses in a material, for example at the surface of a material, hence the element is rotating in that plane. If a normal stress is now included in the 3rd direction, it will be acting mutually perpendicularly to the other principal stresses by default, and hence this will become the 3rd principal stress, σ_3. By definition σ_1 is algebraically larger than σ_2, but σ_3 can take any value.

2.2 Material Properties and Standard Tests

The qualities of a material for selection are adjudged by means of standard material properties and parameters. These material properties are evaluated by means of standard tests, which perform identical operations on each material, to assess the relative material characteristics. This section will describe the material properties that are gleaned through two of the main standard tests: the tensile test, and hardness tests.

2.2.1 Tensile tests & Stress-strain curves

The most frequently used standard test, which evaluates the stress-strain characteristics of a material through stages of loading, is known as the tensile test. The practice involves applying a uniaxial stress to a bar of material, similarly to Figure 2.1, and measuring the resultant strain. The load and hence the stress, is gradually increased until the material fractures, with the strain measured at each step. The material properties are then defined according to the strain response to the increasing stress.

The strain response to the applied stress is constructed into the primary output of the tensile test, known as the stress-strain curve. The strain (ε) is placed on the x-axis and the stress (σ) is on the y-axis. The diagram charts the change in the relationship between stress and strain as the stress is increased gradually. An example of a stress-strain curve is given below in Figure 2.8, for aluminium.

The stress-strain curves for different materials will have different characteristics, but for the sake of the current discussion, the focus will remain on metal curves, particularly aluminium-type curves. The various stages of the curve form the basis for extracting material parameters.

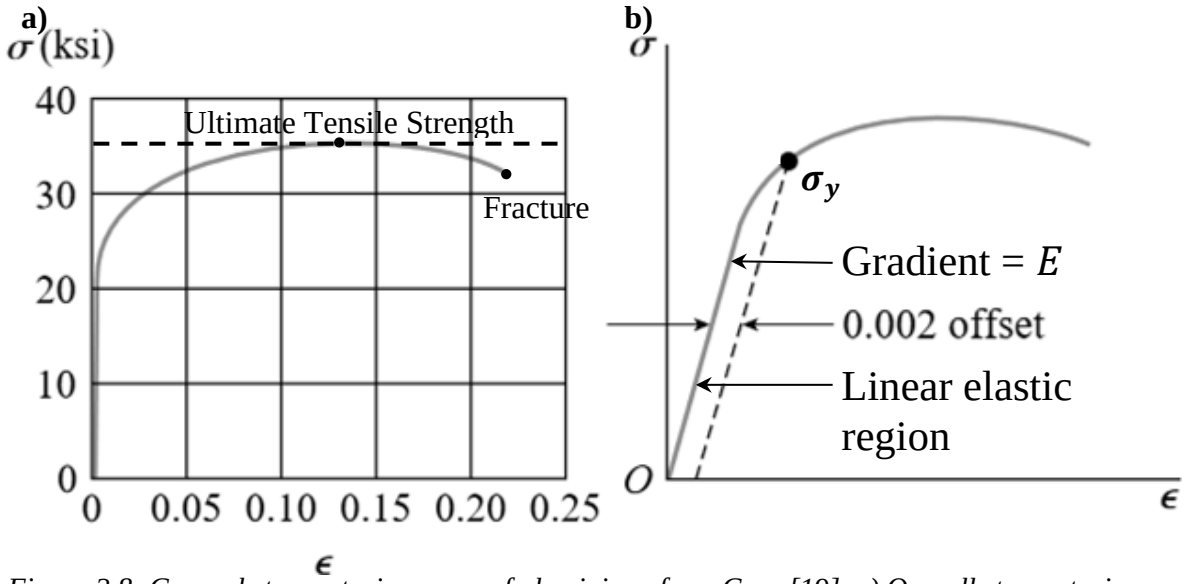

Figure 2.8: General stress-strain curves of aluminium, from Gere [19]. a) Overall stress strain curve showing ultimate tensile strength and fracture points, b) Not-to-scale curve to show linear elastic region and 0.002 offset convention for yield stress

The initial 'straight-line' region is known as the linear elastic region, governed by Hooke's Law. Hooke's Law states that for low stress values, the relation between stress and strain is linear and proportional, i.e. an increase in the stress will lead to a proportional increase in the amount of strain. In this region all of the deformation due to the stress will be elastic, i.e. reversible. The equation describing Hooke's Law in one dimension is given below in equation (2.9).

$$\sigma = E\varepsilon \tag{2.9}$$

The constant E, known as the modulus of elasticity or Young's modulus, is the first parameter obtained from the tensile test. It represents the gradient of the stress strain curve in the initial linear region and is the factor which connects the stress and strain in Hooke's Law. It will change depending on the material, with more ductile materials showing more strain for a particular increase in stress than stiffer materials. E can also be thought of as a measure of the stiffness, as it is analogous to the constant k in the force-displacement equation: $F = kx$.

The point at which the relation between stress and strain ceases to be elastic is known as the yield point or yield stress ($\sigma_y, S_y, Y, \sigma_0$) of the material. With elastic deformation, a removal of the applied stress will lead to the strain also returning to zero. After the yield point however, the deformation is no longer purely elastic, but instead a certain amount will be irreversibly plastic. When plastic deformation occurs, there will be a certain amount of strain that will permanently remain upon unloading and not all of the strain will be recovered. This is illustrated below in Figure 2.9.

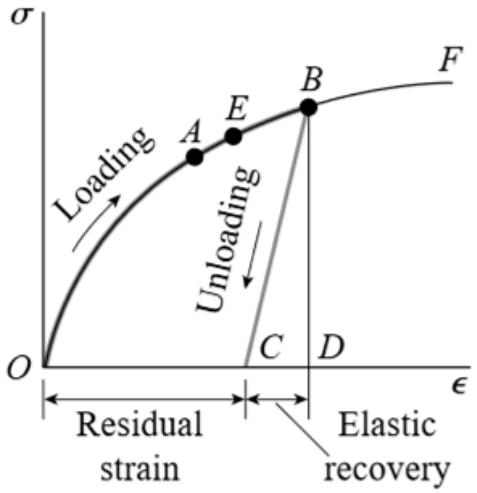

Figure 2.9: Example curve from Gere [19], showing permanent plastic strain upon unloading past yield point

The '0.002 offset' method is used to estimate the yield point of a smooth curve such as aluminium, as shown above in Figure 2.8 b). The yield point generally occurs around the point when the relationship between stress and strain is no longer linear. However, for smooth curves similar to the aluminium curve, it is not necessarily clear where this occurs. Therefore the '0.002 offset' method is usually employed; a straight line is drawn parallel to the initial linear part of the curve but starting at a strain of 0.002. The point at which this line intersects the stress-strain curve is taken as the yield point.

As the stress increases, the curve reaches a peak (Figure 2.8 a)), known as the ultimate tensile stress (UTS or σ_u). At this point, the material does not require any more increase in

stress to continue deforming in fact, it will continue to deform at lower stresses until it fractures, at which point the curve ends.

2.2.2 Mathematical approximations for stress-strain curves

Whilst the initial part of the stress-strain curve is related to Hooke's Law, the behaviour of the curve after the yield point is not clearly defined, therefore mathematical approximations are used. The curve after the yield point is in the plastic regime, the behaviour of which is not clearly known, and as such a clear relation such as Hooke's Law is not defined for the regime. Instead the general expected shape of the curve can be approximated mathematically through empirical observations.

The approximation can either choose to divide the curve into linear and non-linear segments and approximate each individually (Figure 2.10 a)), or instead approximate the curve in its entirety as one equation (Figure 2.10 b)) [11] [21]. Naturally, if one chooses to divide the curve, the linear portion would be approximated through Hooke's Law. The approximation will often form the relation using certain material parameters mentioned previously such as E and the yield stress.

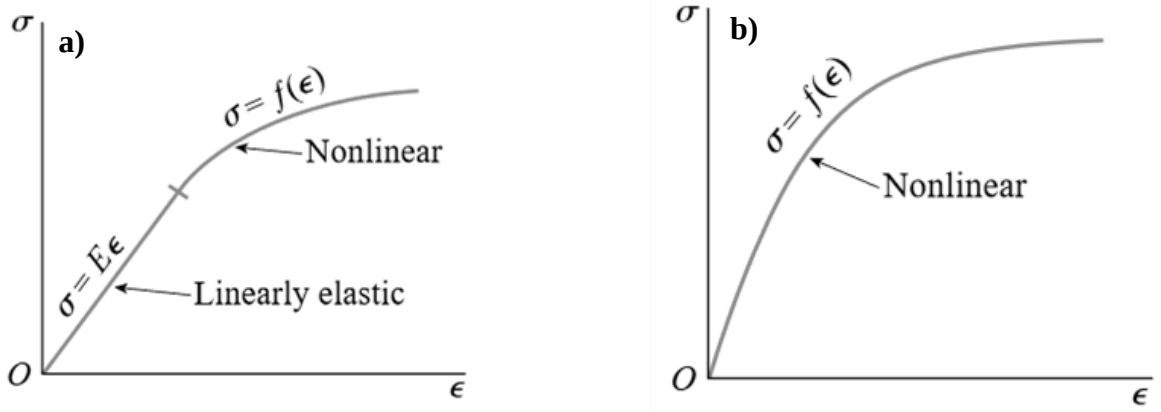

Figure 2.10: Examples of approximations of stress-strain curves, from Gere [19]. a) Divided curve, linear approximation followed by nonlinear after yield point, b) singular approximation of entire curve

In terms of simplicity, it would be preferable to approximate through a single equation, yet dividing the curve is likely to be more accurate, both theoretically and in terms of curve fitting. Theoretically, it appears more accurate to separate the approximations for the elastic

and plastic parts of the curve, as they occur through different processes, although they do occur simultaneously after the yield point. Additionally, there is an accepted theoretical relation for the linear portion, which is not the case for the non-linear section.

The most prominent empirically-derived approximation for stress-strain curves is known as the Ramberg-Osgood equation ((2.10)). Aside from stress and strain, the equation consists of material parameters: yield stress (σ_0), and modulus of elasticity (E). Additionally, fit parameters α and m describe the material's strain-hardening behaviour (more on strain hardening in Section 2.4).

$$\varepsilon = \frac{\sigma}{E} + \frac{\sigma_0 \alpha}{E}\left(\frac{\sigma}{\sigma_0}\right)^{m-1} \tag{2.10}$$

The Ramberg-Osgood equation is divided into two terms describing the linear and non-linear behaviour. The first term describes the linear behaviour, and as such is just Hooke's Law when taken on its own ($\varepsilon = \frac{\sigma}{E}$). The second term describes the non-linear behaviour after the yield point, therefore the stress used in the second term is relative to the yield stress (σ/σ_0). This use of the stress, along with the presence of the exponent, means that the second term will be small until the applied stress reaches the yield stress.

The advantage of the equation is that it would be able to incorporate both elastic and plastic deformation in the post-yield stage, but this leads to its disadvantage of including plastic strains in the elastic regime. The inclusion of the elastic and plastic terms in the equation is in accordance with expectations, as both deformation types occur after the yield point. However, before the yield point, the deformation should be purely elastic and although the second term will be small below the yield point, the equation does still imply plastic strains before yielding.

2.2.3 Hardness measurements

The hardness reflects “the ability of a body to counter the penetration of another body with a certain resistance” [22], and has multiple established tests for its measurement, each test having an associated ‘hardness number’. These include Vickers, Rockwell and Brinell, to name a few. This discussion will focus on the Brinell hardness, primarily due to the frequency of its use for aluminium alloys.

It has become standard practice to include hardness measurements in the data tables for a material. A standard data table for a particular material will include properties such as yield stress, ultimate tensile strength and modulus of elasticity, as gleaned from a tensile test, along with hardness measurements. These pieces of information are nearly always available in tables for most metals. In this way, it is useful to link any new parameters to the ones found in these standard tables.

Mainstream hardness measurements employ the use of indenters to impact the surface of materials and measure the resulting indentations to infer the hardness. The types of indenters vary between wedge, cone and ball-shaped indenters, to name a few. There are standardised sizes for the indenters and standardised forces applied to the indenters, depending on the type of test and the purpose. Different hardness tests will use different aspects of the indentation to form their hardness numbers.

The Brinell hardness test involves the indentation of the material surface with a spherical indenter, as shown in Figure 2.11 (from Herrmann) [22], which is subsequently removed and the surface area of the remaining permanent indentation is measured.

The Brinell hardness number is the force applied over the surface area of the indentation. The ‘force’ used is often in fact the mass and so denoted as ‘kilogram-force’. The equation for the Brinell hardness number, H_B, is given in equation (2.11) below (from Megson) [20], with d being the diameter of the indentation, and D being the diameter of the indenter.

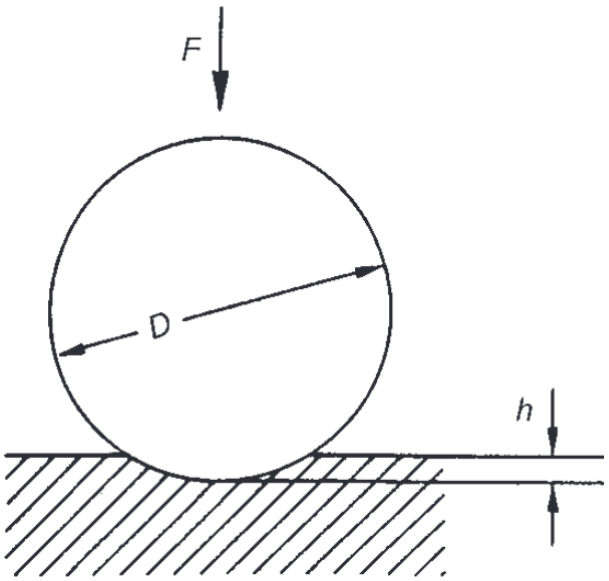

$$H_B = \frac{2F}{\pi D\left[D - \sqrt{D^2 - d^2}\right]} \quad \textbf{(2.11)}$$

Figure 2.11: Schematic diagram from Herrmann, showing Brinell hardness test [22]

2.3 Yielding & the von Mises Criterion

The yield stress or yield point has already been introduced in uniaxial tension as the point at which the deformation ceases to be purely elastic, but the focus now is on the definition of the yield point for more complex stress states. A three-dimensional stress state including shear stresses at a point would mean the criterion for yielding is no longer as simple as a single value, instead a yield criterion will depend on the combination of stresses. This section will describe the causes of yielding and will describe the formulation of the most commonly used yield criterion, the von Mises yield criterion [23].

2.3.1 Hydrostatic & Deviatoric stresses

Yielding and plastic deformation are considered to be driven by deviatoric stresses [24], hence the von Mises yield criterion is based upon the concept of deviatoric stresses. A given stress tensor can be divided into two components: the hydrostatic stress tensor, and the deviatoric stress tensor, as depicted below in Figure 2.12 from Rees [25].

Hydrostatic stresses are the portion of the overall stress tensor that cause a uniform deformation in all 3 directions. In other words, the hydrostatic stresses would cause a change in size, but not shape. The hydrostatic stress (σ_0) is then the mean of the three normal stresses.

If the original tensor is as shown in equation (2.4), then the hydrostatic stress is defined as in equation (2.12) below. The hydrostatic stress tensor is then as seen in equation (2.13).

$$\sigma_0 = \frac{1}{3}\sigma_{kk} = \frac{\sigma_{11} + \sigma_{22} + \sigma_{33}}{3}$$

(2.12)

$$\sigma_{ij}^0 = \begin{pmatrix} \sigma_0 & 0 & 0 \\ 0 & \sigma_0 & 0 \\ 0 & 0 & \sigma_0 \end{pmatrix}$$

(2.13)

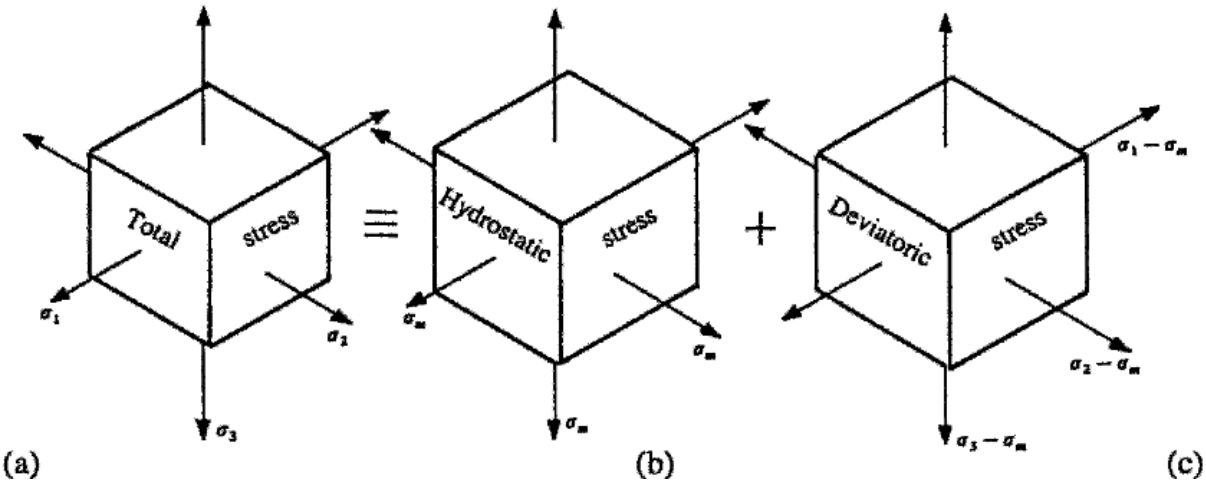

Figure 2.12: Figure from Rees, showing the breakdown of the a) total stress tensor into b) hydrostatic and c) deviatoric stresses for the triaxial case [25]

The deviatoric stresses are then the stresses which will cause a shape change, and as such the deviatoric stress tensor is defined as the overall stress tensor minus the hydrostatic stress tensor. Consequently, the deviatoric stress tensor would include both the parts of the normal stresses which would cause shape change, and the shear stresses present in the original tensor. Thus, if the original tensor (σ_{ij}) is as (2.4), then the deviatoric stress tensor, denotes as s_{ij} will be as equation (2.14).

$$s_{ij} = \sigma_{ij} - \sigma_{ij}^0 = \begin{pmatrix} \sigma_{11} - \sigma_0 & \sigma_{12} & \sigma_{13} \\ \sigma_{21} & \sigma_{22} - \sigma_0 & \sigma_{23} \\ \sigma_{31} & \sigma_{32} & \sigma_{33} - \sigma_0 \end{pmatrix}$$

(2.14)

2.3.2 von Mises yield surface & criterion

The basis of the von Mises yield criterion is that the hydrostatic stresses have no influence upon the yielding of the material, and it is the deviatoric stress which in fact leads to the yielding. This is nicely illustrated in geometric form in Figure 2.13, a commonly seen figure (in this case from Chakrabarty [24]) depicting the yield criterion in principal stress space. The arrow Q depicts a general stress state, and the arrows G and P represent the hydrostatic and deviatoric components of the stress state, respectively. The line H represents the hydrostatic axis, i.e. the hydrostatic components of various stress states.

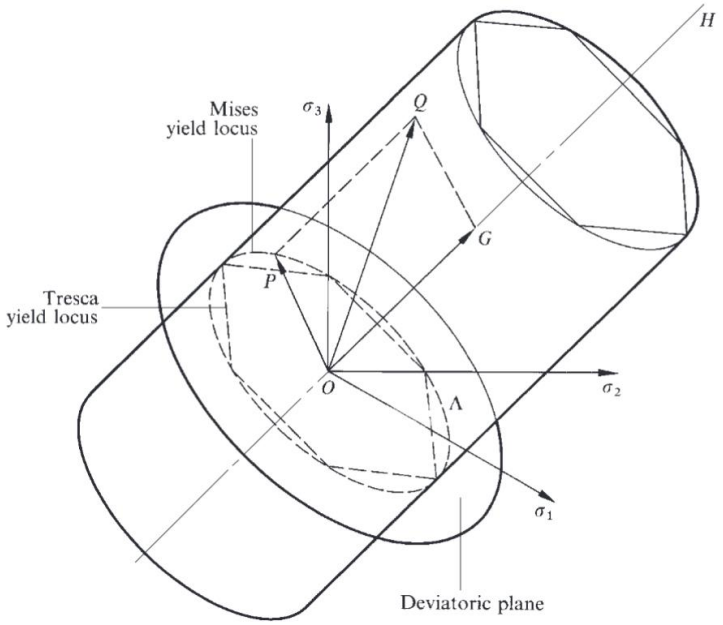

Figure 2.13: Figure from Chakrabarty [24], showing yield surface in principal stress space. Figure shows the 'hydrostatic line' H, and the deviatoric plane which cuts through.

Firstly, the diagram provides a useful portrayal of the extension of a yield criterion to three dimensions. In a single dimension a yield criterion is simply two points: the positive and negative yield stress value as seen in the tensile test, with a negative value corresponding to uniaxial compression. In two dimensions the criterion will take the form of a locus, and in three dimensions it will take the form of a surface such as the one depicted above. Stress states which are within the cylinder are in the elastic regime, stress states which have reached the surface of the cylinder are yielding (deforming plastically).

Secondly, it can be seen from the diagram that the hydrostatic stress has no effect on the yielding in this criterion. The hydrostatic axis is co-linear with the central axis of the cylinder representing the yield surface, hence no change in the hydrostatic stress will cause the stress state to reach the surface. The deviatoric component is perpendicular to the axis of the cylinder, hence a change will cause the stress state to reach the yield surface.

A key facet of the von Mises yield criterion is that a complex three-dimensional stress state is related to the yield stress in simple uniaxial loading, as shown in equation (2.15) [25]. This equation is one of the multiple formulations of the von Mises yield criterion; it makes use of the principal stresses of the stress state. This formulation is displayed because it is commonly used, and it is used in the development of the theory later in Chapter 4.

$$(\sigma_1 - \sigma_2)^2 + (\sigma_2 - \sigma_3)^2 + (\sigma_1 - \sigma_3)^2 = 2\sigma_y^2 \quad \textbf{(2.15)}$$

2.4 Plasticity & Strain-Hardening

Having established a yield criterion, it is pertinent to discuss the behaviour of a material that has entered the domain of plasticity. Plasticity is a complex field and it is difficult to clearly and completely describe a material's behaviour during plastic deformation. However, it is worth introducing a couple of useful concepts involved in plasticity.

2.4.1 Plastic deformation & True stress-strain curve

The key difference between elastic and plastic deformation is that they are caused by different mechanisms. Elastic deformation involves the stretching or compressing of the bonds between the atoms, but with the atoms staying in their original planes, therefore when the load is removed the atoms return to their original positions. On the other hand, plastic deformation is initiated by slip along a plane, causing a dislocation in the plane. The progression of plastic deformation is caused by the dislocations moving through the material. The dislocations in the

plane of atoms block the atoms from returning to their original positions, hence plastic deformation is irreversible.

The concept of true stresses and strains can prove to be important when in the plasticity domain. Thus far in stress-strain curves, they have been defined as in equations (2.1) and (2.2), where the stress and strain are defined according to the original area and length, respectively. These are called 'engineering' stresses and strains and are suitable for the linear region, as one does not expect noteworthy change in the cross-sectional area. In the plastic region however, the cross-sectional area can decrease significantly, leading to a true stress value that is incompatible with the engineering value.

The true stresses and strains are hence defined according to instantaneous values. The true stress σ_t is the load P applied divided by the 'current' cross-sectional area A_c, and the true strain ε_t is an integral value up to the 'current' length l of the bar. These definitions are given in equation (2.16) [26]. Practically, these are more complex to measure than in the simple tensile test, but they are useful theoretical tools.

$$\sigma_t = \frac{P}{A_c}, \qquad \varepsilon_t = \int_{l_0}^{l} \frac{dl}{l} \tag{2.16}$$

The true stress-strain curve is then naturally using the true stresses and strains, as shown in Figure 2.14. The curve appears in large part similar to the engineering stress-strain curve. An important difference however, can be seen when viewing the negative part. In compression, the curve would not be the same as in tension when using engineering values, due to the area changing inversely for each. In true stress-strain curves however, the curves for tension and compression can be considered the same.

The curve also shows the concept introduced already, of permanent strain upon unloading. After the material has been loaded past the yield point, when it is unloaded there is

an offset on the strain axis corresponding to the permanent plastic strain. Upon subsequent reloading of the material, the new path that is followed begins from the offset point (point E). The graph shows a slight mismatch between the unloading and reloading line, leading to a hysteresis loop. This type of behaviour can often be neglected, as it does not have a major effect.

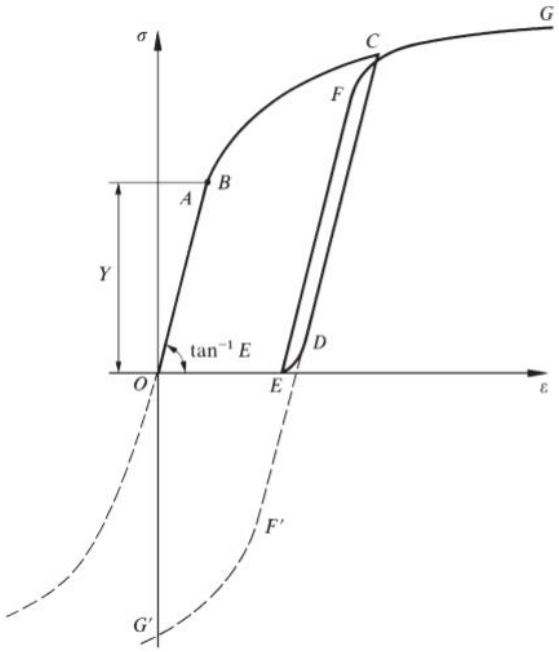

Figure 2.14: True stress-strain curve from Chakrabarty, showing unloading and reverse loading [24].

2.4.2 Strain-hardening curve & exponent

If the stress-strain curve of a material after the yield point is horizontal, such as in Figure 2.15 below, this is known as a perfectly plastic material. The plastic deformation being exhibited is also purely plastic, there is no elastic deformation occurring. The point to note here is that the stress-strain curves viewed thus far do not exhibit this behaviour; they are not perfectly plastic materials but rather strain-hardening materials.

A strain-hardening material is one that will increase its yield stress as a result of plastic deformation. A changing yield stress is often also called the 'flow stress', i.e. the stress required to keep the material flowing or plastically deforming. An increase would mean an increase in the applied stress would be necessary in order to continue plastic deformation. A perfectly

plastic material will not have a changing yield stress, hence once the yield stress is reached, the material will continue to deform without any additional increase in applied stress. In practice, this does not fully occur but there can be regions of perfectly plastic behaviour, prior to the material subsequently strain-hardening.

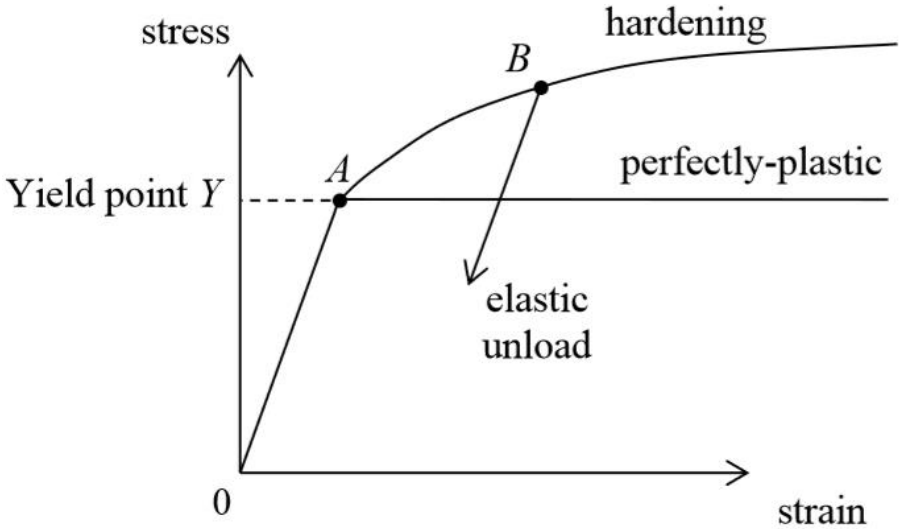

Figure 2.15: Stress-strain curve diagram from Kelly, showing difference in curves of perfectly-plastic and strain-hardening materials [26]

The increase of the yield stress can be observed when looking at reloading curves. In a strain-hardening material such as in Figure 2.14, when the material has been unloaded after plastic deformation, the subsequent reloading curve follows a linear path up to a new yield point (C). This point represents a significant increase in the yield stress (from A) due to the plastic deformation.

A noteworthy point about the curve is that the amount of stress increase required to induce a certain increase in strain reduces as higher values of strain are reached. This indicates that there is a limit to the strain-hardening, and at a certain point, the increase in stress required would be negligible to the point where it can be considered perfectly plastic. Hence, a heavily pre-strained material would not exhibit significant strain-hardening.

Strain hardening behaviour appears to follow a power law, therefore the strain-hardening region after the yield point has often been modelled mathematically for various

materials. A general equation to show the type of behaviour shows a simple power-law relation between the stress and the strain, as in equation (2.17). This equation is known as the Ludwik power law equation [24].

$$\sigma = C\varepsilon^{n} \tag{2.17}$$

The value of C and n are constants of the material. The value of n is key, it is known as the strain-hardening exponent. The value for n can be compared to the curves of Figure 2.15. If n is 0, this reflects a material with no strain-hardening, with a horizontal line after the yield point. A value of 1 for n will reflect a linear strain-hardening, with a straight line of gradient C.

There have been further equations developed to incorporate the strain-hardening exponent into more complex relations involving material parameters. A direct parallel can be drawn at this point to the previous equation introduced for approximating stress-strain curves, the Ramberg-Osgood equation (equation (2.10)).

It is indeed true that the Ramberg-Osgood equation is in essence an extension of the power-law equation, except that it models the entire curve, instead of simply the plastic portion. The Ramberg-Osgood curve is formulated as the strain as the function of the stress, and hence the exponent of the Ramberg-Osgood curve, m, can be related to the strain-hardening exponent as $m = \frac{1}{n}$.

2.4.3 Yield surface change & Bauschinger effect

The increase in the yield stress due to plastic deformation is in fact a changing of the yield surface. In the case of a static yield surface, a material will yield when the state of stress is on the yield surface/locus. As the yield surface doesn't change, it will remain on the surface, and hence keep yielding, reflecting perfectly plastic behaviour. In the case of strain-hardening however, when the state of stress reaches the yield surface and plastic deformation begins, the

plastic deformation induces a change in the yield surface, requiring a change in the stress state to continue yielding.

There are two main assumptions used for yield surface change, the first of which is a change in size, also known as isotropic hardening. Isotropic hardening is the equal increase in size in all directions of the yield surface. This means that the yield surface will only expand in size, maintaining the same shape and position. This can be viewed in Figure 2.16 for an arbitrary circular (in 2-D) yield surface, with the arrow representing the state of stress.

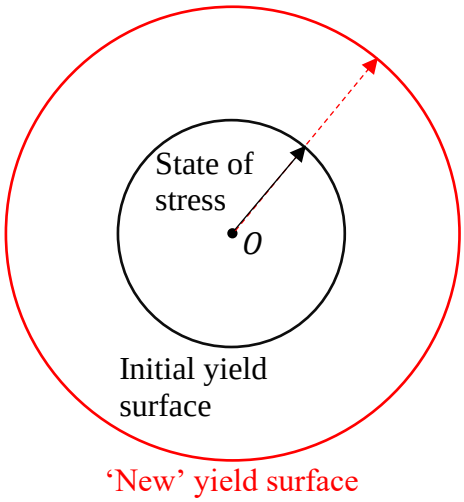

Figure 2.16: Figure showing change in yield surface for isotropic-hardening material

The other type of hardening, known as kinematic hardening, maintains the same yield surface but instead the surface will change in position according to the state of stress that induces yielding. Again, a change/increase in the stress state is required to reach the 'new' yield surface. This formulation is illustrated below in Figure 2.17.

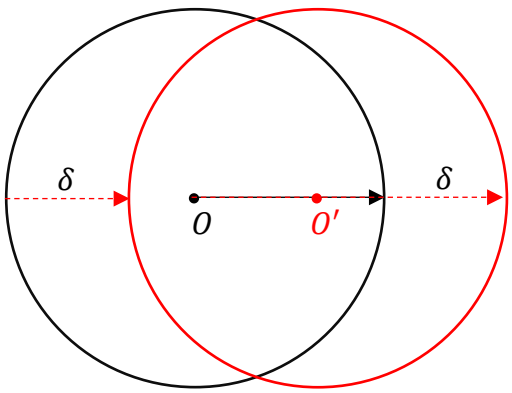

Figure 2.17: Figure showing change in yield surface for kinematic-hardening material

It is likely that both theories are too simple and the reality is some combination of both, which can be seen through observation of Figure 2.18, from Kelly [26]. In an isotropic-hardening case the increase in yield stress would be identical in both tension and compression, and in a kinematically-hardening case the increase in tensile yield stress would be mirrored by an equal decrease in the compressive yield stress. That the reality is somewhere in between serves to illustrate that neither is entirely correct.

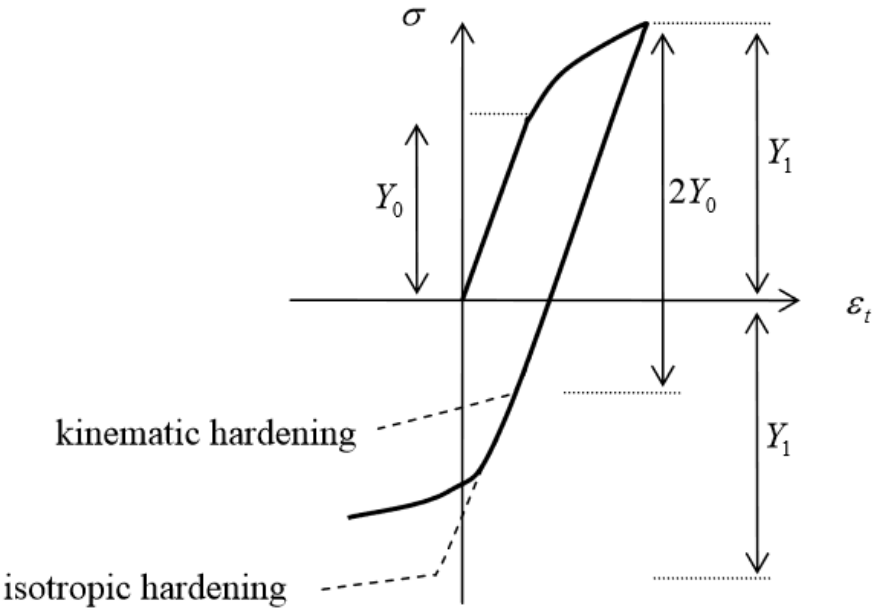

Figure 2.18: Stress-strain curve with reverse loading from Kelly [26], showing Bauschinger effect (solid line), in comparison with models of kinematic and isotropic hardening

The figure does show that strain-hardening in tension results in a lower yield stress in compression. This phenomenon is known as the Bauschinger effect, and has been attributed to various causes. It has been observed to occur in various real metals, such as copper and aluminium alloys [27] [28]. In order to accurately model the Bauschinger effect, hardening models would likely have to combine aspects of both kinematic and isotropic hardening.

2.5 Residual Stresses

The focus of this thesis is the concept of residual stresses which, unlike conventional stresses, continue to exist in a specimen in the absence of any external load. Hence, they are considered ‘locked-in’ stresses. It is important to understand the nature of residual stresses and how they form in order to measure them.

The nature of residual stresses is that they are ‘self-equilibrating’, meaning that since they exist in the absence of an external force or moment, the overall force and moment in a plane must equate to zero, as shown by equation (2.18) below [29]. In essence what this will mean is that localised areas of compressive residual stress will need to be balanced out by tensile stresses. Take for example a cross-section of a specimen. Often what is found is that the stresses at the surface are compressive, which are balanced by tensile stresses through the centre of the cross-section. Figure 2.19 below from Schajer illustrates this [3].

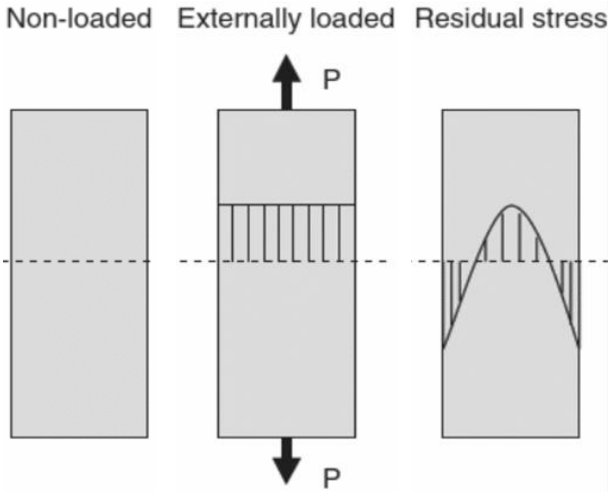

Figure 2.19: Diagram from Schajer, showing stress profiles at different states of loading [3]

$$\int \sigma dA = 0$$

$$\int \sigma z dA = 0 \qquad \textbf{(2.18)}$$

One of the main drivers behind residual stresses, especially mechanical, is incompatibility and “misfit strains”. Plastic deformation in materials is a producer of residual stresses. Plastic deformation is generally non-uniform and hence, when a part of a specimen deforms plastically, certain parts will attempt to unload elastically when the load is removed, but will be unable to fully unload due to the plastically deformed area, leading to localised areas of residual stresses.

The combination of plastic loading in certain regions of the material, with the attempted elastic unloading of the whole, results in residual stress profiles. This is nicely illustrated in Figure 2.20 below from Urriolagoitia-Sosa et al., which displays their method for the

estimation of the residual stress profile due to bending in a bar of material [30], by superimposing loading and elastic unloading.

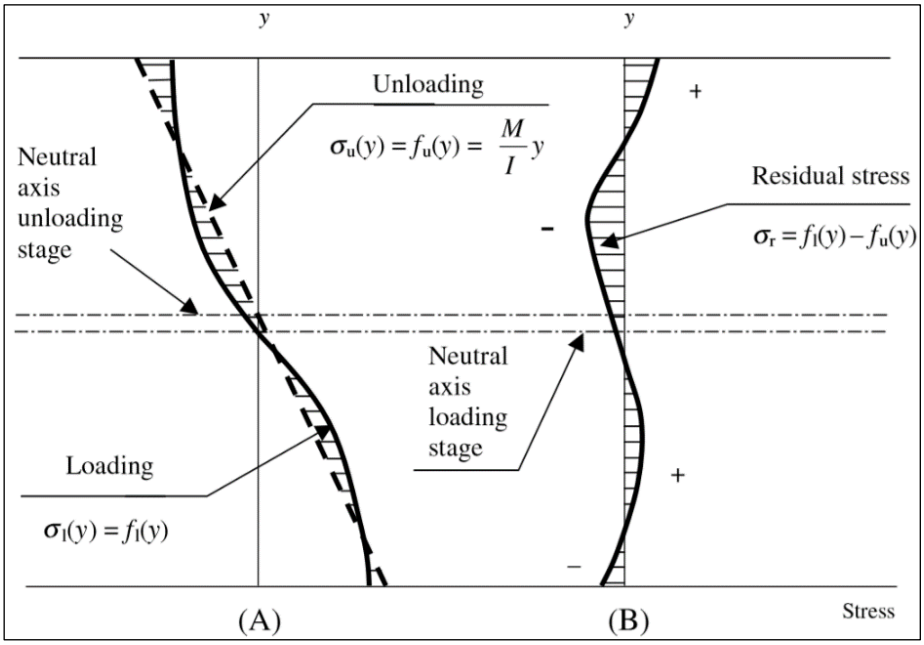

Figure 2.20: Figure from Urriolagoitia-Sosa et al., showing the procedure for their calculation of residual stress profiles due to bending, where (A) gives the loading and unloading curves, and (B) gives the calculated residual stress profile [30]

In addition, as seen in Figure 2.21, Su posited that a predominantly compressive loading would result in tensile residual stresses when the strain is returned to zero and vice-versa [31].

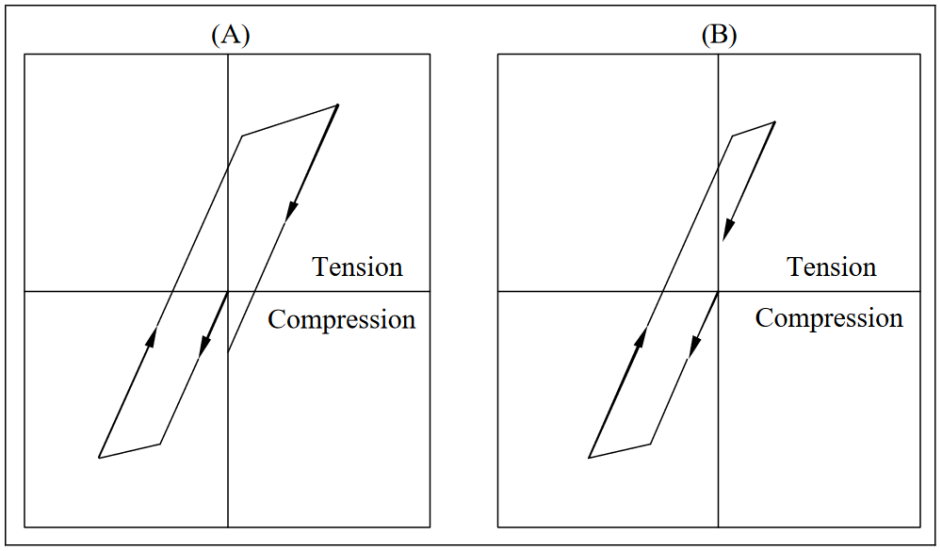

Figure 2.21: Figure from Su, showing their proposition for residual stresses left from loading history, (A) Predominantly tensile, (B) Predominantly compressive [31]

Residual stresses are often divided into three types, depending on the length scale over which they operate, and self-equilibrate. Type I do so over the largest distance, and are hence considered ‘macro’ residual stresses. According to Schajer, they “extend over distances from mm upwards” [3]. Type II residual stresses act over scales of the grain sizes, or between grains, and are hence ‘micro’ stresses. Type III stresses act over the smallest scales, generally at the atomic level.

3 Current Residual Stress Measurement Methods

There are methods already present which aim to directly measure the residual stresses, by observing their effects on the material or to their effects when the equilibrium is breached. This section will aim to first give a general overview of the three types of methods present and give a brief look into one of the key methods of each type, describing its procedure, advantages and drawbacks. Some alternatives will also be discussed briefly, and the suitability for the use of the method will be discussed.

3.1 Categories of methods

Since they exist in a system where there are no applied stresses, the residual stresses present in the material are in a state of equilibrium with themselves, and are hence, as put by Schajer [3], “locked-in”.

Furthermore, the need to exist in an equilibrium means that there are different local regions of residual stress, as the residual stresses need to balance out over the piece of material such that it remains in equilibrium. Hence, the nature of residual stresses makes them difficult to measure directly.

Instead their effects are measured and related to the stresses themselves. In order to achieve this, three types of residual stress measurement methods exist: non-destructive, semi-destructive, and destructive methods.

Non-destructive methods are ones that do not affect the state of the material at all in the process of measurement, semi-destructive methods involve a certain amount of damage to the material, but still keep the material usable.

Destructive methods essentially involve the total destruction of the piece of material (in terms of usability in service at least), and hence are more of an academic method. The various methods and their types are illustrated in Figure 3.1 from Rossini et al. [29].

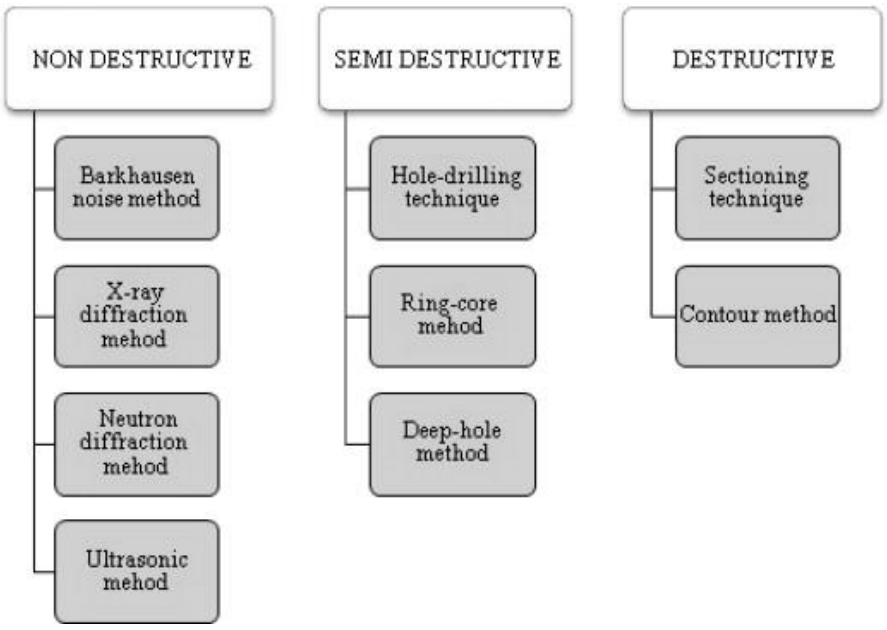

Figure 3.1: Chart from Rossini et al. [29], showing various categories of residual stress measurement, and the techniques within.

3.2 Non-Destructive Methods – X-Ray Diffraction

Non-destructive methods involve no damage to the material in question. Instead the non-destructive methods observe the effects of the presence of stresses in the material on certain types of waves. Primarily, non-destructive methods tend to be diffraction-based methods.

3.2.1 Overview of diffraction

The general theory of diffraction methods is that the presence of residual stresses will alter the spacing between planes of atoms, which are the strains. The strains present are used to calculate the residual stresses. X-ray diffraction (XRD), which tends to be the most oft-used method in residual stress measurement, measures strain in atomic planes through, as the name suggests, the diffraction of X-ray waves. This is illustrated in Figure 3.2 from He [32].

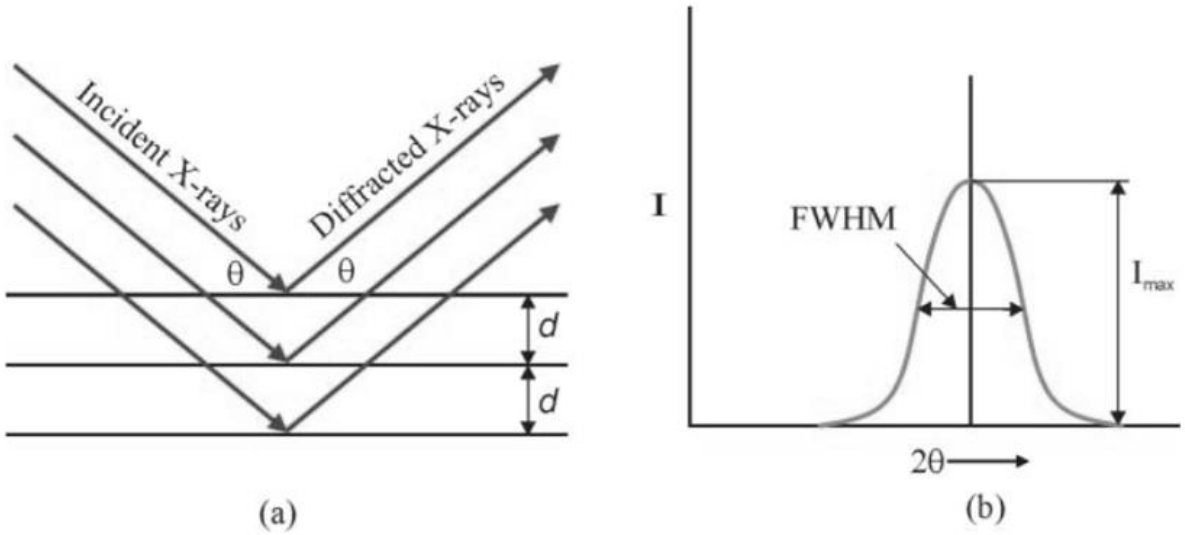

Figure 3.2: Figure from He [32], showing diffraction theory. a) incident vs. diffracted rays in planar lattice spacing d, and b) diffraction peak intensity vs. twice diffraction angle, θ.

The altered spacing will mean a shift in the position of the peak of the diffracted radiation, which constructively interferes with itself. The angle of the peak of the diffracted radiation is related to the planar spacing, therefore the change in the peak position is used with the Bragg's Law relation (equation (3.1)) to calculate the change in the planar spacing [29] [32]. Bragg's Law relates the wavelength of the incident radiation, λ, to the planar spacing and diffraction angle. This method will naturally require an initial measurement of the planar spacing in a 'stress-free' sample of material in order to identify the initial planar spacing.

$$n\lambda = 2d \sin\theta \tag{3.1}$$

3.2.2 Theory & Procedure

X-ray diffraction is a very commonly used method in the industry, due to its non-destructive nature, and its convenience with regard to portability. This makes it naturally useful for in-situ measurements, especially to assess the residual stresses in a final part. Its non-destructive nature makes it possible to measure a final part, as the measurement process will not affect the part in any way.

The basic outline of the X-ray diffraction method has been outlined above. The shift of the diffraction peak enables one to calculate the elastic strain, and subsequent stress. This method requires a 'zero' position for the diffraction peak, given that it is the shift in the diffraction peak that measures the strain.

There are therefore two potential ways to establish the 'zero' position. One can use data already present, collected from past experiments. This method is however subject to being able to obtain data for the exact material in question, and in any case may not fully reflect the material being used. The other way would be to establish the zero state for the same material by using a version of the material with all of the stresses released, i.e. at a zero-stress state. This would give a value for the diffraction peak position, and hence the lattice spacing in the absence of stresses.

A potential zero-stress state could be a fully annealed material, or a powdered version of the material where all of the stresses have been released [13]. Each will still have their issues, the annealing may not remove stresses, and the powdered form of the material may still have Type III stresses affecting the measurement. Nevertheless, it is useful to establish a zero-stress position to account for systematic error.

The procedure for X-ray diffraction measurement and calculation tends to be rather more complex than the simple outline given previously. There is not necessarily a need to describe in detail the mathematical manipulations required in calculating the strain from XRD, but a general view of the procedure would not go amiss.

The key issue in the X-ray diffraction measurement procedure is the orientation of the laboratory and the orientation of the sample. The illustration of the entire system is presented in Figure 3.3 below, from Schajer [3]. The 'S' axes represent the sample, and the 'L' axes the laboratory.

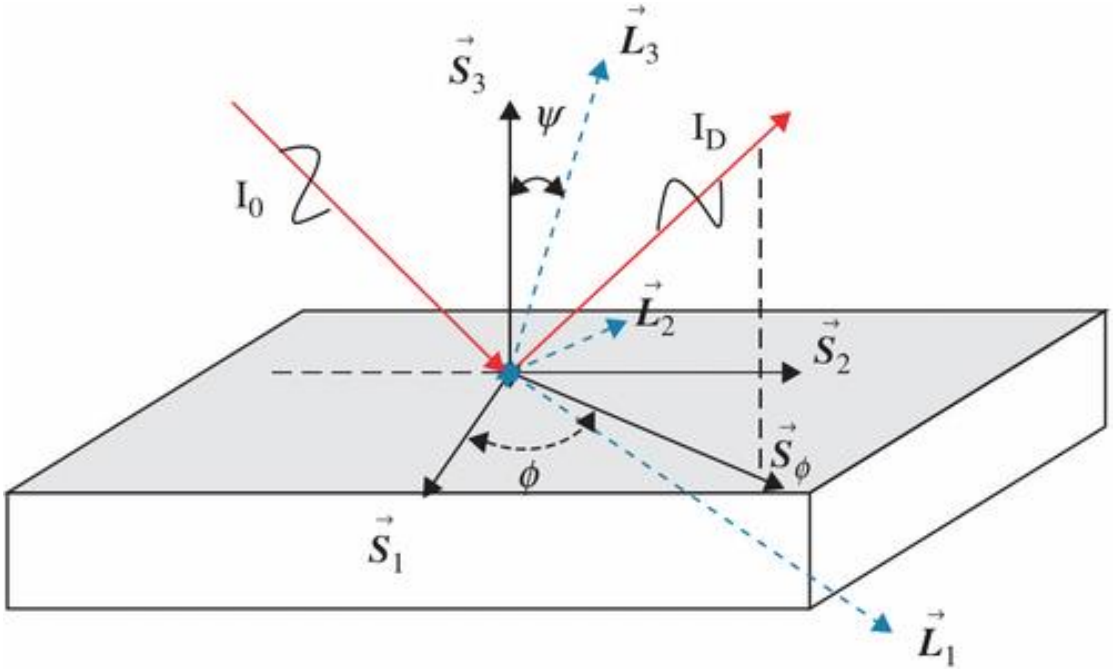

Figure 3.3: Schematic illustration of X-ray diffraction, from Schajer [3].

The angles that determine the orientation of the laboratory system in relation to the sample are ϕ and ψ. The atomic spacing $(d_{hkl})_{\phi\psi}$ is then found in the direction of the L_3 axis above, and the strain component in this direction is calculated using equation (3.2), with d_0 being the initial atomic spacing. Note that the primed term represents the laboratory frame [3].

The crystal upon which the incident beam acts must be orientated correctly for it to diffract. Nonetheless, there should be enough crystals in a small area for this to occur. X-ray diffraction in fact works on a small volume, and the values obtained are averages across the volume. In a crystalline material, each crystal will not be orientated in the same direction, and in the required direction for X-ray diffraction for a particular tilt of the beam, and for these crystals there will be no contribution to the diffraction peak, as shown in Figure 3.4 from Schajer [3]. With a variation of the tilts, the atomic spacing of different grains, which will only scatter at particular tilts can be obtained [3].

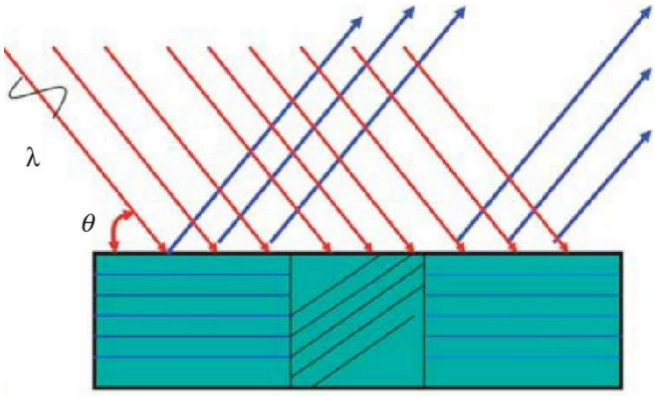

Figure 3.4: Schematic diagram from Schajer, showing that crystal grains at different orientations may not scatter [3]

$$(\varepsilon'_{33})_{\phi\psi} = \frac{(d_{hkl})_{\phi\psi} - d_0}{d_0} \tag{3.2}$$

The element of the stress tensor, ε'_{33}, in the laboratory frame can be subsequently be converted to a stress element in the stress tensor of the sample's frame of reference. This requires a tensor transformation, using a transformation matrix. In equation (3.3) below, the direction cosine matrix is given, which transforms between the laboratory frame and the sample's frame. Simultaneously, the expression for the tensor transformation between ε'_{33} and a strain element in the sample frame, ε_{kl}, is also given in equation (3.3) [3].

$$\varepsilon'_{33} = a_{3k}a_{3l}\varepsilon_{kl} \qquad a_{ik} = \begin{bmatrix} \cos\phi\cos\psi & \sin\phi\cos\psi & -\sin\psi \\ -\sin\phi & \cos\phi & 0 \\ \cos\phi\sin\psi & \sin\phi\sin\psi & \cos\psi \end{bmatrix} \tag{3.3}$$

The subsequent computation of the stresses from the strains above appears to make an assumption of elasticity for the residual stresses, as the calculation makes use of Hooke's Law, in tensor form as given in equation (3.4) below. The term C_{ijkl} is a fourth order tensor, known as the stiffness tensor, and is essentially an extension of the Young's modulus in three-dimensions.

$$\sigma_{ij} = C_{ijkl}\varepsilon_{kl} \tag{3.4}$$

There are naturally certain amounts of mathematical and statistical minutiae to deal with in real situations, apart from the simple procedure indicated here, but this suffices to give an overview of the process.

One of the key defining attributes of X-ray diffraction which make it favourable for in-situ use would be that it is an established method that has been around for a sufficient amount of time, and so firstly has established standards for operation, which clearly help in giving an element of consistency across various usages of the method [3]. This means that it has been used enough to be confident of its usability.

The method has also evolved such that it is able to be used in a portable sense, and so is helpful for use in-situ, without the need for transport to a facility. An example of the type of instrumentation used in modern X-ray diffraction is shown in Figure 3.5 below from Bunaciu [33].

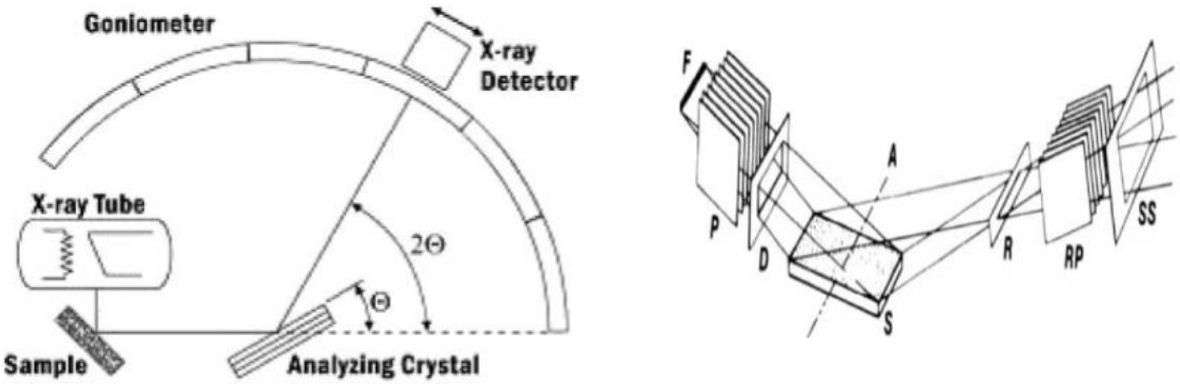

Figure 3.5: Schematic views of general X-ray diffractometers, from Bunaciu [33]

It has a certain amount of potential in terms of its analysis as well, particularly with the diffraction peak. The primary desired component of the diffraction peak is its position. However, the size and the width of the peak is also of interest in terms of analysis. The 'full-width half-maximum' of the peak as shown in Figure 3.2, has the potential to indicate the distribution of the stresses, as if the peak is wide, this would indicate a wide range of diffraction angles for the X-rays, and so the presence of a large range of strains and stresses.

Again, this can be compared to the ‘zero-stress’ case to weed out the inherent factors causing a widening of the peak. Through observing the increase in the width of the diffraction peak, the uniformity of the residual stresses can be analysed along with the simple value obtained through the observation of the shift in position.

The key drawback in X-ray diffraction is indeed, as mentioned earlier, the inability to penetrate too deep into the surface of a material, with Schajer stating that the depth at which stress evaluations can be performed with X-ray diffraction is 0.025mm. This essentially limits the usability to surface measurements. This is the trade-off one will have to make for a method that is entirely non-destructive and fairly portable.

These are the two areas that would likely have to be sacrificed in order to improve upon X-ray diffraction, and the alternatives do indeed have to sacrifice one of these. For example, the non-destructive methods that have been posited as alternatives, such as neutron and synchrotron diffraction, would have to sacrifice the portability (and cost) as they would require specialised facilities. The secondary alternatives would be the methods that cause damage to the specimen, the destructive methods.

3.2.3 Variants & Combinations

One of the key attractive qualities of X-ray diffraction is its ability to be used as a portion of, or in combination with other methods. For example, in the thesis by Spence, the author develops a framework for measuring the ‘stressed surface layer’ of a sample whose surface had been machined.

This framework makes use of a testing method which measures the curvature of the sample post-machining, and combines it with X-ray diffraction measurements of the machined surface to calculate the thickness of the stressed layer [13]. This type of combination of methods with X-ray diffraction is possible due to its non-invasive and non-destructive nature.

Interestingly enough, techniques have also cropped up which subvert the non-destructive nature of X-ray diffraction to a certain extent, in order to improve some other characteristics. An oft-used one in this regard is a semi-destructive variant of X-ray diffraction which employs the use of incremental material removal from the surface at which the X-ray diffraction measurement is performed. X-ray diffraction is then performed at increasing depths in order to characterise the residual stresses at increasing depths.

This method will require a correction, as the material layer removal itself will cause relaxation of stresses at the surface, hence the correction will need to take this into account in combination with the X-ray diffraction measurements at each depth level. The corrections themselves just make use of elasticity theory in calculation, as done by Moore & Evans [34].

A promising method for the estimation of the overall distribution of residual stresses, called the 'Eigenstrain Reconstruction Method' was posited by Jun & Korsunsky [35]. This method uses surface measurements of strain using X-ray diffraction, and combines it with their 'Eigenstrain Reconstruction' theoretical model in order to estimate the residual stress distribution.

These types of combinations of X-ray diffraction with other methods of determining residual stresses add another dimension to the favourable characteristics of X-ray diffraction as a method. Nevertheless, the more accurate residual stress measurements with X-ray diffraction often require some form of layer/material removal which affects the non-destructive nature.

3.2.4 Alternative diffraction methods

The general problem with X-ray diffraction tends to be the depth of penetration, hence the other diffraction methods present and used try to solve this issue by replacing X-rays with other types of radiation, which would be able to penetrate a piece of material.

The key alternative to X-ray diffraction in this regard would be neutron diffraction, which is able to penetrate much deeper into a piece of material. The issue with radiation that is able to penetrate significantly more would be availability and cost. For example, with neutron diffraction, access to a reactor may be necessary. Therefore it may likely not be possible to have a neutron source in the vicinity [29] [36].

Similarly, X-ray diffraction has also been used using synchrotron X-rays, which are able to attain much higher energies than simple X-rays, but once again would require the ability to use a synchrotron particle accelerator, which would certainly make it inconvenient, and unsuitable for quick, in-situ measurements of residual stresses [3].

An alternative to diffraction measurements, and one which has been gaining in popularity in recent times, is the ultrasonic method. In this method, rather than using diffraction of radiation, the use of sound waves is employed. This method makes use of the 'acoustoelastic' effect, which is the effect where the speed of an acoustic wave propagating through the material is altered by the presence of stresses in the material [3].

This method is relatively new but shows a lot of promise. The equipment required is convenient and cheap as compared to other non-destructive methods and is able to achieve a greater depth than regular X-ray diffraction. Additionally, as it does not involve radiation like the other methods, the dangers of resulting harm are decreased, leading to a decreased need for safety precautions. These factors make the ultrasonic method rather convenient for in-situ use in the measurement of residual stresses.

The disadvantages lie in the measurements returned, which tend to be bulk measurements over the volume. Moreover, this method will have limited resolution as the effect of the residual stresses on the acoustic wave is limited [29].

3.3 Semi-Destructive Methods – Hole Drilling

3.3.1 General overview

The semi-destructive techniques involve a certain infringement into the material, without necessarily compromising the overall piece of material entirely, especially in the case of large pieces. The semi-destructive techniques are mostly some variation of hole-drilling methods, which involve drilling a certain amount into the piece of material.

The introductory method here would be simply the hole-drilling method. As with most destructive and semi-destructive methods, hold-drilling involves measuring the reaction of the material to the disruption of the state of equilibrium.

In these cases, this involves mechanically 'damaging' the material to a certain extent, such that the equilibrium of the distribution of stresses is broken, and the material must adjust itself in order to re-establish the equilibrium. The readjustment of the material will take the form of a deformation at the location of the mechanical infringement. The measurement of the deformation (strain) can infer the original stresses present.

In the case of hole-drilling, this mechanical infringement is the drilling of a hole in a specified location where one desires to measure the residual stresses. The resulting deformation is measured using strain gauges, which are placed at certain angles around the hole, from which the x-y strains can be calculated. The general layout of this procedure can be viewed in Figure 3.6 a) from Schajer [3].

These strains can subsequently be used to determine the stresses originally existing in the material through Hooke's Law. Hole-drilling is one of the well-established methods of residual stress testing, and to this end it has a standard procedure for operation.

Along with X-ray diffraction, hole-drilling tends to be the most commonly used residual stress measurement method, and the most frequently used among the techniques involving damage. It has been in use for decades, and so also has a standard procedure for use, similarly

to X-ray diffraction. This lends a certain amount of trustworthiness to the method, as it is still in use and has been for such an extended period of time [3].

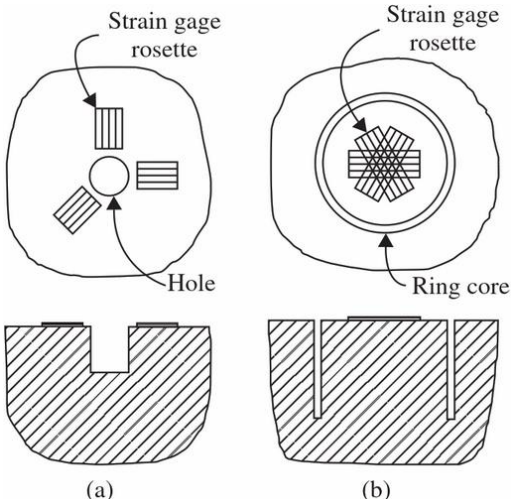

Figure 3.6: Figure from Schajer, showing layout of strain gauge rosette and hole in a) hole-drilling method, and b) ring-core method [3]

3.3.2 Theory & Procedure

Basic hole-drilling involves the use of strain-gauges to measure the deformation. In short, strain gauges are three electronic devices, placed upon the surface of a material in a certain orientation, which measure the strain by the change in the resistance of the electric circuit.

The strains at the orientation of the strain gauge 'rosette', as it is called, can be converted to the strains at the x-y orientation of the sample through transformation equations, in a similar manner to the calculation of principal stresses shown earlier in Section 2.1.4. The transformation equations for the three strain gauges in a rosette to the x-y strains are given in equation (3.5) below [37].

$$\varepsilon_a = \frac{\varepsilon_x + \varepsilon_y}{2} + \frac{\varepsilon_x - \varepsilon_y}{2}\cos 2\theta_a + \frac{\gamma_{xy}}{2}\sin 2\theta_a$$

$$\varepsilon_b = \frac{\varepsilon_x + \varepsilon_y}{2} + \frac{\varepsilon_x - \varepsilon_y}{2}\cos 2\theta_b + \frac{\gamma_{xy}}{2}\sin 2\theta_b$$

$$\varepsilon_c = \frac{\varepsilon_x + \varepsilon_y}{2} + \frac{\varepsilon_x - \varepsilon_y}{2}\cos 2\theta_c + \frac{\gamma_{xy}}{2}\sin 2\theta_c \quad \textbf{(3.5)}$$

In the equation above ε_a, ε_b, and ε_c are the three strains on the three gauges, and θ_a, θ_b and θ_c are their angles, as shown in Figure 3.7 [37]. These equations can then be solved simultaneously to derive the three unknowns, ε_x, ε_y, and γ_{xy}. The drilled hole results in the deformation of the area around the hole, which is picked up by the strain gauges, and from this the stresses are inferred. Strain gauges have certain standard angles at which they tend to be placed, for example at 0^0, 45^0, and 90^0 from the horizontal.

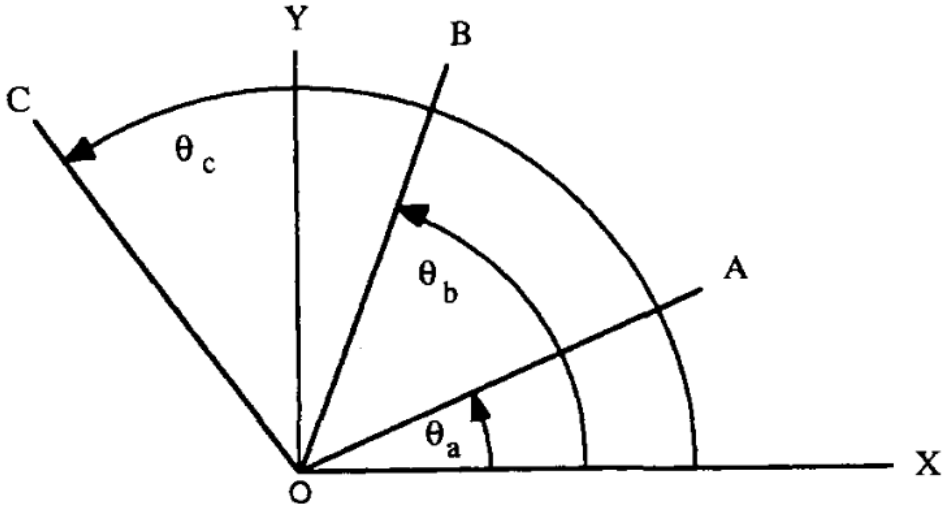

Figure 3.7: Diagram from Murray & Miller, showing angles of strain gauges in rosette [37]

The hole-drilling method using strain gauges has positive characteristics, which has led to it being one of the favoured and established methods for residual stress measurement over the years. The accuracy which modern strain gauges are able to attain plays a big part in this. According to Schajer, the strains associated with hole-drilling can be at the sub-mm strain level, hence the qualities of the modern strain gauge are crucial [3].

In addition, Schajer notes the "compact and portable" nature of the method, which correlates with expectation as strain gauges are readily available, and machinery to drill the holes should be present easily enough at a manufacturer or consumer who wishes to test the material [3]. This would make it rather convenient for in-situ use.

3.3.3 Variants & Alternatives

An interesting variant for the hole-drilling method, but one which compromises its portability somewhat, is the use of optical techniques to measure the strains caused by the hole-drilling [3]. This could be instrumentation such as interferometers, where an optical path difference is used to evaluate the strains present.

This would be as an alternative to the use of strain gauges, and the advantage it offers is a full map on the surface of the strains, rather than simply the strains in the orientations and locations of the gauges. This type of instrumentation would likely not be as portable as strain gauges, and thus the testing would have to be performed in an optical laboratory, which detracts from the convenience.

The primary variation that has cropped up for hole-drilling is the ring-core method. This is essentially a reversal of the hole drilling method. Where the hole-drilling method would drill a hole and place strain gauges around the hole, the ring-core method would drill a ring into the material, with the strain gauges then forming the rosette in the middle of the ring. The layout of the ring-core method in comparison to the hole-drilling is shown in Figure 3.6 b) from Schajer [3].

Given that the two methods are “mathematically identical” [3], the motivation behind the development and usage of the ring-core method as an alternative to the standard hole-drilling was that, as put by Schajer, “the ring-core method has the advantage of producing larger relieved strains and has superior capability to measure very large residual stresses close to the material yield stress” [3].

As is indicated by the figure above, the standard hole-drilling method and the ring-core method both seem to act fairly close to the surface. This is naturally a relative statement, since compared to X-ray diffraction, they would act rather deep in the surface.

Nevertheless, another evolution of the hole-drilling method was developed called the deep hole-drilling method, in order to evaluate the stresses locked deep inside a piece of material. This method involves drilling an initial 'pilot' hole and installing a strain cell in the hole created. The area near the hole is then further 'over-cored' or trepanned out, and the relaxed strains are measured [3] [29].

These tend to be the main methods of which one thinks regarding semi-destructive methods. There are naturally other semi-destructive methods involving various ways of systematically damaging the component and measuring the reaction.

An additional type of semi-destructive method, which was discussed in the previous section, is a variant on a non-destructive method, which is using X-ray diffraction but combining it with layer removal, such that measurements can be made deeper into the sample. This exists in a somewhat grey area for categorisation, as it is still a diffraction-based method, but simultaneously is a semi-destructive method.

3.4 Destructive Methods – Contour Method

3.4.1 General overview

The final type of residual stress measurement methods is destructive testing. Destructive testing also involves the releasing of residual stresses by mechanical material removal, and the subsequent measurement of the deformation. Depending on perception, and intended usage of parts, it is certainly possible that some 'semi-destructive' methods available could in fact be considered as being fully destructive. Nevertheless, the distinction is made between semi and fully destructive, where fully destructive involves more critical damage to a part in order to fully evaluate the stresses present.

In this regard, two main methods spring to mind: the sectioning technique and the contour method. Of these two, the sectioning technique can be considered the more destructive.

The contour method could perhaps still involve the future usability of the material, but that is an entirely subjective issue.

The fully destructive method that has been chosen for an in-depth review is the contour method. This is not particularly well-established, or necessarily widely used, however in the opinion of the author, it is interesting to view for its analytical capabilities.

As this is a fully destructive method in any case the convenience is already limited, as the part cannot be used after the technique has been performed. As such, one would expect the use of completely destructive methods to be mainly an exercise of gaining knowledge of the material and to which types of residual stress distributions certain processes will lead. In this regard, the contour method can provide plenty of insight.

The contour method will involve cutting a sample of material into two pieces, in order to evaluate the stresses in a cross-section. The sectioning method enables the user to measure the residual stresses parallel to the cut direction. In contrast, the contour method will measure the stresses perpendicular to the cut direction, in the cross-section [3]. It is a relatively new method, having only sprung up in the year 2000 [29].

The major advantage of the contour method is that it is able to provide an entire map of the residual stress distribution over a cross-section. The procedure works by cutting through a workpiece, after which the material at the surface of the cut will deform, again to maintain the equilibrium. This deformation is measured, then through the use of analytical equations and finite element methods, the residual stresses required to form such a deformation upon relaxation are computed. This gives a 2-D map of the stresses perpendicular to the cut surface.

This method would have a very high resolution and has a lot of potential for analysis [29]. The key problem with this method would be that the nature of the cut would mean that it is likely a singular process, and could not be repeated multiple times over the workpiece.

3.4.2 Theory & Procedure

The methodology appears fairly simple, albeit with some hefty calculations required, which can be done on a computer. The computation after measurement would be the most challenging aspect, as it would require the construction of a finite element model of the sample in question, and hence this would require an operator with significant expertise.

Aside from the computation, the main drawback here is the equipment required would not be easily portable [3]. The equipment would once again likely involve some kind of optical technique for measuring the deformation, and as such the convenience is not a great attribute for this technique.

The procedure of the contour method is simple enough to describe. A part with residual stresses within is cut in two. At the cross-section of the cut, the residual stresses will relax, and the part will deform. This deformation can be measured using an optical technique such as interferometry.

At this point the finite element analysis will begin: a finite element model of the part is created with constitutive equations describing the behaviour of the material in response to stresses, and the deformations measured will be used as displacement boundary condition inputs [3].

With this, the part can be analysed such that the finite element model will be able to calculate the stresses required to force the part into its original shape, and hence obtain the original stresses that were present. This approach uses the superposition principle, which is excellently illustrated in the diagram by Schajer in Figure 3.8 and equation (3.6) below.

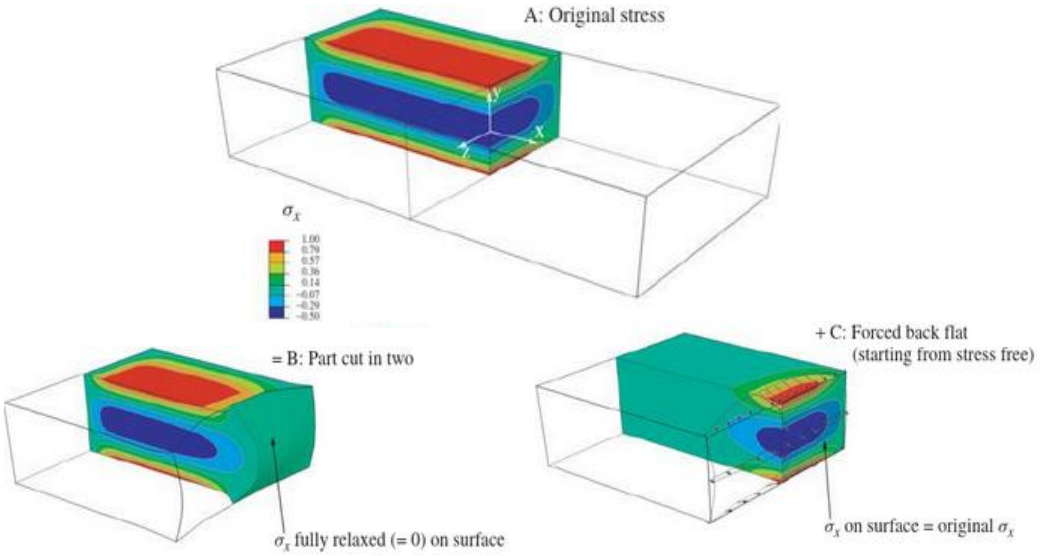

Figure 3.8: Diagram from Schajer, showing superposition principle for contour method [3]

$$\sigma^A(x,y,z) = \sigma^B(x,y,z) + \sigma^C(x,y,z) \quad \textbf{(3.6)}$$

The key issue with this technique is the inability to compute the shear stresses. The measurement of the cut surface will only be able to obtain the normal displacements and not the individual transverse displacements caused by shear stresses. The overall transverse displacement could perhaps be measured, however the individual transverse displacements contributing to the whole would not be known, and hence the distribution of the shear stresses would not be possible to obtain.

The reason that the individual normal displacements and stresses can be known despite any shear stresses and transverse displacements present is due to the averaging procedure that the contour method employs. Since the part will be cut in two, there will in fact be two cut surfaces upon which the measurements can be performed. Shear stresses will naturally need to act inversely on each surface in order to maintain the equilibrium. Therefore, as the measurements are averaged over the two cut surfaces, the shear effect will no longer be present, and the normal stresses can be calculated.

This also leads to more accurate normal stress values, as they are averaged over both surfaces, reducing error. Additionally, any lack of symmetry due to the cut not being perfectly

straight will also disappear as the surfaces are averaged. This is again illustrated nicely in Figure 3.9 below from Schajer [3].

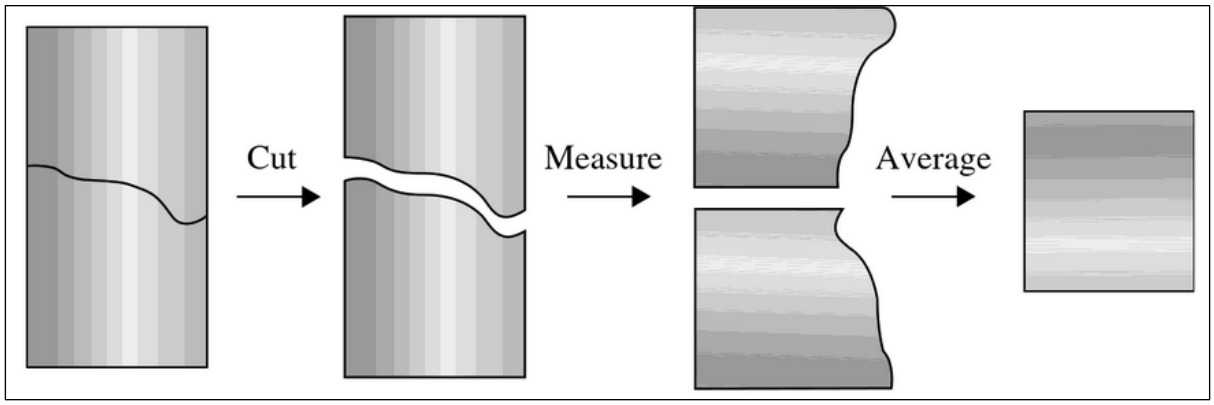

Figure 3.9: Figure from Schajer [3], showing how the averaging procedure in the contour method removes the problem of asymmetric cutting

The contour method additionally shows much promise with regards to potential for analysis. The fact that it is able to create an entire map of the cross-section leads to many possibilities as to how to analyse this map. As this is an entirely destructive process, the analysis becomes particularly important, as using the contour method would be most useful when attempting to gain information and knowledge about the materials and processes.

In the opinion of the author, one of the more interesting options would be to observe the patterns present in the distribution throughout the cross-section. This type of analysis could be performed across materials and processes, and in this way an idea could be gained as to what types of patterns are observed in particular materials and processes.

In terms of the analysis of the patterns being observed across a map of this type, the use of two-dimensional polynomial sets could well be useful. These are frequently used in optics, with Zernike polynomials being often employed to analyse interferometry maps on mirrors.

The Zernike polynomials use a system of polar coordinates which are useful for circular maps [38]. However, it will often be the case in materials that the part will be of a rectangular cross-section, and the subsequent map obtained using the contour method will also take a rectangular shape. It is therefore pertinent to use a set of two-dimensional polynomials which use rectangular coordinates.

There are a number of candidates for this purpose. In a paper titled *"Analyzing optics test data on rectangular apertures using 2-D Chebyshev polynomials",* Liu et al. extended a one-dimensional polynomial set, called the Chebyshev polynomials, to two dimensions, with fairly successful results [39].

This was done by multiplying the Chebyshev polynomials in each direction, in various combinations to obtain the two-dimensional Chebyshev polynomial set. The one-dimensional Chebyshev polynomials are defined by the recurrence relation shown in (3.7) from Clement [40].

$$T_0 = 1, \qquad T_1 = x$$

$$T_{n+1} = 2xT_n - T_{n-1}$$

(3.7)

The corresponding patterns associated with each polynomial in the two-dimensional set is shown in Figure 3.10 from Liu et al. [39]. As can be seen from the figure, the polynomial set can be used to describe a wide array of patterns, with higher order polynomials corresponding to more complex patterns.

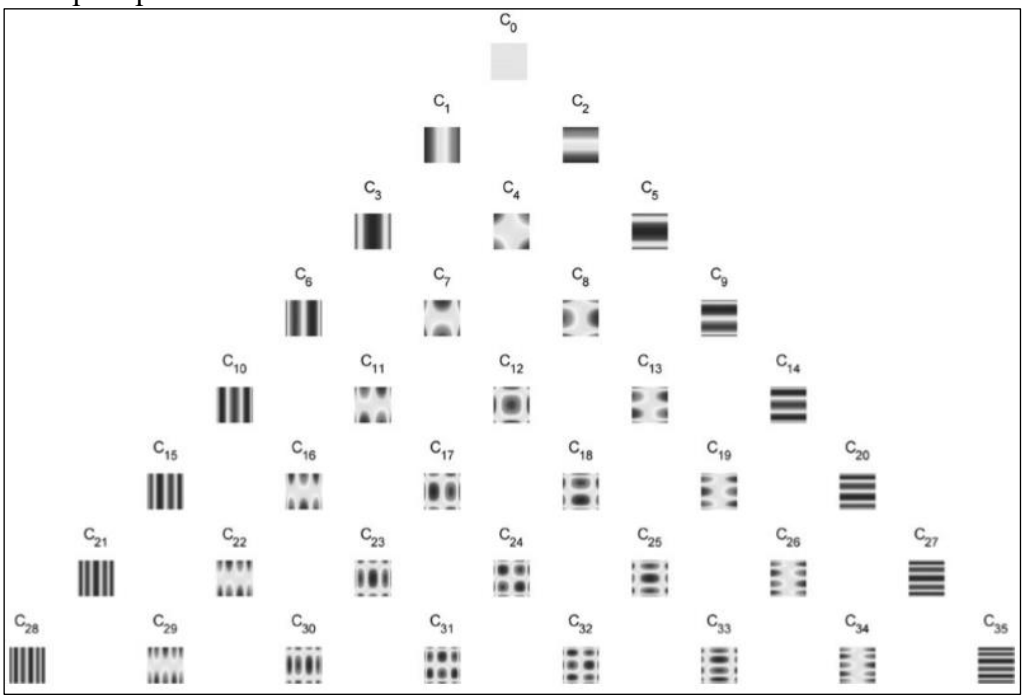

Figure 3.10: Figure from Liu, showing the patterns described by 2-D Chebyshev polynomials up to the 35th 2-D Chebyshev polynomial [39].

3.4.3 Alternative destructive methods

Alternative destructive methods to the contour method are of particular importance, as the contour method is relatively young, having only been introduced in 2000, and is therefore fairly untested in comparison to established methods such as X-ray diffraction and hole-drilling [3].

The main alternative destructive method being described here is the sectioning technique. The sectioning method is one that involves sequentially slicing 'longitudinal' strips of material from a piece of material, measuring the change in length, and inferring the original longitudinal stresses. The key assumption with this method is the assumption of negligible transverse stresses, which may prove a somewhat limiting factor [41]. The steps of the sectioning method are shown in Figure 3.11 from Tebedge [41].

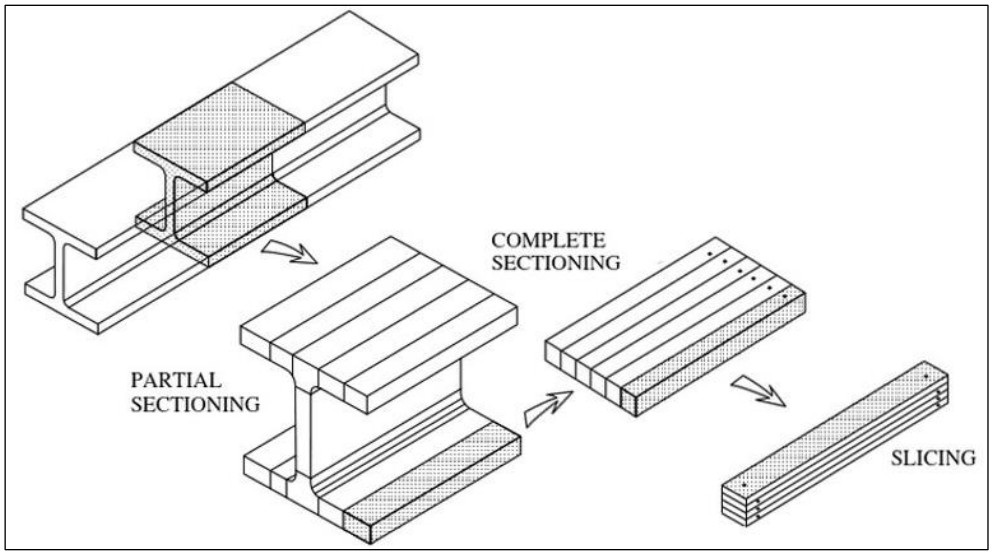

Figure 3.11: Diagram from Tebedge [41], showing sectioning procedure for an I-beam

3.5 Analysis of methods

3.5.1 Relative qualities of methods

Each of the posited methods above has their own merit, even simply due to each one's characterisation as destructive or non-destructive method. It is generally clear that the destructive methods will offer more in terms of quality of data, greater analytical capabilities, and more complete definitions of the stress.

X-ray diffraction offers the convenience of not having to damage the components and also has additional capabilities which the other methods cannot offer. Firstly, X-ray diffraction is completely repeatable; many measurements can be taken at multiple locations all across the sample. The only limiting factor in terms of geometry is the depth of penetration, as the X-rays can only really measure the surface stresses.

Secondly, the timing of the measurements is a crucial factor. With a damaging technique, the measurement must be performed before the part is in its final state, as at that point no more damage can come to it. X-ray diffraction has no such limitation, and so it can measure the residual stresses at the end of the production procedure.

This is especially key for precision components, given that the dimensions must be within a very small range, and hence it is unlikely a significant stress-relieving procedure can be performed at the end. Since the machining procedure will likely be one of the final steps in the production, and it is likely to introduce stresses at the machined surfaces, a capability to measure the stresses after the completion of the machining without causing damage becomes crucial.

Finally, as described before, the non-destructive nature of X-ray diffraction has enabled it to be combined to form a part of another larger technique for calculating residual stresses, or factors related to the residual stresses. In the PhD dissertation by Spence as described earlier, it performed both roles, measuring the residual stresses at the surface, with these values also being used in combination with the curvature to assess the thickness of the stressed layer at the surface caused by machining [13].

These factors make X-ray diffraction an attractive and versatile option, however the limitation caused by the lack of penetration of the X-rays makes the quality of data comparatively low, and the accuracy is affected due to this limitation. Nevertheless, it is a well-

established method with a standard operating procedure, and the equipment required is fairly readily available, hence this method remains a key one for these purposes.

The hole-drilling method takes up the middle ground in terms of destructiveness, but offers a decent amount in terms of data, and the quality thereof. The method has a certain amount of repeatability on a large piece of material, such that the measurement procedure of the previous attempt does not affect the subsequent measurement.

Its main advantage would be the data produced, it is able to obtain the full 2-D stress tensor for the plane stress state at a particular point (or more realistically small area), and hence is able to provide more detailed data than X-ray diffraction. It should theoretically also be usable on every face of a sample, provided the measurements are far enough apart.

This is also an established procedure, and has standard operating procedure, giving it a certain amount of reliability for use, and also makes use of fairly simple equipment, possibly more so than X-ray diffraction.

The drawbacks in comparison to X-ray diffraction would be in terms of its situational usability and its versatility. If the sample is small, the measurements cannot be repeated, and they cannot be taken at all at the end of the production of the part. The repeatability is additionally limited to a few attempts. It also does not have the ability to be combined with other methods as easily and readily as X-ray diffraction.

The data that is produced however, is rather good. The ability to obtain a 2-D stress tensor with shear stresses (and at multiple locations for a large part) is an attractive prospect, with the potential to build an idea of the distribution of the stresses.

Representing the destructive techniques is the contour method. It was chosen for its interesting nature with regards to analysis and quality of data. It should certainly be noted that, as stated before, this is a comparatively very young method, having only been introduced in 2000 [3].

Being an entirely destructive method, the strength of this method lies in the quality of the data. This method has essentially no repeatability hence is obviously not to be used at the end of the production. Additionally, the equipment required is not simple. The cutting procedure will need to be performed using wire EDM, in order not to cause stresses during cutting. The measurement of the contour will also require specialised instrumentation, and hence would need to be performed in a laboratory setting [3].

The data that is produced however, is of a high quality. Only normal stresses are obtained, as opposed to the shear stresses possible with hole-drilling, but these normal stresses are obtained over a whole cross-section, giving a detailed map of the stress distribution. This gives it not only detailed data, but at a depth into the material that is not obtainable for the other two methods described here. Naturally this will only be possible at a single cross-section of the material, yet it is still a high level of data.

Lastly, the potential for analysis is high, as described in Section 3.4. The possibility to be able to describe the patterns observed mathematically, and to then be potentially be able to link the results to materials or processes is attractive as an academic endeavour.

It can therefore be seen that each method is able to provide its own combination of benefits and shortcomings. It is up to the discretion of the user to decide which method is most beneficial for their particular situation, as it is unlikely that any one of the methods described above can be described as the ‘best’, and the value of each is dependent upon the state of affairs.

It is not necessarily the best approach to reduce the complexities of the offerings of each technique into a simple summary, but nonetheless Table 3.1 below attempts to summarise each method’s relative capabilities with regards to certain parameters, which had been described in the preceding paragraphs.

The parameters chosen as important were the data quality, simplicity and availability of equipment, repeatability of measurement, versatility of method, analytic capabilities,

situational usability (for example at end of production), and history of method. These characteristics may not cover everything a user finds important, but should hopefully provide a reasonable summary.

	Equipment	*Data quality*	*Repeatability*	*Versatility*	*Analytic capabilities*	*Usability*	*History*
X-ray diffraction	Simple, X-ray diffractometer	Low, surface measurement	Full	High	Reasonable, can use FWHM	Very high	Well-established
Hole-drilling	Simpler, drill & strain gauges	Fairly high	Some	Medium	Good, plane stress data	Mediocre	Well-established
Contour Method	More complex wire EDM & contour measurement	High, map of cross-section	None, unless large sample	Low	High, pattern observation of cross-section	Limited	Relatively new (2000)

Table 3.1: Table showing relative qualities of the three methods for various characteristics

4 Theory of Method

This section will describe the theoretical formulation of the relation between hardness and residual stress, with the aim of using this relation to infer residual stresses through hardness measurements. The relationship between hardness and residual stress in literature is explored, using a relation derived by Frankel et al. [5].

This is first modified through a simple assumption of the stress state, to obtain a simple relation in rectangular coordinates. This relation is used in comparison with observations from literature on the relationship between hardness and yield stress, to provide a justification for the use of the basic methodology.

After the justification of the basic relation, a more complex stress state assumption is used to modify the Frankel et al. model, leading to a more complete final relation describing the hardness-residual stress connection.

Subsequently, a rough proposal is presented to describe methods of obtaining the parameters required for the use of the final relation, along with ideas for the implementation of the theory. Finally, an analysis of the final relation is presented; the suitability, qualities and limitations of the relation are examined.

This relation is later tested in MATLAB through the testing of the various parameters involved. A discussion is then presented about the results.

4.1 Initial Hardness-Residual stress relation

One of the key ideas of this project was that the residual stresses present in a specimen would affect the hardness number measured. This effect had long been observed and suspected in the past [5] [4]. The purpose was therefore to obtain a quantitative relation for this effect through literature study, with the goal of being able to use hardness measurements in order to infer or estimate the residual stress state in the material.

The general observation seems to be that compressive residual stresses would increase the hardness, and tensile residual stresses would have the inverse effect. This was supported theoretically by Tsui et al. by means of the diagram in Figure 4.1, for uniaxial residual stresses [4]. The figure displays the effect on the maximum shear stress, which govern plastic deformation and in turn affect the hardness.

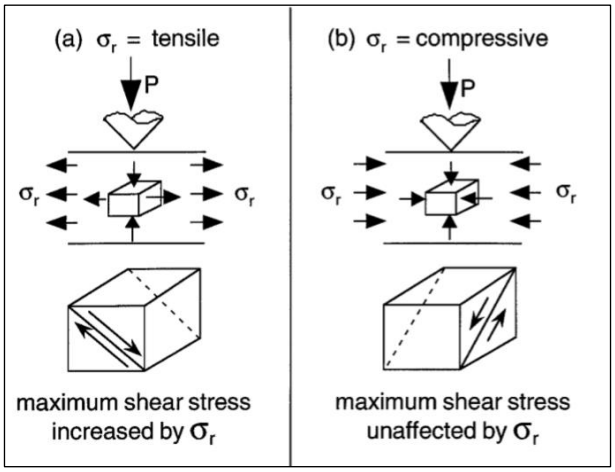

Figure 4.1: Effect of applied stress on the maximum shear stress, and hence hardness [4]

The strength of the observed effect was not particularly striking; the paper by Tsui et al. showed a roughly 20% effect of the residual stresses on the hardness. Nevertheless, the potential was there to exploit the effect to try to measure the residual stresses.

In their paper, Frankel et al. developed a semi-empirical equation attempting to describe how these residual stresses would affect the hardness value, by linking the stresses to the criterion describing the onset of yielding. The method presented in this thesis will base itself on their findings but will subsequently make modifications to suit purposes.

4.1.1 Theoretical formulation from literature

The methodology proposed by Frankel et al. used a simple measure of hardness known as the Meyer hardness number [42]. Meyer hardness is a measurement of the mean pressure applied by an indenter which, for the purposes of the theory in the Frankel paper, was a spherical one. Consequently, the Meyer number is the load applied divided by the projected

area of the indentation, leading to equation (4.1) below. P_m is the mean pressure or Meyer hardness, W is the load applied, and d is the diameter of the indentation.

$$P_m = \frac{4W}{\pi d^2}$$

(4.1)

The paper goes on to describe the state of stress at an element at the indenter tip, shown in Figure 4.2 a). Since this paper required cylinder stresses, the stresses used were the circumferential 'hoop' stresses and radial stresses, σ_H and σ_R. The Frankel et al. paper states that "this figure is adapted from the one given without residual stresses by Shaw, Hoshi and Henry" [43].

The reference paper by Shaw, Hoshi and Henry could not be viewed, however given the explanation provided by Frankel et al., the state of stress due to the indenter would appear to be the state of stress shown in the Frankel paper (Figure 4.2 a)), but in the absence of the in-plane residual stress components, σ_H and σ_R. The original state of stress due to the indenter at its tip would subsequently correspond to Figure 4.2 b). Frankel et al. state this "relates to the situation in which the load W is still applied but the deformation has stopped" [5].

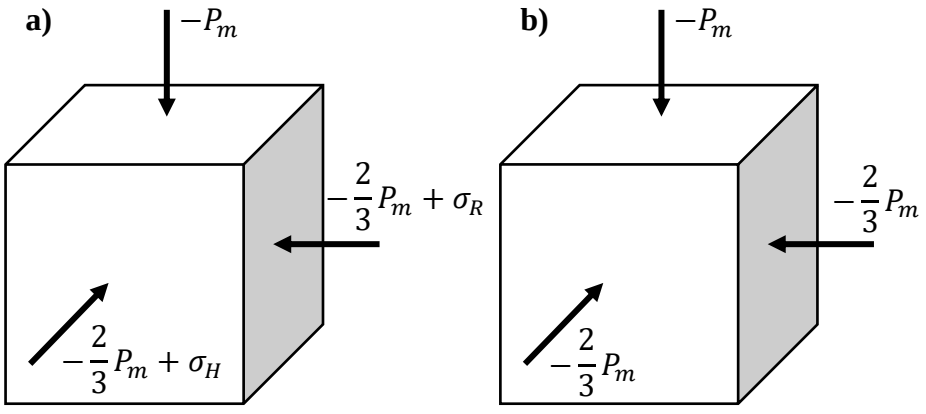

Figure 4.2: Element showing state of stress at indenter tip. a) State of stress shown in Frankel et al. paper [5], and b) presumed original state of stress without residual stresses from Shaw, Hoshi and Henry [43], which was used by Frankel et al.

A note on the direction of the arrows and signs, which are depicted in Figure 4.2 as they were in the Frankel et al. paper. However, the signs are negative for P_m, suggesting that the mean pressure is tensile. It seems though, that in the use of the values in the von Mises criterion (equation (2.15)), they are indeed negative, and so compressive. This is the theoretically logical way to think of it, as one would expect an indenter to apply a compressive stress. The depiction shown above was likely just an attempt to illustrate the direction of the pressure applied, which causes confusion when combined with a negative value shown for P_m.

The paper makes use of the three stresses as shown in Figure 4.2 a) as the principal stresses in the von Mises yield criterion. This implies that the stress state due to the indenter (Figure 4.2 b)) is a triaxial stress state, to which the biaxial in-plane residual stresses are added. The full stress state in Figure 4.2 a) is therefore also triaxial, without shear stresses, which would make the stresses in the diagram the principal stresses.

As opposed to the source paper, the requirement here is to include the in-plane residual stresses in rectangular (x-y) coordinates. Following the same procedure as the Frankel et al. paper, biaxial in-plane residual stresses are added to the triaxial stress state in Figure 4.2 b), except the residual stresses are in rectangular coordinates.

As an initial step, the biaxial residual stress state used is an equi-biaxial stress state. This formulation was obtained from a paper by Lee & Kwon, and details a plane-stress state where the two normal stresses have the same value, σ_{res} [6]. There are no shear stresses, as this is a biaxial stress state, therefore the stress tensor representing the assumed residual stress state is given in equation (4.2) below.

$$\sigma^{res} = \begin{pmatrix} \sigma_{res} & 0 & 0 \\ 0 & \sigma_{res} & 0 \\ 0 & 0 & 0 \end{pmatrix} \tag{4.2}$$

This is naturally a rather simple state of stress; however, it suffices for the first step. Now, the overall state of stress at the tip is the sum of the stress states in Figure 4.2 b) and equation (4.2). The overall stress tensor that will be used initially is given in equation (4.3).

$$\sigma = \begin{pmatrix} \sigma_{res} - \frac{2}{3}P_m & 0 & 0 \\ 0 & \sigma_{res} - \frac{2}{3}P_m & 0 \\ 0 & 0 & -P_m \end{pmatrix}$$

(4.3)

Following the procedure of Frankel et al., the stress state above is used as in input into the von Mises yield criterion, in order to obtain the limiting value for P_m which would cause yielding. As a recap, the von Mises yield criterion is defined, for the principal stresses, as equation (4.4). σ_y is the yield stress of the material, σ_{1-3} represent the three principal stresses. In the triaxial stress state of equation (4.3), the stresses are the principal stresses, therefore σ_{1-3} are defined as in equation (4.5).

$$(\sigma_1 - \sigma_2)^2 + (\sigma_2 - \sigma_3)^2 + (\sigma_3 - \sigma_1)^2 = 2\sigma_y^2$$

(4.4)

$$\sigma_1 = \sigma_2 = \sigma_{res} - \frac{2}{3}P_m$$

$$\sigma_3 = -P_m$$

(4.5)

Inputting these principal stress values into the von Mises equation leads to the derivation to the point shown in equation(s) (4.6).

$$2\sigma_y^2 = \left(\sigma_{res} + \frac{1}{3}P_m\right)^2 + \left(-\sigma_{res} - \frac{1}{3}P_m\right)^2$$

$$\cancel{2}\sigma_y^2 = \cancel{2}\left(\sigma_{res} + \frac{1}{3}P_m\right)^2$$

(4.6)

Due to the root, there are two possible solutions for the above equation, depending on whether one chooses the positive or negative root. The solution from positive root is shown below in equation (4.7), with the solution from the negative root being the same but with a $-\sigma_y$.

$$P_m = 3\left(\sigma_y - \sigma_{res}\right) \tag{4.7}$$

At this point a couple of assumptions and limitations need to be made regarding the usability, the first of which is that only the solution corresponding to the positive root should be used. As the hardness in reality does not seem to depend on whether the yield stress is compressive or tensile (as will be seen later), the positive root should be utilised.

Secondly, it must be assumed that the residual stresses are elastic, i.e. below the nominal yield stress. While higher values of residual stress may be possible in reality, this would likely require localised strain-hardening and hence a higher localised value for the yield stress (since P_m cannot be negative). This is difficult to incorporate into the relation, and so it would instead be pertinent to limit the usability of the relation to elastic residual stresses.

4.1.2 Justification with Hardness-Yield stress relationship

The formulation of the relation in equation (4.7), shared a certain similarity with the existing relation between hardness and yield stress, and it is logical that the residual stresses are affecting this relationship. Ergo, the comparison between equation (4.7) and the hardness-yield relation provides a good basis for analysis of the methodology.

There is a well-established relationship between the hardness of a material and its yield stress, even before empirical evidence had been obtained. Seeing as the hardness of a material is defined as its ability to resist plastic deformation, it is natural that its yield stress reflects the hardness value.

Tabor conducted experiments on materials and formulated a relation between the mean pressure applied to the yield stress, Y, of the material [7]. He found that, to a first approximation, the relation could be presented as equation (4.8), where the constant c was around 3.

$$P_m = cY \tag{4.8}$$

The constant factor of 3 matches the factor of 3 in equation (4.7), which provides encouragement. Additionally, the tests were conducted for different metals, with the results remaining fairly consistent, lending support to the usability of the relation. The results for three of the metals - tellurium lead, copper and mild steel – are shown below in Table 4.1.

Metal	*Y (kg/mm^2)*	*P_m (kg/mm^2)*	*Ratio (P_m/Y)*
Tellurium lead	2.1	6.1	2.9
Copper	31	88	2.8
Mild Steel	65	190	2.8

Table 4.1: Table from Tabor, showing experimental results for ratio of mean pressure and yield stress [7]

The results of Tabor are partly supplemented by those of Tiryakioğlu et al., when they tested the aluminium alloy 7010 [8]. They preselected a value of **2.82** for c to fit their data, and found that this value provided an excellent fit. They also noted however, that the line did not pass through the origin and had an offset, which was attributed to strain-hardening occurring due to the indentation process.

There is, to a certain extent, some further support for the general form of equation (4.7), provided in a paper by Swadener et al. [9]. They note (as did Tabor) that in the initial stages of plastic deformation and yielding, the factor c is around 1.07. Swadener et al. use this factor, and then introduce residual stresses into the formulation. They state that, for a biaxial residual stress present in the material, σ^R, the yield condition is given by equation (4.9) below, stating also that σ^R is positive for tension and negative for compression [9].

$$p_m = 1.07(\sigma_y - \sigma^R) \tag{4.9}$$

The value of around 1.1 is related to the beginning of plastic deformation during indentation, with the value of 3 being when there is a large region of plasticity covering the area around the indentation [7]. Tabor states that "This transition in the value of P_m from $1.1Y$ to about $3Y$ is part of the intrinsic mechanism of plastic deformation and is distinct from the effects produced by work-hardening" [7].

It is likely the value of 1.07 was employed due to the use of nanoindentation, hence they were using low loads and observing the onset of plastic deformation. The set-up described by Frankel et al. appeared to be for a standard hardness test, and "relates to the situation in which the load W is still applied but the deformation has stopped" [5]. Therefore, the value of 3 in this case appears reasonable.

Howlader et al. suggest that the yield stress is affected by the residual stress: "changes of the mechanical properties depend mainly on the magnitude of residual stresses" [44]. The same mechanism that increases the yield stress, strain-hardening due to plastic deformation, also generates residual stresses. The residual stresses are known to be linked to the plastic deformation of a material, due to a misfit strain existing between the part of the material that attempts to unload elastically, and the part of the material that is permanently plastically deformed [30]

Therefore, with the above in mind, one can refer back to equation (4.7) and note an 'effective yield stress' as in equation (4.10). This suggests the relationship between hardness and yield stress is as in equation (4.8), and that the effect of the residual stress is to adjust the value of the yield stress in the relation, hence 'effective yield stress'.

$$\sigma_y^{eff} = \left(\sigma_y - \sigma_{res}\right) \tag{4.10}$$

The effect of residual stresses on the yielding are as expected through past literature: a compressive residual stress value (σ_{res} will be negative) leads to an increased effective yield

stress, hence reduced plastic deformation and a higher hardness number. A tensile residual stress value will have the inverse effect. In essence, what seems to be the case is that Equation (4.7), along with its accompanying simplifications, reduces the residual stress value to the bulk effect it has on the yield stress.

While care should be taken when analysing a simplified case such as this, the assumptions made should still be valid for the analysis above. The equi-biaxial assumption, which assumes the same residual stress value in both directions, is in line with hardness-yield relations, which assume the same yield stress in all directions.

4.2 Modification to stress state & Final relation

The preceding section provided justification for the methodology employed through the comparison of the simple relation and literature observations. The necessity is present now to develop the relation somewhat, in order to achieve a more complete final relation. To this end, complexity needs to be introduced.

4.2.1 Stress ratio parameter

The primary area in which complexity needs to be introduced is the residual stress state, where the previous assumption of equi-biaxiality can now be considered too simple. The state will still be assumed to be biaxial, but the stresses in the two directions should no longer be equal by default.

Lee & Kwon tested the effects of stresses on hardness measurements through the use of applied biaxial stresses. They applied stresses of varying values to a piece of material in the x and y directions. The stress state they applied was defined as in equation (4.11). The observations on the applied stress state could be extended to localised residual stresses as well.

$$\begin{pmatrix} \sigma_x^{app} & 0 & 0 \\ 0 & \sigma_y^{app} & 0 \\ 0 & 0 & 0 \end{pmatrix} = \begin{pmatrix} \sigma_x^{app} & 0 & 0 \\ 0 & \kappa\sigma_x^{app} & 0 \\ 0 & 0 & 0 \end{pmatrix} \quad \textbf{(4.11)}$$

The relation between the two components of the stress tensor above is governed by the stress ratio parameter, κ. κ represents the stress ratio of the two orthogonal components of the stress, σ_x^{app} and σ_y^{app}, which are the major and minor stresses. Table 4.2 below, paraphrased from a segment of a table in the Lee & Kwon paper, shows the value for κ corresponding to various stress states.

Stress Ratio, κ = $\frac{\sigma_y^{app}}{\sigma_x^{app}}$	*Stress state*
1.0	Equi-biaxial
0 < κ < 1.0	Biaxial (same sign)
0	Uniaxial
-1 < κ < 0	Biaxial (opposite sign)
-1	Pure Shear

Table 4.2: Stress states corresponding to κ values (partial from Lee & Kwon [10])

In the same way, this can be used to define a stress tensor in relation to the major residual stress component in the plane of the surface, σ_{res}, and this tensor is shown below in equation (4.12). Using this formulation in combination with the same tensor of the mean pressure applied by the indenter, results in an overall tensor as in equation (4.13).

$$\sigma^{res} = \begin{pmatrix} \sigma_{res} & 0 & 0 \\ 0 & \kappa\sigma_{res} & 0 \\ 0 & 0 & 0 \end{pmatrix} \tag{4.12}$$

$$\sigma = \begin{pmatrix} \sigma_{res} - \frac{2}{3}P_m & 0 & 0 \\ 0 & \kappa\sigma_{res} - \frac{2}{3}P_m & 0 \\ 0 & 0 & -P_m \end{pmatrix} \tag{4.13}$$

Now once again as previously, the principal stresses shown can be used in the von Mises yield criterion, resulting in equation (4.14). Due to the added factor of the κ, the equation will not now cancel out as conveniently as it did in the formulation of equation (4.7). A certain amount of simplification can be made by collecting terms such that the equation reduces to equation (4.15). The full derivation can be found in Appendix A.

$$\left(\sigma_{res}(1-\kappa)\right)^2 + \left(\kappa\sigma_{res} + \frac{1}{3}P_m\right)^2 + \left(-\frac{1}{3}P_m - \sigma_{res}\right)^2 = 2\sigma_y^2$$

(4.14)

$$\sigma_y^2 = (\kappa^2 - \kappa + 1)\sigma_{res}^2 + \frac{1}{3}(\kappa + 1)\sigma_{res}P_m + \frac{1}{9}P_m^2$$

(4.15)

Similarly to earlier, when solving this equation for a parameter, only the 'positive' root was taken. The use of the positive root had support through the observation of the equation used in the source paper by Frankel et al., where the authors appear to be taking the positive root as well. This can be seen in the equations below, equation (4.16) showing the von Mises criterion for their situation.

Equation (4.17) shows the rearrangement in terms of p, which is the mean pressure or Meyer's hardness, as shown earlier. The positive sign ahead of the second term in equation (4.17) indicates the taking of the positive root. (Note: the angle brackets are 'average' stresses they used with a fitting parameter, which is described in the following section).

$$(\sigma_H - \sigma_R)^2 + \left(-\frac{2}{3}p + \sigma_R + p\right)^2 + \left(-p + \frac{2}{3}p - \sigma_H\right)^2 = 2S_y^2$$

(4.16)

$$p = -\frac{3}{2}(\langle\sigma_H\rangle + \langle\sigma_R\rangle) + 3\left[S_y^2 - \frac{3}{4}(\langle\sigma_H\rangle - \langle\sigma_R\rangle)^2\right]^{\frac{1}{2}}$$

(4.17)

4.2.2 α - Fitting Parameter

In the paper by Frankel et al., when using the assumption that the residual stresses simply add up with the stresses from the indenter (as in Figure 4.2 a)), it was found that the model was overestimating the effect of the residual stresses.

Hence, a fit parameter known as α was introduced, which would adjust the value of the residual stresses such that they would have a diminished effect, depending on what was

required from the fit. α was multiplied by the residual stresses to give the 'average residual stresses', and the average residual stresses were used in the model. Therefore, α is also introduced here. α is multiplied by the residual stress to give the 'average residual stress' as in equation (4.18).

$$\langle \sigma_{res} \rangle = \alpha \cdot \sigma_{res} \tag{4.18}$$

Since $\langle \sigma_{res} \rangle$ gets used in the model, there is no change in the functioning of the model, but one can consider the σ_{res} in future uses of the model as being $\langle \sigma_{res} \rangle$. As α is not a known quantity, it cannot be directly included in the testing in Chapter 5. In any case, the primary interest will be extracting residual stress values from known hardness values using the model, consequently the implementation of α will only need to be performed at the end.

4.3 Standardisation of Parameters

This section is focussed on the areas in which information is required such that the equation can be used. This information will need to be collected through some alternative residual stress measurement method, as detailed in Chapter 3. The hope is that once sufficient data has been collected, there can be standardisation of certain parameters, which can then be stored in data tables and used in future measurements.

4.3.1 κ – stress ratio parameter

The first parameter for which information is required in the usage of the relation in equation (4.15) is the stress ratio κ, determining the axiality of the residual stress state. At this stage, it is an unknown in the equation, and although its influence has not proved immense in the figures in the following section, it is significant enough to warrant quantification.

This seems to be a parameter which has a decent amount of potential for standardisation for particular processes. Since there are standard processes which materials will go through

during the production, it would suggest that there will be standard states of stress occurring. Certain processes would likely tend to produce certain types of stress states in the material.

The idea behind standardising κ therefore, would be fairly simple: once the material has undergone a process such as cold-working, the stresses in the plane of the surface can be measured, and the ratio of the stresses measured can be used to establish a value for κ. A bulk of repeated measurements can then be used to obtain a standard value for κ for the process, assuming sufficient consistency exists in the values obtained.

These measurements could be conducted at various locations, with both the hope of confirming consistency, and to obtain average values of longitudinal and transverse stresses. The locations should, whilst being far enough apart to avoid interference, be in a similar region of the bulk material, i.e. a measurement at the edge of the piece should not follow a measurement in the middle.

The measurement of the stresses in order to establish κ would need to be performed using one of the current residual stress measurement methods, the choice of which is down to the discretion of the user, depending on personal preference and situational suitability. Nevertheless, the hole-drilling method is posited here for the sake of a hypothetical proposal, due to its accuracy and relative repeatability.

The procedure for hole-drilling is already described; the measurement makes use of strain gauge rosettes, which are able to obtain the strains (and hence stresses) in any orientation in the plane of the surface. The expected orientation of the principal axes is coincident with the longitudinal and transverse axes, but if not, it is a simple calculation to obtain the principal orientations.

The ratio of the minor principal stress divided by the major would give κ. The hope for this testing is to observe standard values for κ for each procedure, which could then be used as

data tables in the use of κ in estimating residual stress from hardness measurement. A chart for a rough potential testing procedure is shown below in Figure 4.3.

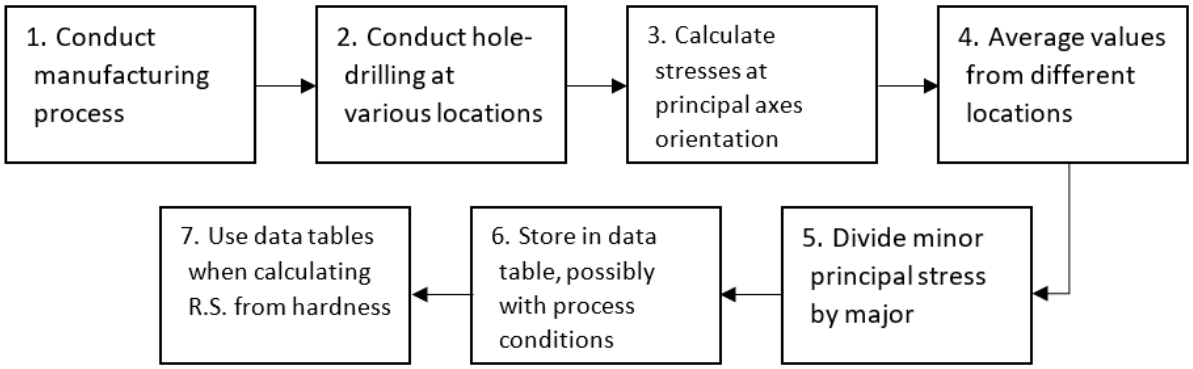

Figure 4.3: Chart showing rough potential procedure for establishing κ for use in residual stress measurement with theory shown earlier.

4.3.2 α – fit parameter

One of the key issues with the model mentioned in the source paper by Frankel et al. was the over-estimation of the effect of the residual stresses on the hardness measurement [5]. They found that the measured values for the residual stresses were overestimating the hardness values, and hence they introduced the fitting parameter α in order to satisfactorily fit the data.

When extracting residual stress values from hardness data, the use of the parameter α will only need to be performed at the end, in order to adjust the value of σ_{res}. Hence in this usage, α would not be used as a fit parameter. Therefore, the need to know the value of the parameter to use becomes crucial, especially as it likely will not be a constant across materials and processes.

The solution may be to standardise the parameter by repeated uses of the procedure performed by Frankel et al., who measured the residual stresses and fit their model to the hardness-residual stress data using the fit parameter α. By repeating this procedure for different materials and processes, one could standardise α by noting the value required to fit the data in each case.

The choice of X-ray diffraction for the measurement appears to be more suitable in this case, as the procedure requires both the measurement of hardness and residual stresses in the

same location. The residual stresses would need to be measured first, and the use of hole-drilling would cause damage at the location, preventing the subsequent measurement of hardness. If one deemed it necessary to have consistency in measurement methods, then the measurement of the stresses for κ could also be performed using X-ray diffraction.

The procedure for establishing α for a particular material and/or procedure should also be fairly simple. Taking X-ray diffraction as the measurement method, it can be performed at various locations on the piece. However, while X-ray diffraction can be performed at any location on the piece, the points will need to be well-spaced out, as the hardness measurements will need to be far enough apart so as to not influence each other.

Once sufficient data has been collected, with hopefully a decent range in the hardness and residual stress values, the values can be used in equation (4.15), with the use of the stresses as in equation (4.18) to introduce α. Regression analysis can be used to estimate the value of α for which the data fits best, and thus α can be recorded.

Frankel et al. also posited that α has a dependence on the yield stress, so these can be recorded simultaneously or, as done by Frankel et al., the equation could be solved for both α and σ_y. Once again, a chart is shown below in Figure 4.4 indicating a rough procedure for the procurement of α.

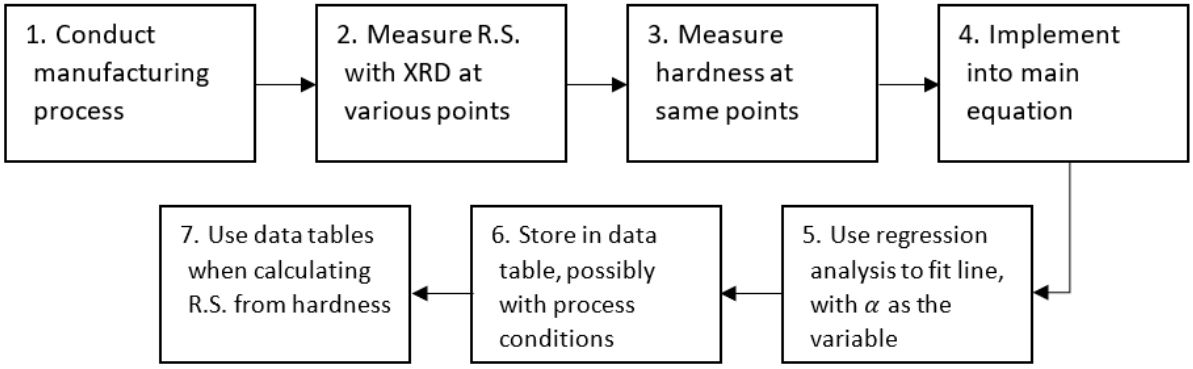

Figure 4.4: Chart showing rough potential procedure for estimating α

4.3.3 Cross-sectional profiles

An important limitation of using hardness measurements as a method for estimating residual stresses is that it is limited to near-surface measurements, therefore a possible method

to gain some idea of the stresses in the core after using hardness tests is to use cross-sectional stress profiles.

One can make use of the self-equilibrating aspect of residual stresses to estimate stresses in the core. As explained earlier, the overall residual stress across a cross-section of the material will be 0. Hence, compressive residual stresses at the surface tend to be balanced out by tensile residual stresses in the core of the material. Using this fact, one can use standard cross-sectional profiles in combination with residual stress measurements at the surface to gain an estimation of the stresses in the centre.

To achieve this, standardisation must once again be employed, in order to have known residual stress profiles that can be used in combination with the surface measurements. If the profiles can be quantified mathematically into an equation, the surface measurements can be used as boundary conditions to the equation, which could be solved to gain an estimate the residual stresses at the centre.

This will once again involve the use of one of the existing residual stress measurement methods, which will have to be destructive in this case, as this would be the most appropriate way to measure stresses in the centre. For this purpose, the contour method seems to have potential, given its ability to provide an entire 2-D map of the cross-section. This can once again be performed for specific manufacturing processes, to standardise residual stress profiles observed for each process.

Caution must be employed when using the contour method given its relative novelty as a measurement method. Additionally, it has the drawback of only being capable of measuring the normal stresses. This means it reduces to a one-dimensional measurement; if a cross-section is measured, only the stresses acting normal to the cut surface will be measurable.

The wealth of data provided however, means that the contour method does have advantages for this purpose. The map that is provided can be used to gain residual stress profiles

in multiple locations along the depth or the height, hence giving multiple options from a single cut. However, a single cut will likely be all that is possible for a particular piece of material, given the destructive nature.

Using profiles to estimate residual stress distributions based on surface measurements is rather reliant on a certain amount of regularity and symmetry in the residual stress profiles, which may not always be the case in the real world. There is some encouragement offered when one views some of the past experimentation conducted in this area, as there have been measurements made of residual stress profiles, with some promising results.

As an example, Prime & Hill conducted residual stress profile measurements on a plate of aluminium alloy 7050-T74 [45]. While their aim was to justify their stress relaxation technique, the profiles they obtained are able to offer useful insights to the problem at hand. They made use of a destructive measurement method, known as the Crack Compliance Method [46]. The details are unimportant here, but they were able to obtain residual stress profiles in both the rolling and transverse directions using this method. The profiles they obtained can be viewed in Figure 4.5 a) and b) below.

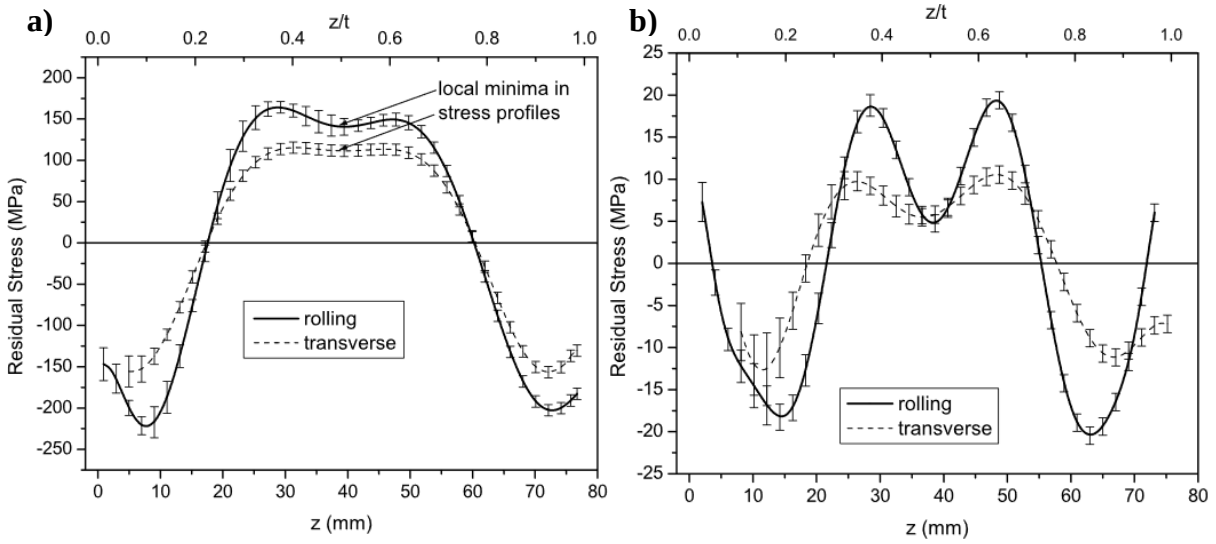

Figure 4.5: Figures from Prime & Hill, showing residual stress profiles for a plate of aluminium alloy 7050-T74, a) before and b) after a stress relaxation treatment [45]

Setting aside the changes in the magnitudes of residual stress and the change in the shapes of the profiles due to the relaxation treatment, it can be seen both figures show encouraging profiles, with regularity and symmetry. The shapes of the profiles seem to be describable by orders of polynomial that are not particularly high.

This provides some encouragement with regards to being able to predict residual stresses within the core of a material using surface measurements. There are certainly issues to overcome, as one does not necessarily know the exact shape that the profile will take, but a rough estimate will nevertheless provide helpful information.

The paper also features a figure on a thinner plate of the same alloy but with a slightly different tratment, 7050-T7451, which shows a less encouraging profile. The profile is shown in Figure 4.6 below [45]. This figure seems to have a similar shape to the ones above, but is significantly more asymmetrical, leading to challenges in trying to estimate stresses in the centre. This can perhaps be attributed to the thinness of the plate, but it should be kept in mind that it is not a given that the stress profiles will be nicely symmetrical.

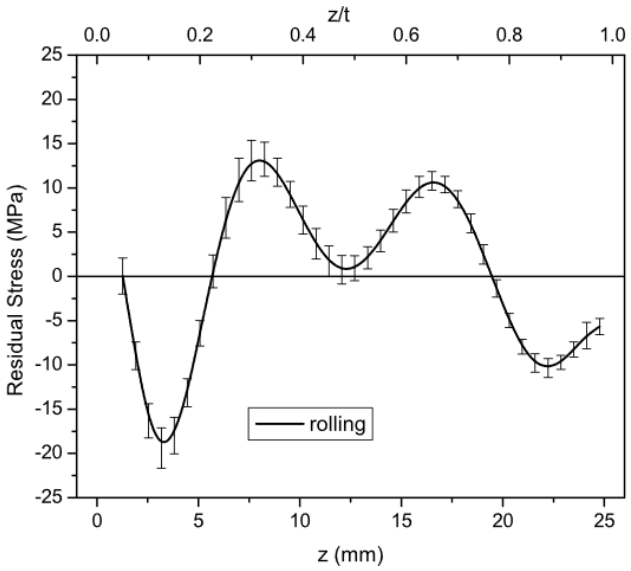

Figure 4.6: Figure from Prime & Hill, showing residual stress profile for a 25mm plate of aluminium alloy 7050-T7451 [45]

In addition to the experimental data shown, Schajer has provided expected residual stress profiles and gradients for a couple of common processes which are performed on metals,

namely welding and machining [3]. These are shown in Figure 4.7 a) and b) below [3]. This indicates there are already standard expected residual stress profiles for certain operations, which further aids in the attempt to describe core stresses using surface measurements.

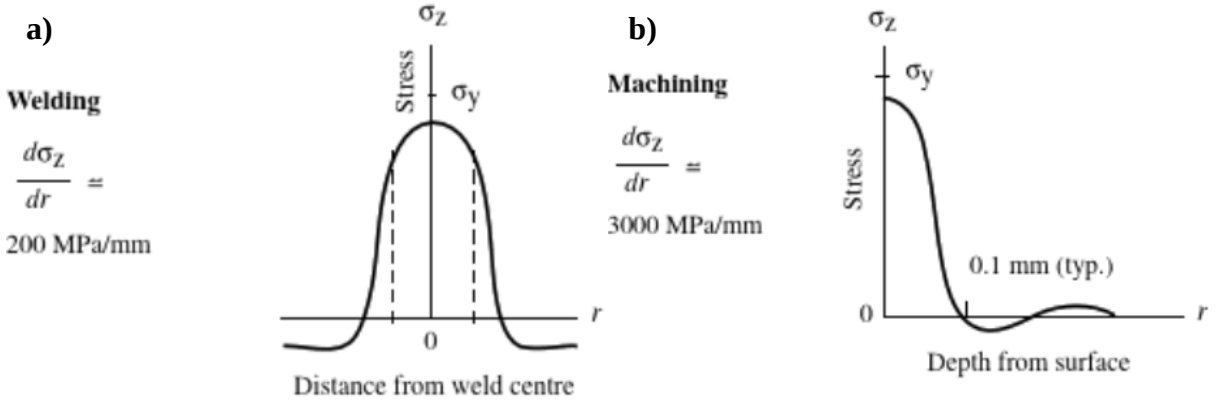

Figure 4.7: Diagrams from Schajer, showing expected residual stress profiles and gradients for a) welding and b) machining [3]

4.4 Analysis of derived relation

It is deemed necessary at this point to examine and analyse the final relation obtained earlier in equation (4.15), such that a clear image can be formed of its qualities and shortcomings. The sensibility of the steps taken to arrive at the final relation will be analysed, along with the accompanying assumptions and simplifications. The limitations of the relation due to the assumptions and simplifications are discussed for their potential to hinder the usage of the relation in measuring residual stresses.

4.4.1 Logicality of formulation

The simplistic nature of the initial ideas leads to certain reservations about the quality of the relation. However, given that first, the initial set-up was taken from a paper by Frankel et al. where it appeared to function quite well and second, the subsequent steps taken to adapt the relation for the current purposes were not a huge leap, lends a little reliability to the relation.

Firstly, the explanation put forth by Frankel et al. for the initial stress state due to the indenter was that it "relates to the situation in which the load W is still applied but the deformation has stopped" [5]. This appears a logical manner in which to define the value of P_m.

At the stage mentioned, the mean pressure being applied is at the limit of yielding, since the deformation has stopped. Therefore, it is logical to use this value in the von Mises yield criterion, as this is the value that places the stress state on the border of yielding.

The biaxial stress state, which assumes no shear stresses, implies that the stresses are also the principal stresses. While it does seem simplistic to exclude shear stresses, the assumption still seems fairly reasonable. One could expect that the principal stresses are oriented to the longitudinal and transverse directions. If they are not, the relation would obtain the principal stresses, which are nonetheless useful to know. Additionally, the use of biaxial stress states has been employed by other authors, hence there is a reasonable justification for the usage [10] [6] [11].

The biaxial stress assumption goes hand in hand with the plane stress assumption, as there is the assumption of no residual stress in the z-direction. This has also been previously used, not least by Frankel et al. in their paper, where they use only hoop and radial stresses and ignore the axial stresses of the cylinder. This assumption seems also to be fairly valid, given the past usage, and the expectation that the stresses will be mostly in-plane. This approach in defining the stress state as plane stress is naturally a simplification to help with calculation, nevertheless it appears valid.

The initial use of the equi-biaxial state, taken from a paper by Lee & Kwon, was considered to be a reasonable first assumption, and in the end turned out to provide a useful basis for justification of the methodology. The relation obtained using this stress state had certain similarities to the observed relationship between hardness and yield stress, from which the explanation could be formed that equi-biaxial residual stresses were adding to, or subtracting from, the yield stress [7] [8]. Coupled with a similar relation and explanation from Swadener et al., this provided a good justification for the overall process used [9].

The subsequent expansion through the use of the non-equi-biaxial stress state with the κ parameter was a way to more accurately define the stress state at the surface. This adds some necessary complexity to the equation. The steps taken to build upon and supplement the relation, by sourcing a stress state from another paper by Lee & Kwon [10], seem to be fairly logical without any immense leaps into the unknown. The use of the stress state with κ by Lee & Kwon and also subsequently by Huber & Heerens, adds further support [11].

As to the quality of the relation obtained, and whether or not it is capable of rigorously defining and predicting the effect of residual stresses on hardness measurements, this is opaquer. Therefore, in order to assess this, the following discussion will centre on the inherent limitations of the relation derived.

4.4.2 Limitations of relation

As with any derived relation, the one obtained in equation (4.15) has to make a certain amount of assumptions and simplifications, and as such it becomes limited to some extent. These limitations must be addressed now to attempt to analyse their impact on the overall quality and usability of the relation.

The parameter α was introduced as a fit parameter by Frankel et al., hence it is not a clearly defined physical quantity. The authors provided the justification that the need for α was due to the lack of orthogonality of the stresses as the indenter would penetrate deeper into the material. It is unclear whether or not the assumption of orthogonality of the stresses is valid or not, but their use of α as a parameter in the fitting seemed to function well, as their fits to data appeared satisfactory. However, it was still not defined as a physical quantity. The authors mentioned an analytical derivation for α in a subsequent paper, but I was unable to locate this.

A key point to mention at this point is regarding the ineffectiveness of measuring residual stresses with hardness measurements using low loads. This has particularly emerged as people have attempted to make use of nanoindentation to measure residual stresses. Tsui et

al. noted that when ‘real’ contact areas were measured using optical methods, that nanoindentation hardness appeared to have no real dependence on the residual/applied stress state, in contrast to observations from conventional hardness tests [4]. These observations are echoed somewhat by a follow-up paper to the one by Frankel et al., by Schroeder et al., which stated that the effect of residual stresses on hardness get “washed out” for tests with lower loads, in their case Rockwell-A and Microdur Vickers testers [47].

The root of the issue seems to be that the tests carried out with lower loads with less plastic deformation, such as low-load Rockwell and nanoindentation tests, do not show a significant effect of the residual stress on the hardness [47]. It has already been noted earlier that even for higher loads, the effect is observable but limited.

Schroeder et al. say that the effect is detectable for Rockwell-C and Rockwell-D measurements and in the book by Herrmann, the maximum load used in the Rockwell measurements is 1.373 kN [47] [22]. Given that, in Brinell testing the loads tend to be higher, for example in Table 5.1 the load is 500kg which corresponds to roughly 5kN, the loads should hopefully be high enough that this effect is clearly present.

This is naturally not an exact equivalency, given the shape of indenter as a diamond for Rockwell-C and D, as well as the difference in procedure. Nevertheless, the tests by Schroeder et al. were conducted for gun steel, and one would expect aluminium alloys to exhibit more plastic deformation, due to their lower yield strength [47].

An important limitation which needed to be imposed on the use of the relation was one of elasticity in the residual stresses. Due to the formation of the equation being rooted in the limiting case of a von Mises yield criterion, it cannot handle residual stress states which would exceed the yield criterion. This is exhibited when one attempts to use a tensile residual stress above the yield, which causes the hardness to drop below zero, which is naturally not possible.

This limitation could perhaps be circumvented through the use of higher localised yield stress values, which would likely be necessary to sustain higher values of residual stresses. However, higher localised yield stress values would be difficult to incorporate into the relation, as one would not know what the local yield stress value would be.

A potential option is to, as done by Frankel et al., use the yield stress as a fit parameter rather than as a known quantity. Therefore, the model would be run using both α and σ_y as fit parameters which would be optimised to best fit the data. However, then σ_y would require standardisation in the same way as α, which would be extremely difficult for localised yield stresses. Hence, the decision to limit the usability of the relation to only elastic residual stresses seems reasonable.

A main drawback of the derived relation is that it does not incorporate certain effects observed in real life, such as the Bauschinger effect. In this case, it is not an issue connected with the formation of the equation, but rather an inherent curiosity associated with hardness, which does not seem affected by the Bauschinger effect.

The tests of Tabor indicating an increasing hardness with plastic compressive deformation, combined with the known increase of hardness with increase in yield stress due to strain-hardening, are in contrast with observations of the Bauschinger effect [7] [24]. If the increase in one direction causes a decrease in the other, as the Bauschinger effect indicates, then one would not expect the hardness to increase with yield in either direction. It appears as though the hardness is rather related to the maximum value in magnitude of the yield stress.

Another observation noted by authors in the past is the offset in the relation between hardness and yield stress. This is also not incorporated into the relation. Tiryakioğlu et al. observed the relationship between hardness and yield for aluminium alloy 7010, and found that the relation had an offset, i.e. the line did not pass through the origin, as can be seen in Figure 4.8 below [8].

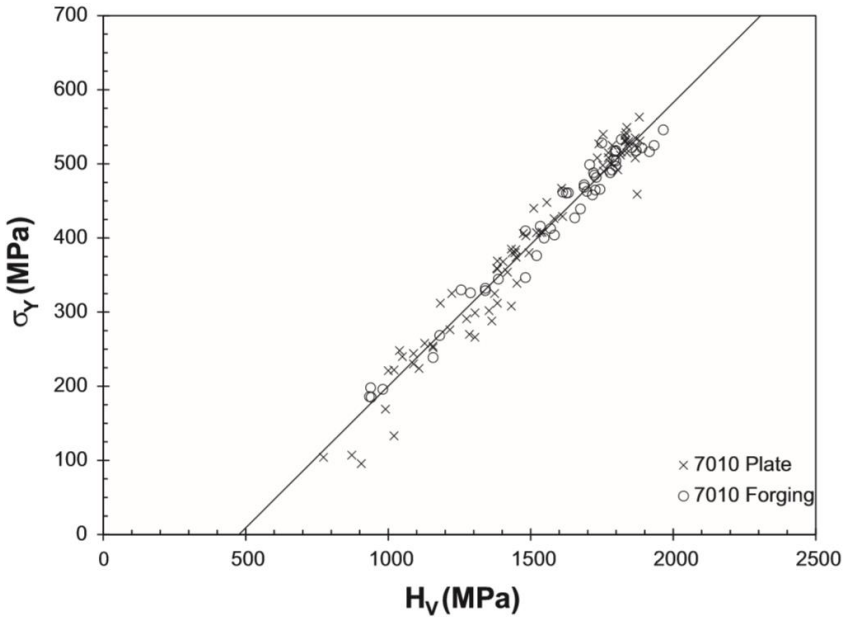

Figure 4.8: Figure from paper by Tiryakioğlu et al., showing the significant offset in the hardness-yield relationship [8]

This offset was attributed to work-hardening occurring during the indentation process itself. Tabor's experiment was conducted on fully work-hardened materials (Table 4.1), and he found the factor c (equation (4.8)) was around 3. Given that the relation used also shows a relation between hardness and yield of 3, it is clear that this does not consider the effects of work-hardening during hardness testing, which can have a significant effect, as seen in the figure above.

This effect would be difficult to incorporate into the relation, as it is not easy to quantify the effect of the work-hardening behaviour. An additional relation would have to be used linking the increase in the yield stress to the incremental plastic deformation caused by the indenter. This would make the relation significantly more complex to formulate and use.

This is perhaps an option for future work, to introduce σ_y as a function of the indentation dimensions. The indentation dimensions could be used in combination with mathematical approximations for the stress-strain curve, to estimate the 'current' yield stress due to the strain-hardening.

It is clear from the above discussion that the theory derived does make a significant amount of assumptions during the formulation, and out of necessity certain aspects must be simplified. This would be the case for the formulation for many theories, but it may be the case that this theory makes rather hefty simplifications. These will naturally lead to limitations in the applicability of the theory, which are indicated above.

A large amount of the limitation of the theory is not clearly known however, and the best way to gain a better understanding would be to rigorously test this theory to observe in which situations it is able to adequately function. Nevertheless, the formulation appears to be logical in nature, and the similarity with past observations of the hardness-yield relationship is encouraging. The theory may well be able to give some indication of the residual stresses present based on hardness measurements, or perhaps be a building block in more robust theories.

5 Testing of relation

In order to analyse the workings of the relation in equation (4.15), it was necessary to conduct some testing, which will be detailed in this section. Initially, real values taken from data tables were used to form a plot, where the values of residual stress could be observed. Subsequently, a more hypothetical path was taken, with certain parameters being varied between arbitrary values to observe the effect on the output. Finally, the results and the analysis are presented.

5.1 Testing methodology – Data & Codes

5.1.1 Test Data

The first step was to obtain test data to use to observe the values of residual stresses being obtained from equation (4.15). This project contained no physical testing, hence there is no produced data to use, which would have been the ideal scenario, as one could control all the elements. Nevertheless, test data from material tables was available, and could be used to gain some idea of the values of residual stress being obtained.

Aluminium alloy 6061 was the desired material to view, hence its data was collected from a table. Table 5.1 below shows the material properties for aluminium 6061, taken from Alcoa Engineered Products [48]. This table provided information required for the usage of the equation, specifically the yield stresses and the Brinell hardness. For the conversion to Meyer hardness, it was necessary that the table contained information about the load and ball size used in the Brinell test.

The alloy has various temper designations, depending on how it has been handled. A hardened state was required, as this would contain residual stresses. Hence, the frequently used temper of T6 was selected, which had a yield stress of 35 ksi and a Brinell hardness of 95 kgf/mm^2. The yield stress and Brinell hardness were converted to N/mm^2 as can be seen in equations (5.1) below.

Temper	Specified Section or Wall Thickness[2] (inches)	Tensile Strength (ksi)				Elongation[3] Percent Min. in 2 inch or 4D[5]	Typical Brinell Hardness (500 kg load/ 10 mm ball)	Typical Ultimate Shearing Strength (ksi)
		Ultimate		Yield (0.2% offset)				
		Min.	Max.	Min.	Max.			
Standard Tempers[1]								
O	All	—	22.0	—	16.0	16	30	12
T1	Up thru 0.625	26.0	—	14.0	—	16	—	—
T4, T4511[4]	All	26.0	—	16.0	—	16	65	24
T51	Up thru 0.625	35.0	—	30.0	—	8	—	—
T6, T6511[4]	Up thru 0.249	38.0	—	35.0	—	8	95	30
	0.250 and over	38.0	—	35.0	—	10	95	30
Alcoa Special Tempers*								
T6S2, T6S15	Up thru 0.249	38.0	—	35.0	—	8	95	30
	0.250 and over	38.0	—	35.0	—	10	95	30
T6S9, T6S10	Up thru 0.249	35.0	—	30.0	—	8	—	—
	0.250 and over	35.0	—	30.0	—	10	—	—
T6S4	All	38.0	—	35.0	—	6	95	—
T6H, T6511H	1.000 and over	42.0	—	38.0	—	10	95	30
T6G, T6511G	3.000 and over	42.0	—	38.0	—	10	95	30
T6X, T6511X	.250 thru 1.999	38.0	—	35.0	—	10	95	30

Table 5.1: Table from Alcoa Engineered Products showing aluminium 6061 material properties [48]

$$\sigma_y = 241.4\ \mathrm{N/mm^2}$$

$$H_B = 931.95\ \mathrm{N/mm^2}$$

(5.1)

5.1.2 MATLAB Functions

Having obtained some basic data to use, the next step was to formulate a system for testing. Given that for a particular specimen the values for σ_y and P_m are known, as above, the unknowns in the model are firstly σ_{res}, the desired output, and the stress ratio, κ. Therefore, it was deemed pertinent to implement the data into the model by means of studying the effect of the stress ratio on the output parameter, the residual stress. The idea was to use varying values of κ for a particular set of σ_y and P_m, and to observe the effects on the value of σ_{res} obtained.

A function was written in MATLAB, named *res_calc*, which would calculate the value for the residual stress parameter as defined in the stress tensor and equation (4.15), when values for σ_y, P_m and κ are put into the function. The function works by using equation (4.15), in the same structure. σ_{res} is defined as a variable using *syms* and, with the inputs as defined in the previous sentence, uses the *solve* function to solve the equation for σ_{res}. As stated before, this will return two roots, and the function only selects the positive root, and returns this value.

It soon became clear during the preliminary trial runs of the *res_calc* function that, for certain values of κ, the function would return σ_{res} values that were not real, i.e. they were in the complex domain. In hindsight, this is not entirely unexpected, given the quadratic nature of the main equation, hence taking a square root could lead to complex solutions for certain values.

A need was present firstly to identify the values for which this occurred. The complex results would occur for values of κ beneath a certain threshold, hence a function was written to calculate this threshold for specific values of P_m and σ_y.

It seems clear that the threshold at which the σ_{res} values cross into the real domain is related to the discriminant of the standard solution to a quadratic equation (5.2):

$$x = \frac{-b \pm \sqrt{b^2 - 4ac}}{2a}$$

(5.2)

So, in equation (4.15) the σ_y^2 was moved to the other side, such that the quadratic equation was equated to 0. Then the constants a, b, and c in the equation above were identified as:

$$a = \kappa^2 - \kappa + 1$$

$$b = \frac{1}{3}(\kappa + 1)P_m$$

$$c = \frac{1}{9}P_m^2 - \sigma_y^2$$

(5.3)

The function *k_thresh* was written to calculate the threshold by stating $b^2 - 4ac = 0$, and calculating the value of κ for which this occurs. The inputs for the function were naturally P_m and σ_y. The solution would be found again using *solve,* which would naturally return two solutions. Hence the limitation was placed that $-1 < \kappa < 1$, such that only the solution in this

interval would be returned. If there were no solutions in this interval, it would mean that there was no threshold for κ, and that any value of κ would return a real value for σ_{res}.

Secondly, the need was also present to exclude the complex results in the function *res_calc.* This was simple enough, as the code could simply instruct *solve* to assume that σ_{res} was real, hence if the solution was complex, the output to *solve* would be an empty matrix. In *res_calc* this was adjusted such that if the solution was empty, the output of *res_calc* would be NaN.

The use of the relation is to be limited to elastic residual stresses only, therefore this needed to be incorporated into the MATLAB testing. As the process for finding the solution to equation (4.15) in *res_calc* placed no limitations on the values for σ_{res}, aside from them having to be real. Hence, it was necessary to know the values of σ_{res} which would exceed elasticity.

Since the residual stress state used in equation (4.15) is more complex than the state in equation (4.7), the limit for elasticity is no longer simply the yield stress. Instead the von Mises criterion needed to be applied for the residual stresses alone. As the stress state is biaxial, the von Mises criterion for plane-stress principal stresses could be used (equation (5.4)) [24].

$$\sigma_1^2 - \sigma_1\sigma_2 + \sigma_2^2 = \sigma_y^2 \tag{5.4}$$

With the biaxial stress state as defined in equation (4.12), the criterion becomes as in equation (5.5), from which the positive root is again taken. This represents the maximum absolute value that σ_{res} can reach before plastic deformation begins. The value would naturally need to be negative if dealing with compressive residual stress.

$$(\kappa^2 - \kappa + 1)\sigma_{res}^2 = \sigma_y^2 \tag{5.5}$$

As the above equation shows, the maximum value for σ_{res} is different depending on the value of κ, hence another function (*res_thresh*) was written to calculate the maximum value for σ_{res} based on inputs of σ_y and κ.

The data used from Table 5.1 used Brinell hardness, whereas the relation in equation (4.15) needed the mean pressure or Meyer hardness. Hence, the final function written was named *pm_hb_conv*, and would convert Brinell hardness to Meyer hardness, given the values of the load (in kg) and ball size used (in mm). Note that if the Brinell hardness was given in N/mm^2, the load would also need to be given in newtons rather than kg. All of the functions can be found in Appendix B.1.

5.1.3 MATLAB Scripts

Once the functions were written to calculate various parameters, scripts were needed to utilise these functions to test the relation in equation (4.15), and display the results. The scripts would test the effects of the various parameters, and can be found in Appendix B.2.

The first script (*ratio_effect*) dealt with the κ threshold, and how its value would change with P_m and σ_y. It was noted that it was in fact the ratio of P_m/σ_y which was governing the location of the κ threshold. Hence *ratio_effect* would select an arbitrary value for σ_y, after which P_m would be decided by the ratio, which would be varied. The value of the κ threshold would then be calculated for each ratio value, and the results of the ratio vs. κ-threshold data would be plotted.

The ratios were varied between a lower limit and an upper limit; the lower limit was set as 3. This was due to observations during experimentation with *k_thresh* that using ratios below 3 were producing no threshold, i.e. for a ratio below 3, σ_{res} would be real for any κ. Hence, it was deemed futile to depict the ratios below 3. The possible reasons for this phenomenon are discussed later.

The upper limit was decided as being 5.2, due to the limitation of elasticity. The maximum possible value for σ_{res} from equation (5.5) was found through differentiation to occur when $\kappa = 0.5$. This maximum value is given as in equation (5.6). Using this relation in equation (4.15), the maximum P_m was found to be as in equation (5.7), hence the maximum ratio of P_m/σ_y was chosen as 5.2.

$$\sigma_{res}^2 = \frac{4}{3}\sigma_y^2 \tag{5.6}$$

$$P = \frac{9}{\sqrt{3}}\sigma_y \approx 5.2\,\sigma_y \tag{5.7}$$

The main script in use, named *Rs_script*, would calculate σ_{res} values for κ values which were varied between -1 and 1. The data used in the script are the Brinell hardness, yield stress, load, ball diameter and κ, which is varied. The script then converts to N/mm^2 if desired and converts the Brinell hardness to Meyer hardness. The script then plots the line showing the σ_{res} value calculated for each κ (for the σ_y and hardness data) using *res_calc*. Additionally, the σ_{res} values which exceed elasticity are calculated using *res_thresh* and shown as a shaded area, and the κ threshold (if present) is also shown.

The final script (*Pm_script*) was essentially a reversal of *Rs_script*, wherein it would calculate P_m for various arbitrary values of σ_{res}. The script would plot lines of σ_{res} vs. P_m, and also vary the κ value between -1 and 1, with each line representing a different κ value.

5.2 Testing results – plots

This section shows the plots produced through the running of the scripts described above. An explanation is provided prior to the presentation of the plots regarding how the parameters were varied for the testing, and the motivations behind the same.

5.2.1 κ parameter threshold

As described previously, the script *ratio_effect* produced plots depicting the variation of the κ threshold with the ratio of P_m/σ_y. Two plots were produced, the first of which varied the ratio between its lower and upper limits, 3 and 5.2, as discussed earlier. This is shown in Figure 5.1 below. Subsequently, a desire was present for a closer view of the region near the lower limit, hence the second plot (Figure 5.2) varied the ratio between 3 and 3.5.

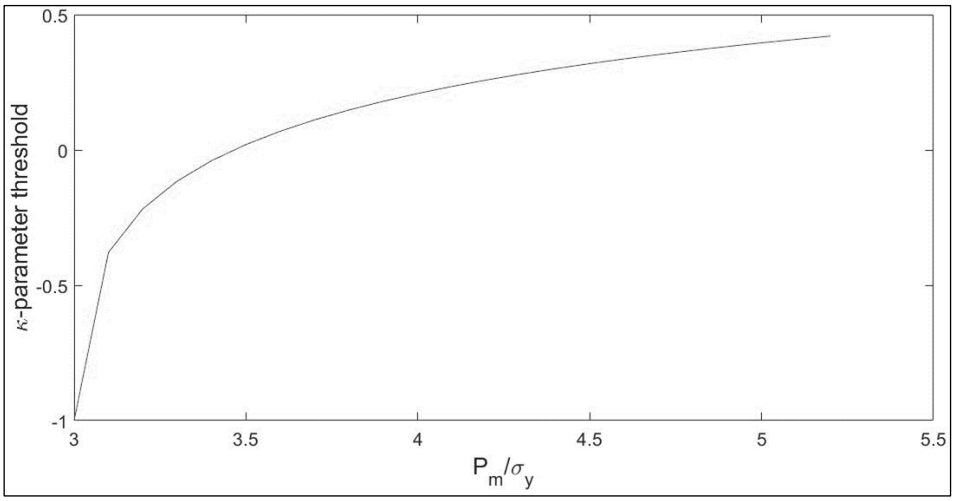

Figure 5.1: Variation in the threshold for κ as the ratio between P_m and σ_y is varied between 3 and 5.2

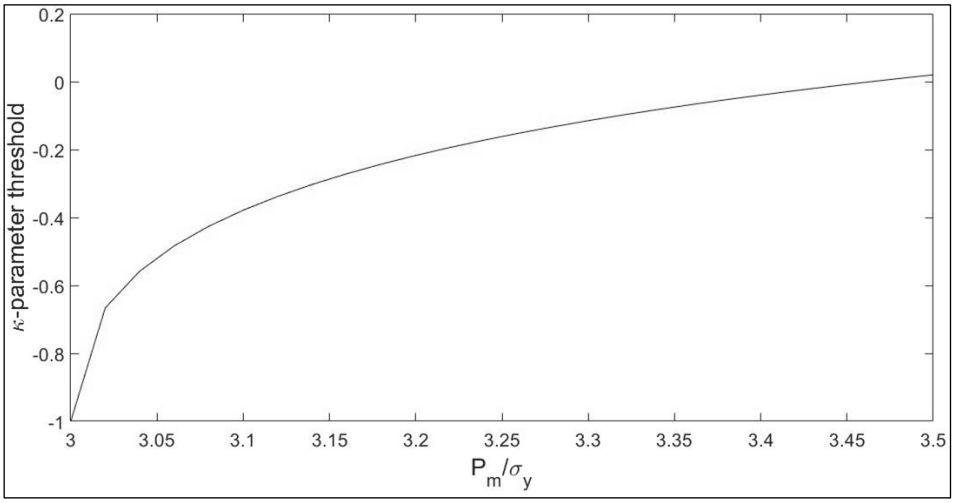

Figure 5.2: Variation in κ threshold as P_m/σ_y is varied between 3 and 3.5

5.2.2 Effect of hardness on σ_{res}, with varying κ

Rs_script was utilised to find values of σ_{res} for particular values of P_m and σ_y, and for the spectrum of κ values. The initial use of *Rs_script* was to show the values of σ_{res} returned

for the real data values of σ_y and H_B in equation (5.1), hence in the first plot (Figure 5.3), *Rs_script* is run for the real data values from the table, so one can observe then results obtained.

In subsequent uses of *Rs_script* and the other scripts however, the data used was generally arbitrary. This was done to observe the effect of changing certain parameters, for which real data was not necessary once a plot had been produced with real data. The yield stress was often held at the same value as in equation (5.1) however, with the other parameters varied as they were more interesting.

Thus, the next plot (Figure 5.4) is a group of four which shows how the plot changes for increasing input values of the hardness. In the script, H_B was varied between the arbitrary values 1079.1, 1177.2, 1373.4 and 1471.5 N/mm^2, while σ_y was held at 241.4 N/mm^2.

The final plot for this script (Figure 5.5) is another group of four plots, which instead observe the changes in the plot for decreasing hardness values. In the script, H_B was varied between the arbitrary values 588.6, 392.4, 196.2 and 0 N/mm^2, while σ_y was held at 241.4 N/mm^2.

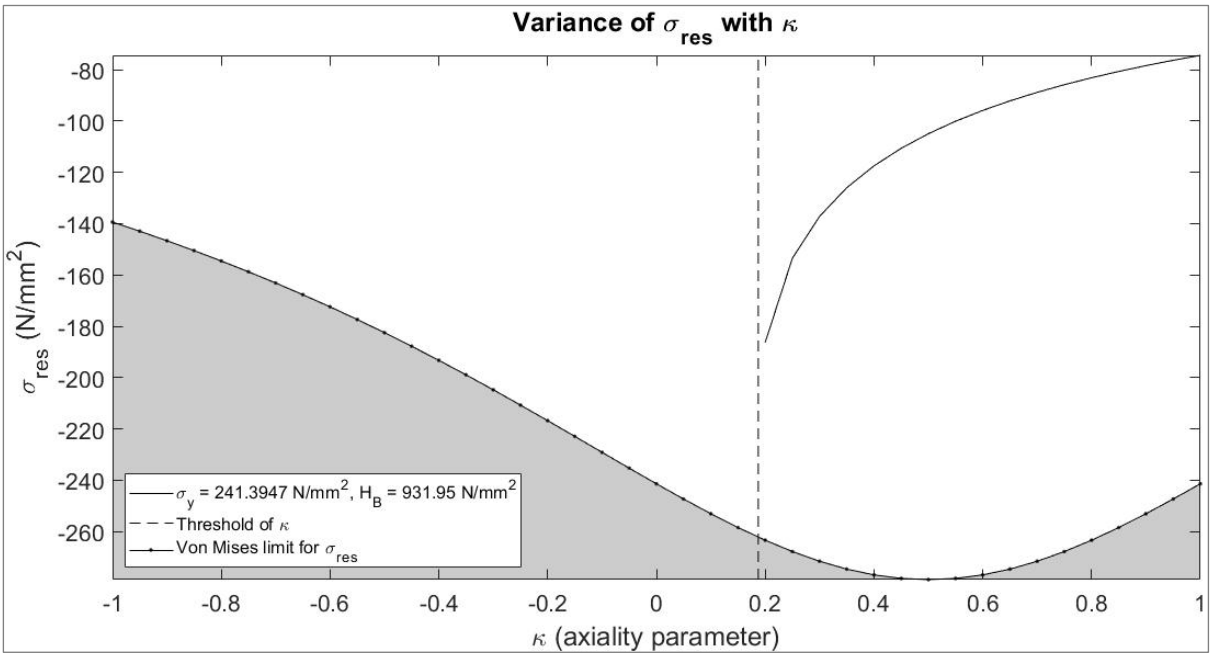

Figure 5.3: Plot of variance of major residual stress value with κ, for $\boldsymbol{\sigma_y = 241.4\ N/mm^2}$ *and* $\boldsymbol{H_B = 931.95\ N/mm^2}$. *Dashed line represents the threshold for κ, and the shaded area representing the* σ_{res} *for each κ which would exceed elasticity.*

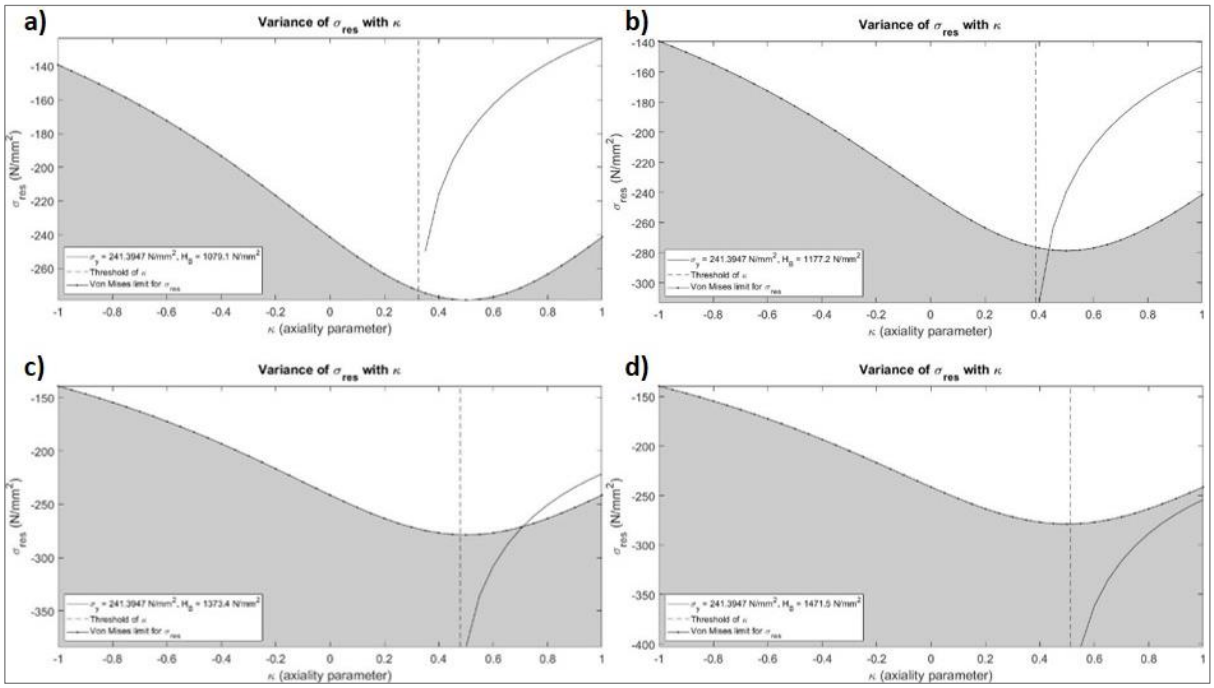

Figure 5.4: Plot of variance of major residual stress value with κ, for $\boldsymbol{\sigma_y = 241.4\ N/mm^2}$*, for increasing hardness values. a)* $\boldsymbol{H_B = 1079.1\ N/mm^2}$*, b)* $\boldsymbol{H_B = 1177.2\ N/mm^2}$*, c)* $\boldsymbol{H_B = 1373.4\ N/mm^2}$ *and d)* $\boldsymbol{H_B = 1471.5\ N/mm^2}$*. Dashed line represents the threshold for κ, and the shaded area representing the* σ_{res} *for each κ which would exceed elasticity.*

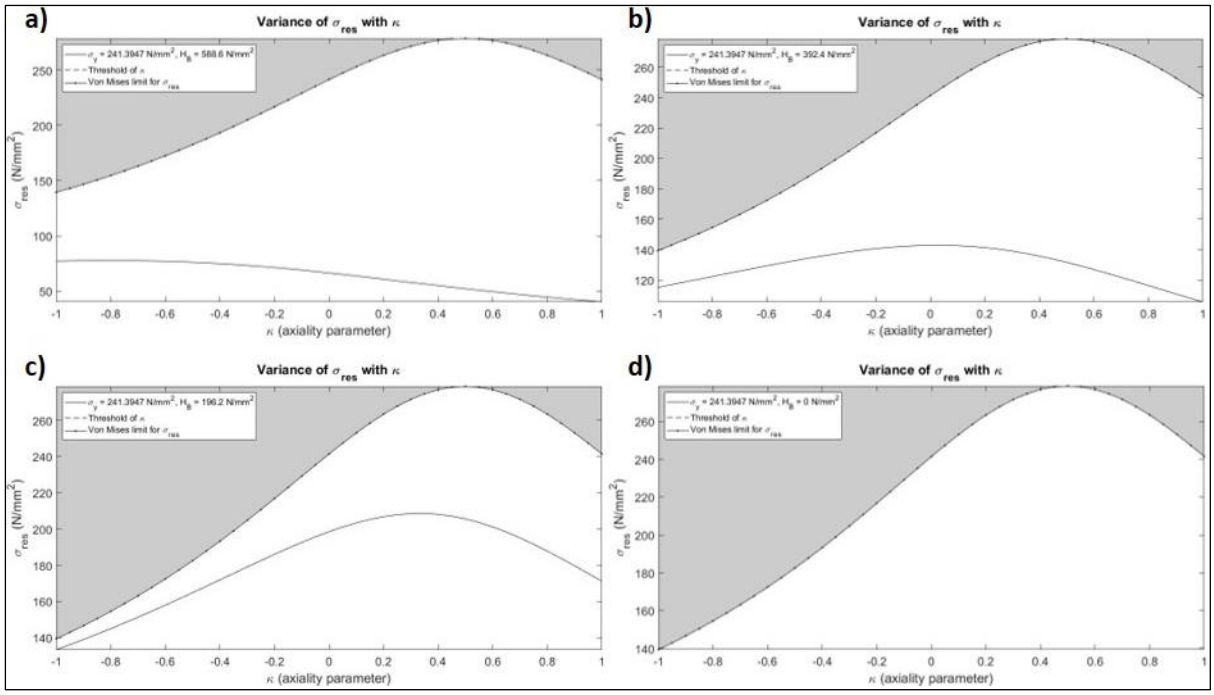

Figure 5.5: Plot of variance of major residual stress value with κ, for $\boldsymbol{\sigma_y = 241.4\ N/mm^2}$*, for decreasing hardness values. a)* $\boldsymbol{H_B = 588.6\ N/mm^2}$*, b)* $\boldsymbol{H_B = 392.4\ N/mm^2}$*, c)* $\boldsymbol{H_B = 196.2\ N/mm^2}$ *and d)* $\boldsymbol{H_B = 0\ N/mm^2}$*. Dashed line represents the threshold for κ, and the shaded area representing the* σ_{res} *for each κ which would exceed elasticity.*

5.2.3 Effect of σ_{res} on hardness

Pm_script calculated the effect that various values of σ_{res} would have on the hardness, whilst also varying κ between -1 and 1 in increments of 0.2. σ_y is arbitrarily set at 98.1 N/mm^2. The first plot (Figure 5.6) depicts compressive stresses varying between 0 and -98.1 N/mm^2, while the second plot (Figure 5.7) depicts tensile stresses varying between 0 and 98.1 N/mm^2.

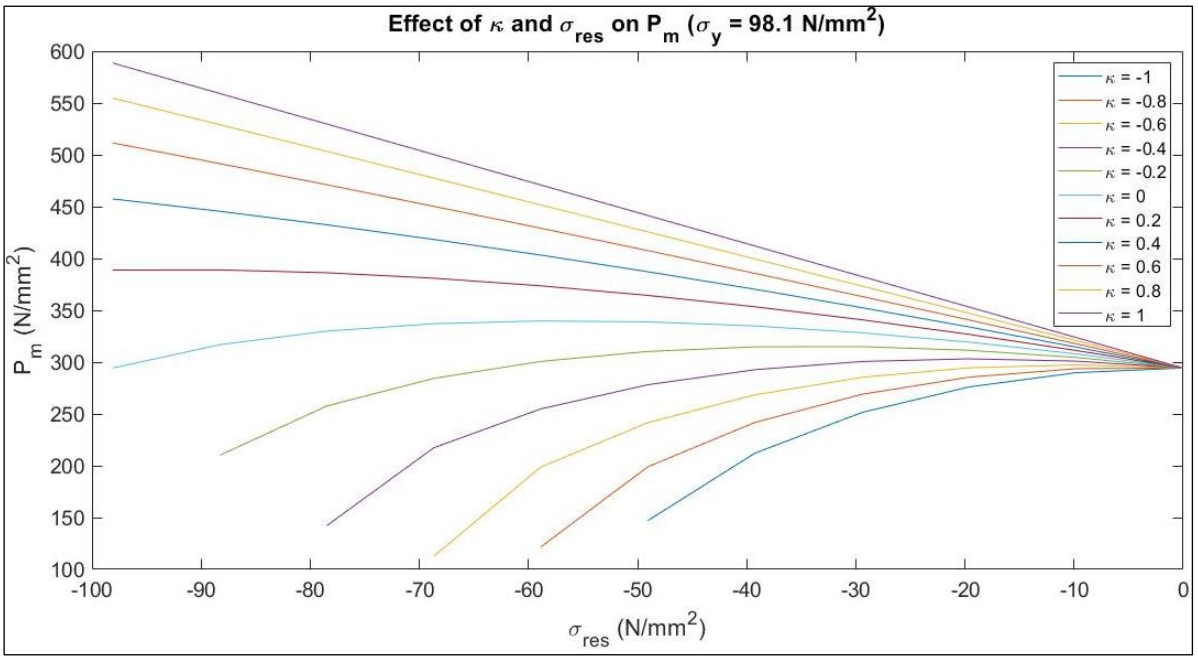

*Figure 5.6: Plot showing effect of varying σ_{res} on P_m, according to equation (4.15), with κ also varied between **-1 and 1**. Compressive σ_{res} values tested, between **0 and -98.1 N/mm^2***

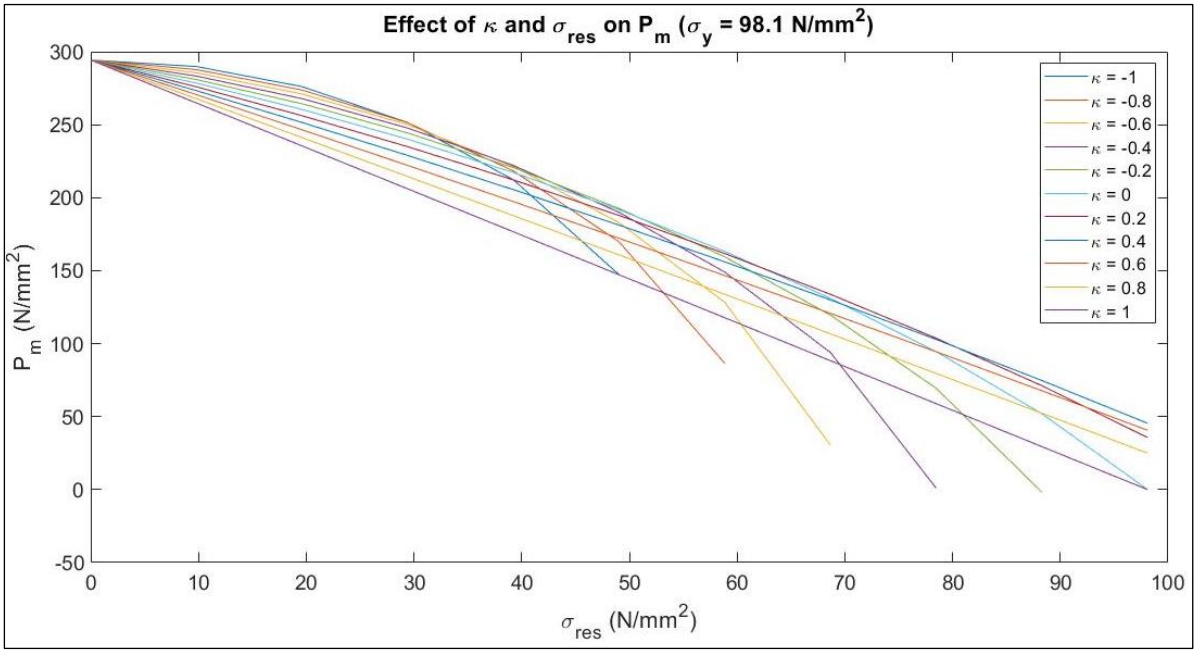

*Figure 5.7: Plot showing effect of varying σ_{res} on P_m, according to equation (4.15), with κ also varied between **-1 and 1**. Tensile σ_{res} values tested, between **0 and 98.1 N/mm^2***

5.3 Sensitivity analysis

Finally, it was also deemed necessary to quantify the effects of the various parameters on σ_{res} by means of a sensitivity analysis. The first step was to establish nominal values for each parameter. σ_y and H_B were the same as the values from the data tables. H_B was converted to P_m for the sensitivity analysis. κ was arbitrarily selected as 0.5, since the value is not known, hence the nominal input values and the resulting output of nominal σ_{res} are given in equation(s) (5.8).

$$\sigma_y = 241.4\ N/mm^2$$

$$P_m = 947.3\ N/mm^2$$

$$\kappa = 0.5$$

$$\sigma_{res} = -104.9\ N/mm^2 \quad \textbf{(5.8)}$$

The sensitivity analysis was then conducted by varying a single parameter by +5% and -5%, while leaving the rest at the nominal values, and noting the resulting value for σ_{res}. The percentage change in σ_{res} was calculated. The results of the sensitivity analysis are given in Table 5.2 below.

Inputs			**Output - σ_{res} (N/mm^2)**	**Percentage Change (%)**
σ_y (N/mm^2)	*Nominal*	241.4	-104.9	-
	+5%	253.5	-86.8	17.3
	-5%	229.3	-123.7	17.9
P_m (N/mm^2)	*Nominal*	947.3	-104.9	-
	+5%	994.7	-128.9	22.9
	-5%	899.9	-81.6	22.2
κ	*Nominal*	0.5	-104.9	-
	+5%	0.525	-102.4	2.4
	-5%	0.475	-107.6	2.6

Table 5.2: Results of sensitivity analysis of parameters σ_y, P_m and κ

5.4 Discussion of Testing

Having obtained results for the hypothetical tests, it comes time to discuss them, to note the various aspects of each plot which are striking, and to provide potential explanations for the same. The parameters tested were κ, σ_{res}, and P_m, with σ_y being kept constant, either at a value obtained from the data tables, or else simply an arbitrary value, to observe the effects of the other parameters.

5.4.1 κ threshold

The first thing to note about these figures is that the ratios begin at 3. As mentioned previously, this was due to another observation, which was that when the ratio was below 3, there was no threshold and all values of κ were possible. This is verified by the observation that, when the ratio equals 3, the threshold is -1, the lower limit of κ.

The importance of the value of 3 for the ratio is that, in the absence of residual stresses, the ratio would be 3, according to the equation. Therefore, if the ratio value is lower than 3, the residual stresses have caused the hardness to reduce. This observation leads to the conclusion that for a reduction in the hardness, any value of κ is possible.

The best way of explaining this phenomenon is through shear stresses. As Tsui states, "shear stresses control plastic deformation" [4], and increased plastic deformation would lead to a reduced hardness. If the value of κ is negative, this means the stresses in the two directions are of opposing signs, leading to a shearing effect, hence reducing the hardness.

If the hardness is reduced by the residual stresses, then it follows that any value of κ can be present. If κ is positive, then the residual stresses in both directions are of the same sign and if the stresses are tensile, this would decrease the hardness as it would subtract from the yield stress. If κ is negative, then there is naturally a shearing effect created due to the stress state, and this would increase plasticity and also reduce the hardness.

On the other hand, if the hardness is increased by the residual stresses, κ is more limited. Since negative values of κ are creating increased plasticity, a significantly increased hardness cannot be obtained with such a stress state in the material. This is also seen in Figure 5.2, where only small increases in hardness are able to have negative κ values.

Interestingly enough, this extends further than the exclusion of negative κ values; as the hardness increases, the κ threshold does as well (up to an asymptote at $\kappa = 1$). This implies that, in order to increase the hardness to certain level, the residual stress state must have a certain amount of equi-biaxiality. In other words, to achieve higher and higher increases in hardness, the residual stress state must be closer and closer to the equi-biaxial state, where the stresses in both directions are equal.

This can perhaps be explained by viewing Figure 5.8 below from Tsui et al., who posited an explanation for the reduced effect of uniaxial compressive residual stresses on indentation hardness [4] [49]. Since the indenter is applying a compressive stress, a uniaxial compressive residual stress in the material does not alter the maximum shear stress, hence does not have a major effect on the hardness. It is perhaps necessary for stresses in both directions to increase the effective yield stress as in equation (4.7).

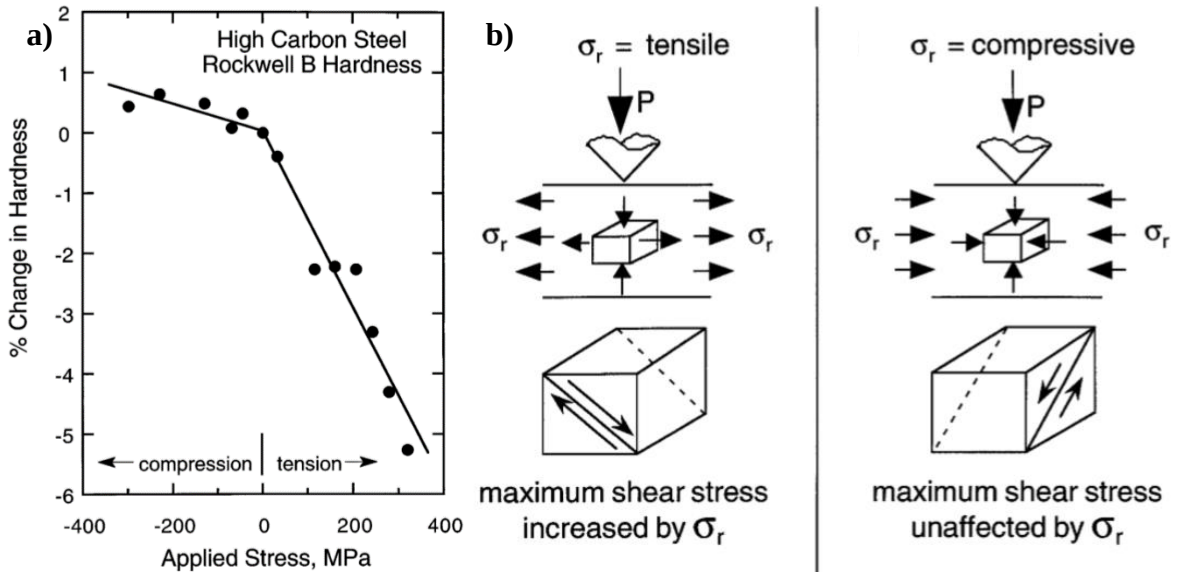

Figure 5.8: a) Graph from Tsui et al. showing reduced effect of uniaxial compressive stress on hardness (data from Sines & Carlson), b) Diagram depicting explanation posited [4] [49]

5.4.2 Effect of hardness on σ_{res}

The 'main' plot in Figure 5.3 shows that for the hardness in question, the residual stresses calculated by the equation remain well within the elastic region. Note that this may not necessarily be the case, due to aspects such as the α parameter, but this is not discussed here.

It can be seen that the maximum magnitude of the limit occurs at $\kappa = 0.5$, as calculated earlier from equation (5.5). Additionally, it can be seen that the minimum value occurs at $\kappa = -1$. This is also to be expected, given that this stress state represents pure shear, hence significantly increasing the plasticity. The respective magnitude values of the maximum and minimum values are roughly 280 N/mm^2, and 140 N/mm^2, respectively. Comparing these values to the nominal value for the yield stress, 241.4 N/mm^2, as one would use for a simple uniaxial stress state, one can see that a change in the two-dimensional residual stress state can have a significant effect on the maximum allowable stress.

The general features of the plot are as expected, with regards to the shape of the curve, the values for σ_{res}, and the threshold for κ. The curve shows negative values for σ_{res} which get lower in magnitude as κ increases. Since the curve depicts a 'hardened' material, this is as it should be, given that compressive residual stresses will increase the hardness, and more equi-biaxial stress states will require a lower major stress value to attain a certain hardness. The threshold for κ, which stands at around 0.2, also correlates with expectations given that there is a significant increase in the hardness.

Moving now to the first group of four figures (Figure 5.4), as expected the values of σ_{res} returned get progressively greater in magnitude and the thresholds for κ increase with the hardness. The combination of these two features means that there are progressively fewer values for σ_{res} which are able to provide this level of hardness.

These values get further limited by the inelastic zone marked by the shaded area. Whilst this zone stays constant, the increasing σ_{res} values means that the curve appears to

progressively sink into this zone until, in Figure 5.4 d) the entirety of the curve is in the inelastic zone. For the hypothetical hardness value in question, this means it cannot be attained by an elastic residual stress state.

In the following set of four figures (Figure 5.5), there is naturally no κ threshold, as all the plots begin at hardness values lower than the nominal value in Figure 5.3. Consequently, the curves encompass the entire range of κ.

Finally, two interesting features of these plots are the shape of the curves and their progression. Whilst in the first set of four plots the shape of the curve was generally similar across the plots, the shape of the second set of plots changes as they progress to lower hardness values. Eventually, when the hardness is 0, the curve matches the von Mises yield curve exactly. This is not unexpected but is a curious feature to note.

5.4.3 Effect of σ_{res} on hardness

Looking first at positive κ values for the curves in Figure 5.6 and Figure 5.7, the curves are fairly expected: increasing compressive stress increases P_m and increasing tensile decreases P_m. They seem rather close to being linear. Although they are not, it remains interesting to note that to the naked eye they could be considered linear.

The negative κ values show a decrease in hardness for increasing σ_{res} magnitude, in both the figures using compressive and tensile σ_{res} values. This is another reflection of the shear stress as seen and explained earlier; the negative κ serves to create a shear effect, leading to a decreased hardness value. The decrease in hardness is more pronounced in Figure 5.7 since the major residual stress value is also tensile.

A final aspect to observe on the two plots is the curve representing the uniaxial residual stress state, which occurs when $\kappa = 0$, and is the pale blue line on the plots. The striking feature is the contrast between the effect of the tensile stresses at $\kappa = 0$ in Figure 5.7, and the

compressive stresses at $\kappa = 0$ in Figure 5.6; an increase in the tensile stresses has a significant effect, while an increase in the compressive stresses has a negligible effect.

This supports the argument presented earlier through Figure 5.8; the uniaxial compressive residual stresses are having little effect because they are not altering the maximum shear stress, contrary to the uniaxial tensile residual stresses. As a result, an increase in the tensile residual stresses has a far greater effect on the hardness than an equal increase in the compressive residual stresses. Bear in mind, it is not a linear relationship between residual stress and hardness.

The sensitivity analysis showed that the measurement of σ_y and P_m will have large effects on the value of σ_{res} returned; the value of κ does not have a large effect for a small variation of 5%. Hence, accurate measurements are most important for the yield stress and hardness values.

In general, the plots seem to follow fairly expected patterns, with the exception of a few curious elements. Additionally, the unexpected factors tended to be explainable from theory with a fair degree of confidence. Therefore, there are no major surprises from the testing of the relation, but it is interesting to view how it functions.

6 Conclusions

6.1 Future Work & Improvements

6.1.1 Spence Creep Model

One area of interest with regards to future work is that of combining findings with other models to obtain further useful data. In this area, the creep model proposed by Spence in his paper appears promising [12] [13]. This could be used to predict the progression of residual stresses over time, and so could be combined with measurements of residual stress made through hardness tests.

Stresses applied on a piece of material will relax over an extended period of time, and hence cause the material to deform to maintain equilibrium; this is known as creep. Even stresses below the yield stress can cause deformation of the material. This makes a material with significant residual stress levels dimensionally unstable if this material forms a part which will be in service for years.

Therefore, Spence developed a creep model to estimate the development of residual stresses. Since standard creep models are for applied stresses, the model developed by Spence required adjustments to make it suitable for use with residual stresses.

It was first determined that the creep would be in the ‘dislocation glide’ and ‘dislocation creep’ regimes (Figure 6.1 a)), due to the expected residual stress value and operating temperature. Additionally, it was argued that creep would remain in the ‘Primary’ stage (Figure 6.1 b)), since the ‘applied’ (residual) stress would constantly change as the material deformed and so the same stress would not remain applied for a long enough time to enter the ‘Secondary’ stage.

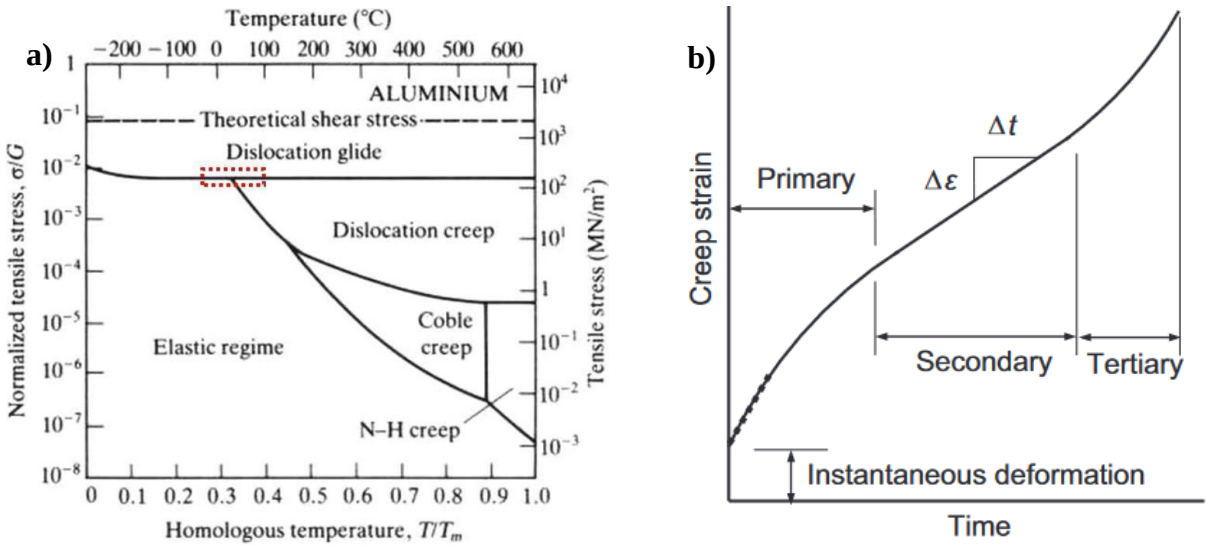

Figure 6.1: Figures from Spence, showing a) Creep regime map for aluminium, and b) Creep mode diagram, indicating creep for residual stresses stays in Primary Creep [12] [13]

In order to use standard creep equations, the definition of stress needed to change from being a constant applied stress to a strain-dependent stress. This new definition of stress is given below in equation (6.1), where σ_{in} is the initial stress and ε_f is the final strain.

$$\sigma = \sigma_{in}\left(1 - \frac{\varepsilon}{\varepsilon_f}\right) \tag{6.1}$$

The definition was then used in the power law creep model for crystalline materials, shown in equation (6.2) below.

$$\dot{\varepsilon} = \frac{k}{T}\sigma^m e^{-\frac{Q_c}{RT}} \tag{6.2}$$

This creep model presents an interesting opportunity for combination with data gleaned from hardness tests regarding the state of residual stress. One can estimate the residual stresses by means of a hardness test, these values can then be used in the creep model to estimate the effect the residual stresses will have on the dimensions over the course of the years in which the part will be in service.

6.1.2 Supplementary work to relation

The relation derived would benefit from improvement through future work. The precise nature of the future work required is difficult to predict, but the areas in which future work would be beneficial can be outlined once more.

Firstly, the standardisation of the parameters κ and α are necessary for the functioning of the relation. Additionally, the standardisation of cross-sectional profiles for certain manufacturing processes would be beneficial if one wishes to know the stresses deeper in a piece of material.

Secondly, the limitations of the relation have been outlined at length previously. It would prove invaluable if some future work is able to remove some of these limitations, such that the relation can be used in more wide variety of situations and provide a better quality of data.

The limitation of elasticity is one such aspect. If the relation could be improved so that this limitation is no longer an issue, then cases with higher values of residual stresses could be handled. These situations are the ones that are more likely to cause problems. However, it would likely be difficult to incorporate local yield stresses into the formulation without losing accuracy in the data.

Another such limitation is the offset in the hardness-yield relationship. This had been attributed to work-hardening due to the indentation, therefore it would be beneficial to conduct work to both confirm work-hardening as the cause, and to incorporate this effect into the relation. This could perhaps be done by defining the yield stress as a function of the indentation dimensions.

6.1.3 Improvements to project

At this point it is pertinent to discuss the shortcomings of elements of the project undertaken, and attempt to posit some alternatives which would have served to improve it. As

with the majority of projects, there were certainly aspects of the execution which were less than ideal, and which could do with some retrospective examination.

First and foremost, the main area in which it would have been beneficial to improve would be the lack of fresh experimental data. With the formation of a model to estimate residual stresses through hardness measurements, it would certainly have been beneficial to test this model with the application on some data collected under conditions that could be precisely attuned, such that the required information to adequately judge the quality of the model derived could be extracted.

Naturally, this would be easier said than done, mainly due to the fact that the scope of the project left little time to satisfactorily design a testing regime to adjudge the model. The process of formulating the model itself took up too much time, hence it was not deemed feasible to subsequently test the model.

Another area of potential improvement would lie in the certain aspects of the decision making on the part of the author. It would be fair to state that too large amount of searching was conducted prior to arriving at the decision to pursue the relation of hardness with residual stress. This decision could have been made earlier, which could potentially have freed up time to conduct testing.

Naturally again this is simple to suggest in hindsight, given that the final direction is known. In the state where the final direction is not known, it becomes rather difficult to adjudge which avenue to pursue, and as such the route taken was often meandering, exploring multiple avenues for a time. This process could have been streamlined, such that there were clear points at which the avenue would be evaluated, and a decision taken on whether to pursue it or not.

6.2 Conclusions

6.2.1 Reflections

The presence of residual stresses in an optical component has potential to disrupt the dimensional stability of the component and diminish the resulting data quality. Machining of the component or the gradual relaxation of the stresses over time (creep) are two key areas where residual stresses could cause deformation of the part. Therefore, there was a need in this project to gain a greater insight into residual stresses.

The primary objective of this project was to define the residual stresses as a material parameter, or to relate them to existing defined material parameters through the use of existing literature on this subject. The intention was to eventually be able to infer the residual stresses present in the part through the measurement of the existing material parameter(s).

In this regard, a partial success can be stated, given that a quantitative relation between hardness and residual stress was found in literature from Frankel et al. [5]. The model was based on stresses applied by the indenter being combined with the residual stresses in the material, which were then used in the von Mises yield criterion.

This relation was additionally adapted from cylindrical coordinates with the use of a simple stress state also obtained from literature to obtain a simple relation in rectangular coordinates [6]. This was used to justify the methodology by comparing the equation to hardness-yield stress observations in literature [7] [8] [9]. The similarities observed formed the basis for justification and explanation.

Subsequently, a more complex stress state from literature was used to obtain a final relation describing the effect of residual stresses on hardness measurements, shown below [10].

$$\sigma_y^2 = (\kappa^2 - \kappa + 1)\sigma_{res}^2 + \frac{1}{3}(\kappa + 1)\sigma_{res}P_m + \frac{1}{9}P_m^2$$

This use of this relation would be to use the results standard tests of indentation hardness, and material tensile tests, as inputs into the relation. This would give an estimate of the residual stresses which are affecting the hardness value at the indentation location on the surface. Repeated hardness measurements at key locations on the piece could give an idea of the residual stresses present at those locations.

The success of the primary objective is mitigated by the limitations in the derived relation. Parameters such as κ above would need to be standardised before the relation could directly be used to infer residual stresses from hardness measurements. Additionally, the relation can only function for elastic residual stresses, does not consider the effects of work-hardening during indentation, and would only measure stresses near the surface of a piece. Moreover, the relation displayed here is theoretical, having not been tested with experimental data, although Frankel et al. did show fairly good fits to their data.

Nevertheless, the relation does show potential for usage; if parameters can be standardised, it should be able to infer residual stresses. The limitations listed above are not all likely to cause a large impact on the usability of the equation. For example, the limitation of elastic residual stresses should still make the relation usable for most scenarios. What is clear is that future work is needed to confirm the functionality or otherwise of the relation, and to potentially improve it.

The equation was tested hypothetically, through the arbitrary variation of certain parameters to observe the effects. The hardness was varied to observe the effect on the residual stresses obtained and vice-versa.

The testing showed no entirely unexplainable surprises but the presence of a threshold for κ, below which only complex values were obtained, was somewhat unexpected. The threshold made logical sense in terms of excluding negative values of κ for increased hardness values, due to shear effects. However, it was not expected that some positive κ values would

also be excluded for the higher hardness values. This was somewhat explainable through the observation that uniaxial compressive residual stresses have a low effect on the hardness, hence a certain amount of biaxiality is required to attain higher hardness levels.

A plot using real values from a data table was also presented as an example, but it is difficult to come to conclusions based on this data, as one could not control all the variables. The data chosen was simply for a temper of aluminium alloy 6061, T6, which was significantly 'hardened'. However, the temper involves multiple operations performed upon it, therefore it could not be confidently stated that the residual stresses were solely affecting the hardness measurement.

The secondary objective of this project was to obtain knowledge of current methods used for measuring residual stresses. In the event that the primary objective proved unattainable, this objective would gain in importance. The knowledge of the methods would then have been used to propose a method for measurement and analysis using one or more of the methods. Given the arguable success of the primary objective however, this objective was limited to the description of the existing methods.

The secondary aim of the project as listed in the introduction was as such partly attained. An overview of the residual stress measurement methods in use today are presented, with a description given of a representative method selected for each measurement method type: non-destructive, semi-destructive and destructive.

The three methods selected were X-ray diffraction, hole-drilling, and the contour method. These three were additionally analysed for their usefulness. Each had their own attributes, with their suitability likely to be determined by the situation to be used, and the preference of the user. Nevertheless, a comparative table is presented at the end of Chapter 3 highlighting their relative qualities.

Rough theoretical procedures were formed to estimate certain parameters of the main equation, in which the current measurement methods were needed in order to measure the residual stresses, such that the parameters could be estimated for certain processes, and standardised. Hence, the knowledge of current residual stress measurement methods has potential use in supplementing the relation obtained.

As for the tertiary objectives, not much progress has been made towards predicting residual stresses. There was some information collected on certain models predicting residual stresses due to machining, but this avenue was not pursued deeply, and is not presented here. This was a difficult objective to attain, hence not considered crucial for the successful completion of the project.

For the development or effect of residual stresses, as was mentioned briefly earlier in this chapter, a creep model by Spence was observed in literature, which would calculate the creep due to residual stresses [12] [13]. While this was not investigated deeply, there is enough to suggest the creep model could well be useful and has potential to be combined with residual stress measurements obtained from hardness tests.

6.2.2 Recommendations

With regards to the primary aim of this project, the main recommendation would be to test this relation fully. Given the theoretical nature of the project, a rigorous testing has not been performed on the relation. The necessity is therefore present to test this relation for various scenarios and states.

First and foremost, the functionality of the equation must be confirmed, or rather the shortcomings must be clearly known, such that the equation can be modified and potentially improved into a more robust theory.

Additionally, as mentioned previously, for the equation to be useful in real situations, certain parameters need to be known, and for this there needs to be further testing. The

parameters κ and α would need to be tested in the hope that one could obtain standard values for these parameters for certain situations. This would likely involve the current measurement methods.

The main recommendation for this project is therefore to conduct rigorous testing. With the weight of sufficient good quality data in support of the relation and the parameters involved, one can confidently make use of the relation, or an improved form of it. A summary of a few proposed future actions is given in the list below:

- Test relation thoroughly through performing hardness and residual stress measurements for various situations
- Standardise κ through measuring axiality of residual stresses for various materials and manufacturing processes, e.g. cold-rolling.
- Standardise α through fitting hardness-residual stress data for various materials and processes.
- Incorporate strain-hardening due to indentation into relation, for example by making σ_y in relation dependent on plastic deformation caused by indentation. Can use mathematical approximations to stress-strain curve to estimate 'new' yield stress.
- Obtain standard residual stress profiles for various processes and materials, such that surface measurements can be used to infer stresses deeper in the part.
- Incorporate local yield stresses into relation, such that it is not limited to elastic residual stresses.

With regards to the secondary objective, although this does not form a large portion of the takeaways from this project, there are some possibilities to explore. The most intriguing among these would be the contour method; it is a relatively new method, and appears to be rather interesting for its analytical capabilities. Perhaps the fitting of two-dimensional polynomials to the surface map produced could be a good way to analyse the patterns of stresses present in the cross-section. One such set of two-dimensional polynomials, known as the Chebyshev polynomials, seem to have interesting capabilities in this area.

To conclude, the use of hardness measurements and the relation derived as a probe for residual stresses certainly has its limitations. It remains however an attractive option with future work since it uses equipment and parameters which are already widely used in the industry.

References

[1] N. English, Space telescopes: capturing the rays of the electromagnetic spectrum, Springer, 2017.

[2] T. Newsander, B. Crowther, G. Gubbels and R. Senden, "Aluminum Alloy AA-6061 and RSA-6061 HeatTreatment for Large Mirror Applications," *Space Dynamics Lab Publications,* no. Paper 102, 2013.

[3] G. S. Schajer, Practical Residual Stress Measurement Methods, John Wiley & Sons, Incorporated, 2013.

[4] T. Tsui, W. Oliver and G. Pharr, "Influences of stress on the measurement of mechanical properties using nanoindentation: Part I. Experimental studies in an aluminum alloy," *Journal of MATERIALS RESEARCH,* vol. 11, no. 3, 1995.

[5] J. Frankel, A. Abbate and W. Scholz, "The effect of residual stresses on hardness measurements," *Experimental Mechanics,* pp. 164-168, 1993.

[6] Y.-H. Lee and D. Kwon, "Measurement of residual-stress effect by nanoindentation on elastically strained (1 0 0) W," *Scripta Materialia,* vol. 49, pp. 459-465, 2003.

[7] D. Tabor, "A simple theory of static and dynamic hardness," *Proceedings of the Royal Society A,* vol. 192, 1948.

[8] M. Tiryakioğlu, J. Robinson, M. Salazar-Guapuriche, Y. Zhao and P. Eason, "Hardness–strength relationships in the aluminum alloy 7010," *Materials Science & Engineering A,* vol. 631, pp. 196-200, 2015.

[9] J. Swadener, B. Taljat and G. Pharr, "Measurement of residual stress by load and depth sensing indentation with spherical indenters," *Journal of Materials Research,* vol. 16, no. 7, pp. 2091-2102, 2001.

[10] Y.-H. Lee and D. Kwon, "Estimation of biaxial surface stress by instrumented indentation with sharp indenters," *Acta Materialia,* vol. 52, pp. 1555-1563, 2004.

[11] N. Huber and J. Heerens, "On the effect of a general residual stress state on indentation and hardness testing," *Acta Materialia,* vol. 56, no. 20, pp. 6205-6213, 2008.

[12] T. W. Spence and M. M. Makhlouf, "The effect of machining-induced residual stresses on the creep characteristics of aluminum alloys," *Materials Science & Engineering A,* vol. 630, pp. 125-130, 2015.

[13] T. Spence, "The Effect of Machining Residual Stresses on the Dimensional Stability of Aluminum Alloys used in Optical Systems," 12 April 2010. [Online]. Available: https://digitalcommons.wpi.edu/etd-dissertations/104. [Accessed 08 August 2019].

[14] S. L. Kakani and A. Kakani, Material science, New Delhi: New Age International, 2004.

[15] J. G. Kaufman, Introduction to Aluminum Alloys and Tempers, Materials Park, Ohio: ASM International, 2000.

[16] United Performance Metals, *6061 Aluminum.*

[17] G. E. Totten, M. A. H. Howes and T. Inoue, Handbook of residual stress and deformation of steel, Materials Park, Ohio: ASM International, 2002.

[18] J. Rondal, "Residual stresses in cold-rolled profiles," *Construction and Building Materials,* pp. 150-164, 1987.

[19] J. M. Gere, Mechanics of Materials, Thomson Learning, 2004.

[20] T. Megson, Structural and Stress Analysis, Amsterdam: Butterworth-Heinemann, 2005.

[21] M. Kamaya, "Ramberg–Osgood type stress–strain curve estimation using yield and ultimate strengths for failure assessments," *International Journal of Pressure Vessels and Piping,* vol. 137, pp. 1-12, 2016.

[22] K. Herrmann, Hardness testing : principles and applications, Materials Park, Ohio: ASM International, 2011.

[23] R. von Mises, "Mechanik der festen Körper im plastisch- deformablen Zustand," *Nachrichten von der Gesellschaft der Wissenschaften zu Göttingen, Mathematisch-Physikalische Klasse,* pp. 582-592, 1913.

[24] J. Chakrabarty, Theory of Plasticity, Amsterdam: Elsevier/Butterworth-Heinemann, 2006.

[25] D. W. A. Rees, Basic Engineering Plasticity : An Introduction with Engineering and Manufacturing Applications, Boston: Elsevier, 2006.

[26] P. Kelly, "Lecture Notes: An introduction to Solid Mechanics," [Online]. Available: http://homepages.engineering.auckland.ac.nz/~pkel015/SolidMechanicsBooks/index.html. [Accessed 15 July 2019].

[27] O. Pedersen, L. Brown and W. Stobbs, "The bauschinger effect in copper," *Acta Metallurgica,* vol. 29, no. 11, pp. 1843-1850, 1981.

[28] R. E. Stoltz and R. M. Pelloux, "The Bauschinger effect in precipitation strengthened aluminum alloys," *Metallurgical Transactions,* vol. 7, no. 9, pp. 1295-1306, 1976.

[29] N. Rossini, M. Dassisti, K. Benyounis and A. Olabi, "Methods of measuring residual stresses in components," *Materials & Design,* vol. 35, pp. 572-588, 2012.

[30] G. Urriolagoitia-Sosa, J. Durodola and N. Fellows, "Determination of Residual Stress in Beams Under Bauschinger Effect Using Surface Strain Measurements," *Strain,* vol. 39, no. 4, pp. 177-185, 2003.

[31] J.-C. Su, "Residual Stress Modeling in Machining Processes," Georgia Institute of Technology, 2006.

[32] B. B. He, Two-Dimensional X-Ray Diffraction, Hoboken, NJ: John Wiley & Sons, Inc., 2018.

[33] A. Bunaciu, E. Udriştioiu and H. Aboul-Enein, "X-ray diffraction: instrumentation and applications," *Critical reviews in analytical chemistry,* vol. 45, no. 4, pp. 289-99, 2015.

[34] M. G. Moore and W. P. Evans, "Mathematical Correction for Stress in Removed Layers in X-Ray Diffraction Residual Stress Analysis," *SAE Transactions,* vol. 66, no. 19580101, pp. 340-345, 1958.

[35] T.-S. Jun and A. M. Korsunsky, "Evaluation of residual stresses and strains using the Eigenstrain Reconstruction Method," *International Journal of Solids and Structures,* vol. 47, no. 13, pp. 1678-1686, 2010.

[36] International Atomic Energy Agency, "Measurement of residual stress in materials using neutrons," in *IAEA*, Vienna, 2005.

[37] W. M. Murray and W. R. Miller, The bonded electrical resistance strain gage : an introduction, New York: Oxford University Press, 1992.

[38] V. Lakshminarayanan and A. Fleck, "Zernike polynomials: a guide," *Journal of Modern Optics,* vol. 58, no. 7, pp. 545-561, 2011.

[39] F. Liu, B. Robinson, P. Reardon and J. Geary, “Analyzing optics test data on rectangular apertures using 2-D Chebyshev polynomials,” *Optical Engineering*, vol. 50, no. 4, 2011.

[40] P. R. Clement, “The Chebyshev approximation method,” *Quarterly of Applied Mathematics*, vol. 11, no. 2, pp. 167-183, 1953.

[41] N. Tebedge, G. Alpsten and L. Tall, “Residual-stress measurement by the sectioning method,” *Experimental Mechanics*, vol. 13, no. 2, pp. 88-96, 1973.

[42] G. Berg and P. Grau, “Meyer’s hardness law and its relation to other measures of ball hardness tests,” *Crystal Research and Technology*, vol. 32, no. 1, pp. 149-154, 1997.

[43] M. Shaw, T. Hoshi and D. Henry, “Reverse Plastic Flow Associated With Plastic Indentation,” *Journal of Engineering for Industry*, vol. 101, no. 2, pp. 104-108, 1979.

[44] M. K. Howlader, J. Marik and M. Jandera, “Cold-Forming Effect on Stainless Steel Sections,” *International Journal of Steel Structures*, vol. 16, no. 2, pp. 317-332, 2016.

[45] M. B. Prime and M. R. Hill, “Residual stress, stress relief, and inhomogeneity in aluminum plate,” *Scripta Materialia*, vol. 46, no. 1, pp. 77-82, 2002.

[46] G. Urriolagoitia-Sosa, B. Romero-Ángeles, L. Hernández-Gómez, C. Torres-Torres and G. Urriolagoitia-Calderón, “Crack-compliance method for assessing residual stress due to loading/unloading history: Numerical and experimental analysis,” *Theoretical and Applied Fracture Mechanics*, vol. 56, no. 3, pp. 188-199, 2011.

[47] S. Schroeder, J. Frankel and A. Abbate, “The relationship between residual stress and hardness and the onset of plastic deformation,” US Army Armament Research, Development and Engineering Center, Watervliet, N.Y., 1995.

[48] Alcoa Engineered Products, “Alloy 6061”.

[49] G. Sines and R. Carlson, “Hardness measurements for the determination of residual stresses,” *ASTM Bulletin*, vol. 180, pp. 35-37, 1952.

[50] R. B. Cruise and L. Gardner, “Strength enhancements induced during cold forming of stainless steel sections,” *Journal of Constructional Steel Research*, vol. 64, no. 11, pp. 1310-1316, 2008.

[51] S. Liang and J.-C. Su, “Residual Stress Modeling in Orthogonal Machining,” *CIRP Annals - Manufacturing Technology*, vol. 56, no. 1, pp. 65-68, 2007.

[52] D. Roylance, “STRESS-STRAIN CURVES,” 2001 August 2001. [Online]. Available: http://web.mit.edu/course/3/3.11/www/modules/ss.pdf. [Accessed 26 July 2019].

Appendix A Full Derivation of Theory

A.1 Frankel, Abbate and Scholz model

Frankel, Abbate and Scholz introduced the formulation based on the stress element shown below in Figure A.1, formulated for cylindrical stresses [5]. These were the circumferential or hoop stresses (σ_H), and the radial stresses (σ_R). This was itself based on the stress element for only the forces on the material at the tip of the indenter due to the indentation pressure, from Shaw, Hoshi and Henry [43]. According to Frankel, Abbate and Scholz, this "relates to the situation in which the load W is still applied but the deformation has stopped" [43], hence giving the P_m value at the border of the yield. Using the three stresses shown as the principal stresses in the von Mises criterion (equation (2.15)), gave them equation (A.1) below, where p is the P_m from the element, and S_y is the yield stress.

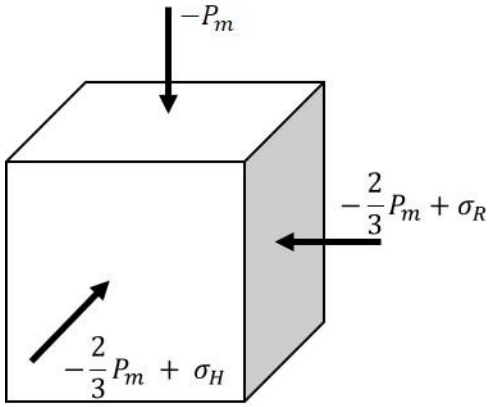

Figure A.1: Stress element from Frankel, Abbate and Scholz, for hoop and radial stresses [5]

$$(\sigma_H - \sigma_R)^2 + \left(-\frac{2}{3}p + \sigma_R + p\right)^2 + \left(-p + \frac{2}{3}p - \sigma_H\right)^2 = 2S_y^2 \quad \textbf{(A.1)}$$

A.2 Equi-Biaxial modification & derivation of initial equation

The formulation above was relevant for the steel tubes used by Frankel, Abbate and Scholz, however for regular purposes, normal rectangular coordinates were needed. The equi-biaxial formulation shown in equation (4.2), was indicated as an assumption in a paper by Lee & Kwon [6], and was used as an initial assumption, where the two orthogonal principal plane

stresses were equal, and of value σ_{res}, leading to an overall stress element as shown below in Figure A.2. The third principal stress would simply be the $-P_m$ from the stress element, as with the plane stress assumption, this is the only stress acting in this direction. The principal stresses are shown in equation (4.5). These principal stresses are used in the von Mises yield criterion once more, and the relation is derived starting from the first part of equation (4.6).

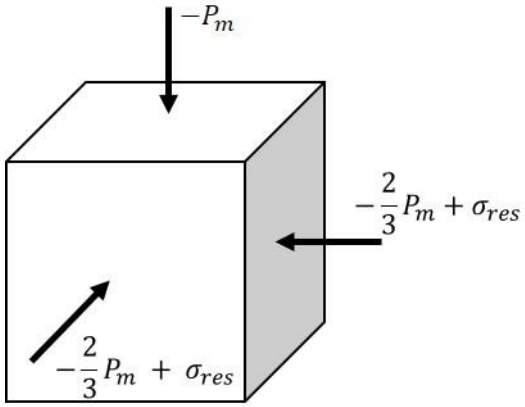

Figure A.2: Stress element using equi-biaxial residual stress state

$$2\sigma_y^2 = \left(\sigma_{res}^2 + \frac{2}{3}\sigma_{res}P_m + \frac{1}{9}P_m^2\right) + \left(\sigma_{res}^2 + \frac{2}{3}\sigma_{res}P_m + \frac{1}{9}P_m^2\right)$$

$$2\sigma_y^2 = 2\left(\sigma_{res} + \frac{1}{3}P_m\right)^2$$

$$\sigma_y^2 = \left(\sigma_{res} + \frac{1}{3}P_m\right)^2 \quad \textbf{(A.2)}$$

Cancelling out the twos on either side results in the second part of equation (4.6). From there on, the assumptions/problems are explained in the text.

A.3 Using κ parameter to give modified equation

The κ parameter, as introduced by Lee & Kwon [10], added an additional modification, such that the state of stress was no longer the simple equi-biaxial. The use of the κ parameter gives a state of stress as shown in equation (4.13), and the input of it into the von Mises criterion

results initially in equation (4.14). Starting from equation (4.14), the derivation is shown in equations (A.3) below.

$$2\sigma_y^2 = \left(\sigma_{res}(1-\kappa)\right)^2 + \left(\kappa\sigma_{res} + \frac{1}{3}P_m\right)^2 + \left(-\frac{1}{3}P_m - \sigma_{res}\right)^2$$

Expanding out gives:

$$2\sigma_y^2 = \sigma_{res}^2(1-\kappa)^2 + \kappa^2\sigma_{res}^2 + \frac{2}{3}\kappa\sigma_{res}P_m + \frac{1}{9}P_m^2 + \sigma_{res}^2 + \frac{2}{3}\sigma_{res}P_m + \frac{1}{9}P_m^2$$

Collecting terms:

$$2\sigma_y^2 = ((1-\kappa)^2 + \kappa^2 + 1)\sigma_{res}^2 + \left(\frac{2}{3}\kappa + \frac{2}{3}\right)\sigma_{res}P_m + \frac{2}{9}P_m^2$$

Simplifying:

$$2\sigma_y^2 = (\kappa^2 - 2\kappa + 1 + \kappa^2 + 1)\sigma_{res}^2 + \frac{2}{3}(\kappa+1)\sigma_{res}P_m + \frac{2}{9}P_m^2$$

$$2\sigma_y^2 = (2\kappa^2 - 2\kappa + 2)\sigma_{res}^2 + \frac{2}{3}(\kappa+1)\sigma_{res}P_m + \frac{2}{9}P_m^2$$

(A.3)

Dividing by the factor of 2, finally gives equation (4.15):

$$\sigma_y^2 = (\kappa^2 - \kappa + 1)\sigma_{res}^2 + \frac{1}{3}(\kappa+1)\sigma_{res}P_m + \frac{1}{9}P_m^2$$

Appendix B MATLAB Codes

B.1 Functions

B.1.1 res_calc

Function to return major $\boldsymbol{\sigma_{res}}$ *value for a given mean pressure, initial yield stress, and* $\boldsymbol{\kappa}$ *parameter.*

```
function res = res_calc(y_0,P_m,k)
%y_0 = yield stress
%k = biaxiality ratio parameter
%P_m = mean pressure
%sig_r = residual stress parameter
%%%%%%%%%%%%%%%%%%% Defining equation and variables %%%%%%%%%%%%%%%%%%%%%%
syms sig_r % Defining RS variable as the one to be solved for.
assume(sig_r,'real') % Limitation that solution must be real
%Constitutive equation defined as from derivation in notes
eqn=(y_0^2)==(k^2-k+1)*(sig_r^2)+(1/3)*(k+1)*sig_r*P_m + (1/9)*(P_m^2);
%%%%%%%%%%%%%%%%%%%%%%%%%%%%%% Calculation %%%%%%%%%%%%%%%%%%%%%%%%%%%%%%%%
r = solve (eqn,sig_r); % Solving equation for residual stress
r1 = vpa(r);
% Assigning output, 'res'.
if isempty(r)== 1 % 'Solve' will return empty if there are no real solutions
res = NaN; % Want to assign the complex solutions as NaN
else
res = r1(2); % Returning only the 'positive' root
end
end
```

B.1.2 k_thresh

Function to calculate threshold of $\boldsymbol{\kappa}$ *for values of* P_m *and* $\boldsymbol{\sigma_{y_0}}$

```
function klim = k_thresh(y_0,P_m) % Inputs of yield stress and mean pressure

%%%%%%%%%%%%%%%%%%%%%%% Defining equation and variables %%%%%%%%%%%%%%%%%%%
syms k % Define variable to be solved for
assume(k >= -1 & k<=1); % Finding only values of k in this interval

%Defining constants a,b, and c of quadratic formula from equation%
a= (k^2-k+1);
```

```
b = (1/3)*(k+1)*P_m;
c = ((1/9)*(P_m^2))-(y_0^2);
%Equation: Threshold defined when part in square root in quadratic
%formula equals 0
eqn1 =(b^2)-4*a*c ==0;

%Solving equation
k1 = solve (eqn1,k);
k2 = vpa(k1);

% Assigning output of function
klim = mean(k2); % mean used here just in case of 2 identical solutions,
%i.e. when curve only touches axis at one point
end
```

B.1.3 pm_hb_conv

Function to calculate P_m value from Brinell hardness (based on equations from Frankel et al. [5]*)*

```
function P_m = pm_hb_conv(H_b,W,D)
%P_m = Mean pressure in kg/mm^2
%H_b = Brinell Hardness number
%W = Load applied during Brinell test in kg
%D = Diameter of ball used in Brinell in mm
if H_b == 0
    P_m = 0;
else
d_D_2 = ((4*W)/(pi*D^2))*((1/H_b)-((W/(pi*D^2))*(1/(H_b^2))));
P_m = H_b*(1+((1/4)*d_D_2));
end
end
```

B.1.4 res_thresh

Function to calculate the von Mises limit for σ_{res} for a particular κ and yield stress

```
function reslim = res_thresh(k,y_0)
syms sig_r
assume(sig_r,'real')
eqn = ((k^2)-k+1)*(sig_r^2)==(y_0^2);
r = solve (eqn,sig_r); % Solving equation for residual stress
```

```
r1 = vpa(r);
reslim = abs(r1(2));
```

B.2 Scripts

B.2.1 Rs_script

Script to calculate and plot the variance of residual stress values as κ *is varied between -1 and 1.*

```
%%%%%%%%%%%%%%%%%%%%%%%%%%%%%% Raw Data %%%%%%%%%%%%%%%%%%%%%%%%%%%%%%%%%%%%
y_0 = 24.607; %Yield stress, kgf/mm^2
H_b = 0; % Brinell Hardness
W = 500; % Load used in Brinell test, in kg
D = 10; % Diameter of Ball used in Brinell test, in mm
k = (-1:0.05:1); % Range of k values being tested

% % Conversion to N/mm^2 (can comment in/out as required)
g = 9.81;
y_0 = y_0*g;
H_b = H_b*g;
W = 500*g;
%%%%%%%%%%%%%%%%% Pre-allocation of arrays %%%%%%%%%%%%%%%%%%%%%%%%%%%%%%%%
res = zeros(length(k),length(H_b)); % empty array for residual stress for
each k
P_m = zeros(1,length(H_b));
reslim = zeros(length(k),length(y_0)); % limit of residual stress for
elasticity
%%%%%%%%%%%%%%%%%%%%%%%% Calculation %%%%%%%%%%%%%%%%%%%%%%%%%%%%%%%%%%%%%%
for j = 1:length(H_b) % Loop through each hardness value
for i = 1:length(k) % Loop through each k value

    % Converting Brinell to mean pressure %
P_m(j) = pm_hb_conv(H_b(j),W,D);
    % - Calculating residual stress value for each k, hardness and yield
    res(i,j) = res_calc(y_0(j),P_m(j),k(i));
    % - Calculating R.S. von Mises limit for each k and y value
   reslim(i,j) = res_thresh(k(i),y_0(j));
end
 % - klim is threshold of k, above which residual stress has real
```

```
    % values
klim = k_thresh(y_0(j),P_m(j));
% Creating legend entries. If 'g' exists, then we are in N/mm^2
if exist('g','var')==1
lgd{j} = ['\sigma_y = ' num2str(y_0(j)) ' N/mm^2, H_B = ' num2str(H_b(j)) '
N/mm^2'];
else
lgd{j} = ['\sigma_y = ' num2str(y_0(j)) ' kgf/mm^2, H_B = ' num2str(H_b(j))
' kgf/mm^2'];
end
%%%%%%%%%%% Plotting of residual stress values vs. k values %%%%%%%%%%%%%
plot(k,res(:,j),'k')
xlim([min(k) max(k)])
hold on
end
if mean(res,'omitnan')<0
    reslim=reslim*(-1);
end
%%%%%%%%%%%%%% Plotting of k-threshold & von Mises limit %%%%%%%%%%%%%%%
if length(H_b)==1 % Plotting k-threshold only if there is one curve
   c = max(res);
   d = min(res);
   c1 = max(reslim);
   d1 = min(reslim);
   mx = max(c,c1);
   mn = min(d,d1);
   mxm = max(abs(mx),abs(mn));

plot([klim klim],[mn mx],'k--')
hold on

plot(k,reslim,'k.-')
a = area(k,reslim,(mxm*sign(mean(res,'omitnan'))),'FaceColor','black');
alpha(a,0.2);
set(a,'EdgeColor','none')
ylim([mn mx])
end
```

```
%%%%%%%%%%%%%%%%%%%%%%%%%%%%%%%% Labels %%%%%%%%%%%%%%%%%%%%%%%%%%%%%%%%
ax=gca;
ax.FontSize=16;
xlabel('\kappa (axiality parameter)','FontSize',18)
ylabel('\sigma_r_e_s (N/mm^2)','FontSize',18)
l = legend(lgd{1:end}, 'Threshold of \kappa','Von Mises limit for
\sigma_r_e_s','FontSize',12,'Location','SouthWest');
if mean(res,'omitnan')>0
    set(l,'Location','NorthWest')
end
title('Variance of \sigma_r_e_s with \kappa','FontSize',18)
hold off
```

B.2.2 ratio_effect

Script to test effect of ratio $P_m/\boldsymbol{\sigma}_y$ on the $\boldsymbol{\kappa}$ threshold value

```
%%%%%%%%%%%%%%%%%%%%%%%%%%%%%%%% Input Data %%%%%%%%%%%%%%%%%%%%%%%%%%%%%%%%
ratio = (3:0.02:3.5); % Range of ratios
y_0 = 10; % Yield stress
P_m = ratio*y_0; % Define P_m
klim = zeros(size(P_m)); % Pre-allocation of klim
%%%%%%%%%%%%%%%%%%%%%%%%%%%%%%%% Calculation %%%%%%%%%%%%%%%%%%%%%%%%%%%%%%%%
for i = 1:length(P_m)
    klim(i) = k_thresh(y_0,P_m(i)); % Using k_thresh at each value
end
%%%%%%%%%%%%%%%%%%%%%%%%%%%%%%%% Plotting Results %%%%%%%%%%%%%%%%%%%%%%%%%%%%%%%%
figure(1)
plot(ratio,klim,'b')
ax = gca;
ax.FontSize=16;
xlabel('P_m/\sigma_y','FontSize',20)
ylabel('\kappa-parameter threshold','FontSize',20)
```

B.2.3 Pm_script

Script to calculate P_m for varying σ_{res} values, also with a changing κ

```
y_0 = 10; % Arbitrary yield stress
sig_r = (0:1:10); % Varying R.S. value, but keeping lower than yield
% Convert to N/mm^2
```

```
y_0 = y_0*9.81;
sig_r = sig_r*9.81;
k =(-1:0.2:1) ;
syms P_m % Defining Pm variable as the one to be solved for.
assume(P_m,'real')
r2 = zeros(length(k),length(sig_r));
for j = 1:length(k)
for i = 1:length(sig_r)
eqn=(y_0^2)==(k(j)^2-k(j)+1)*(sig_r(i)^2)+(1/3)*(k(j)+1)*sig_r(i)*P_m    +
(1/9)*(P_m^2);
%%%%%%%%%%%%%%%%%%%%%%%%%%%%%% Calculation %%%%%%%%%%%%%%%%%%%%%%%%%%%%%%
r = solve (eqn,P_m); % Solving equation for Pm
r1 = vpa(r);

if isempty(r)==1  % 'Solve' will return empty if there are no real solutions
r2(j,i) = NaN; % Want to assign the complex solutions as NaN
else
r2(j,i)=r1(2);% Returning only the 'positive' root
end
end
%%%%%%%%%%% Plotting data, each k value will be a different line %%%%%%%%%%
plot(sig_r,r2(j,:))
lgd{j} = ['\kappa = ' num2str(k(j)) ''];
hold on
end
ax=gca;
ax.FontSize=14;
ylabel('P_m (N/mm^2)','FontSize',16)
xlabel('\sigma_r_e_s (N/mm^2)','FontSize',16)
legend(lgd{1:end},'FontSize',12)
title(['Effect of \kappa and \sigma_r_e_s on P_m (\sigma_y = ' num2str(y_0)
' N/mm^2)'],'FontSize',16)
hold off
```

Published with MATLAB® R2019a